

**STUDY OF MAGNETITE MINERALIZATION ASSOCIATED
WITH NAGA OPHIOLITE BELT AT PHOKPUR IN KIPHIRE
DISTRICT OF NAGALAND**

By

Kenyelo Rengma



*Thesis submitted for the Requirement of
Degree of Doctor of Philosophy
in
Geology
of the
Nagaland University*

2022

TO MY DAD, MOM AND AUNTY

**DEPARTMENT OF GEOLOGY
NAGALAND UNIVERSITY
Kohima Campus, Meriema**

DECLARATION

I, Kenyelo Rengma, hereby declare that the subject matter of this thesis is the record of work done by me. That the content of this thesis did not form basis for the award of any previous degree to me or to the best of my knowledge to anybody else, and that this thesis has not been submitted by me for any research degree to any other University/Institute.

This thesis is being submitted to the Nagaland University for the award of degree of Doctor of Philosophy in Geology under the supervision of Prof. Santosh Kumar Singh of Nagaland University.

Date:
Place: Nagaland University
Kohima Campus, Meriema

(KENYELO RENGMA)
Ph.D. Scholar
Department of Geology
Reg. No. 576/2014 (20th May, 2014)

Supervisor
(Prof. Santosh Kumar Singh)

Head of the Department
(Prof. Santosh Kumar Singh)

NAGALAND



UNIVERSITY

Dr. Santosh Kumar Singh
Professor & Head
Department of Geology
Kohima Campus: Meriema
Kohima – 797 004

Mobile : 09436604764
E-mail:
santoshsingh@nagalanduniversity.ac.in

CERTIFICATE

The thesis presented by Mr. Kenyelo Rengma, bearing Registration No. 576/2014, dated 20th May, 2014 embodies the result of investigations carried out by him under my supervision and guidance during the research period prescribed in the Ph.D. ordinance of Nagaland University and further extensions as per UGC notifications from time to time.

I certify that this work has not been presented for any degree elsewhere and that the candidate has fulfilled all conditions laid down by the Nagaland University.

Date: 20-12-2022

(Prof. Santosh Kumar Singh)
Supervisor



नागालैण्ड विश्वविद्यालय

NAGALAND UNIVERSITY

(संसद द्वारा पारित अधिनियम 1989, क्रमांक 35 के अंतर्गत स्थापित केंद्रीय विश्वविद्यालय)

(A Central University established by the Act of Parliament No.35 of 1989)

मुख्यालय: तुमामी, जुन्हेबोटो (नागालैण्ड), पिनकोड-798627

Headquarters: Lumami, Dist: Zunheboto, (Nagaland), Pin Code-798627

PLAGIARISM-FREE UNDERTAKING

Name of Research Scholar	Kenyelo Rengma
Ph.D. Registration Number	No. 576/2014
Title of Ph.D. thesis	Study of Magnetite Mineralization Associated with Naga Ophiolite Belt at Phokpur in Kiphire District of Nagaland
Name & Institutional Address of the Supervisor / Co-Supervisor	Prof. Santosh Kumar Singh Department of Geology, Nagaland University Kohima Campus, Meriema, Kohima-797004
Name of the Department & School	Department of Geology/ School of Sciences
Date of submission	20.12.2022
Date of plagiarism check	19.12.2022
Percentage of similarity detected by the URKUND software	1%

I hereby declare / certify that the Ph.D. thesis submitted by me is complete in all respects, as per the guidelines of the Nagaland University for this purpose. I also certify that the thesis (soft copy) has been checked for plagiarism using URKUND similarity-check software. It is also certified that the contents of the electronic version of the thesis are the same as the final hard copy of the thesis. A copy of the report generated by the URKUND software is also enclosed.

Kenyelo Rengma
(Name & Signature of the
Scholar)

Date: 20-12-2022

Place: Kohima

Prof. Santosh Kumar Singh
Name & Signature of the Supervisor with seal

ACKNOWLEDGEMENTS

First of all, I express my deepest and sincerest gratitude to my Supervisor Dr. Santosh Kumar Singh, Professor & Head, Department of Geology, Nagaland University, Kohima Campus, Meriema for his selfless, untiring and dedicated guidance extended to me throughout the entire period of my research work.

I am immensely indebted to Nagaland University for providing the opportunity to pursue my Ph.D. and also extending all possible and available facilities.

I also express my heartfelt thanks to Prof. G.T. Thong and Prof. B.V. Rao for their full support, suggestions and encouragement during my research period.

My sincere thanks goes to Shri S. K. Kenye, former Director, Directorate of Geology & Mining, Nagaland, Dimapur for allowing me to pursue my Ph.D. and also for extending all possible facilities available in the Department.

I am very much indebted to Prof. N. V. Chalapathi Rao (In-Charge) and Dr. Dinesh Pandit (Scientist) EPMA Laboratory, Department of Geology, Institute of Science, Banaras Hindu University, Varanasi for electron probe micro analysis of magnetite ore samples of my Ph. D. area.

My heartfelt thanks go to Dr. Moalang Kichu, Mr. Mehilo Apon, Ms. Bendangtola Longchar research scholars and Mr. Vilzoto Valeo, Assistant Geologist, DGM, Nagaland for their help in preparation of geological maps.

I also express my thanks to the leaders of Phokpur village, for all their support and allowing me to do my field work in their jurisdiction.

My sincere thanks go to all persons who helped me during my research work. I would like to make a special mention to Mr. Keyhun Kath, Mr. Hongbe, Mr. Hankimong and Mr. Pheeno for helping me during my field visits.

It would not be complete if I don't mention my father Late Jorhi Rengma, my mother Shasinle Tep and my aunty Late Asüle Tep, who fully supported me morally and prayerfully. I would be failing in my duty if I don't mention my family support especially from my wife Mrs. Lily Tep Rengma and children Jozenlo Tep, Hissolo Tep, Konilo Tep and Gwashalo Tep, who gave constant moral and prayer support throughout my research work.

Lastly, I thank the Almighty God for sustaining me and my family in good health all throughout my research work.

(KENYELO RENGMA)

PARTICULARS OF CANDIDATE

NAME OF THE CANDIDATE : Kenyelo Rengma

DEGREE : PhD

DEPARTMENT : Geology

TITLE OF THESIS:

Study of Magnetite Mineralization Associated With Naga Ophiolite Belt at Phokpur in Kiphire District of Nagaland

DATE OF ADMISSION : 30th August 2013

APPROVAL OF RESEARCH
PROPOSAL : 16th June 2014

REGISTRATION NO. & DATE : 576/2014 (20.5.2014)

(Head of Department)

BIODATA OF THE CANDIDATE

1. Research Paper Published

Rengma K. and Singh S.K. (2021) Ni-Co-Cr-Bearing Phokpur Magnetite Deposit Associated With Naga Ophiolite Belt, North-East India and its Economic Viability. Journal of Scientific Research, BHU. Vol. 65, Issue 1, pp.

2. Workshop Attended

- (i) Attended Basic e-course on PRGS using ArcGIS for pre-field studies from 04th to 10th June 2021, Government of India, GSI, RTD NER, Shillong.

3. Seminar Participated and Presentation

- (i) Attended the National Seminar on “Geology, Geochemistry, Tectonics, Energy and Mineral Resources of Northeast India from 9th to 11th Nov’ 2016, conducted by Department of Geology, Nagaland University, Kohima Campus, Meriema.
- (ii) Participated in the 3rd National Geo-Research Scholars Meet-2019 (NGRSM-2019) from 6th -8th June, 2019 at Wadia Institute of Himalayan Geology, Dehradun and participated in Poster presentation on “Presence of nickel in Phokpur magnetite deposit associated with Naga ophiolite belt and its importance in the national scenario.
- (iii) Participated in the National Conference on Emerging Trends in Environmental Research from 31st to 2nd Nov’ 2019 at Department of Science, Pachhunga University College, Aizawl and presented a poster on “Study of magnetite associated with Naga Ophiolite Belt at Phokpur, Kiphire District of Nagaland, North-East India and was awarded with Best Poster Presentation.

LIST OF TABLES

	Page Nos.
2.1. Lithostratigraphic Succession of Eastern part of Nagaland.....	27
4.1. Paragenetic sequence based on textural relationship.....	51
4.2. Modal percentage of mineral samples of the Phokpur magnetite ore.....	52
4.3. Chemical analyses of Phokpur magnetite ore samples (in %)......	53
5.1: X-ray line used in the analysis along with their counting statistics with respect to natural and synthetic standards.....	58
5.2. Representative EPMA analyses of magnetite grains from the Phokpur magnetite ore samples of Naga Ophiolite Belt.....	60-62
5.3. Representative EPMA analyses of chrome-magnetite grains from the Phokpur magnetite ore samples of Naga Ophiolite Belt.....	63-65
5.4. Representative EPMA analyses of chromite grains from the Phokpur magnetite ore samples of Naga Ophiolite Belt.....	66-69
5.5. EPMA analyses of a selected chrome-magnetite phenocryst along X-Y line from the Phokpur magnetite ore samples of Naga Ophiolite Belt.....	78-82
5.6. Representative EPMA analyses of chlorites in wt% from the Phokpur magnetite ore samples and Fe content reported as total FeO. Structural formulae of chlorite calculated on basis of 28 oxygen atoms.....	90-91
7.1. Paragenetic sequence based on textural relationship.....	104

LIST OF PLATES

	After page No.
Plate I..... Chapter 1.....	20
Plate II, III Chapter 2.....	41
Plate IV to XVII..... Chapter 4.....	58

LIST OF FIGURES

	Page Nos.
Fig. 1.1: Regional geology map of Himalaya showing location of the..... South Ladakh and North Ladakh Ophiolite	4
Fig. 1.2: Geological map of Ladakh-Zaskar area	5
Fig. 1.3: Distribution of Ophiolite at the eastern margin of the Indian plate	8
Fig. 1.4: Geological map of the Andaman Islands	10
Fig. 1.5: Regional tectonic setting of the Himalaya showing all Tethyan ophiolite.... Occurrences and their age of formation	11
Fig. 1.6: Location map of the study area	14
Fig. 2.1: Simplified geological and tectonic map of Nagaland and Manipur	22
Fig. 2.2: Geological map showing the occurrence of chromite, nickeliferous magnetite and base metals in the Naga ophiolite belt	28
Fig. 2.3: Schematic diagram showing the late felsic granite cut-across pillow lava at Salumi in Phek	35
Fig. 2.4: Geological Map of the Phokpur Magnetite Deposit	37
Fig. 2.5: Schematic diagrams showing occurrence of nickeliferous magnetite	38
Fig. 2.6: Lamination of chromite with inter-granular magnetite in nickeliferous magnetite at Matungsekien Ridge, Phokpur magnetite deposit	39
Fig. 2.7: Geological map showing the locations of collected ore samples.	40
Fig 4.1: Binary diagram of (a) Ni versus Co and (b) Co versus Cr plotted for Phokpur Magnetite ore samples from NOB (after Duran et al., 2020).....	55
Fig 4.2: Primitive mantle normalized enrichment pattern of chrome-magnetite ore samples from Phokpur deposit, NOB. Primitive mantle values from Palme and O, Neill (2014).	56
Fig. 5.1 (a): Composition of spinel group minerals plotted in $\text{TiO}_2\text{-FeO-Fe}_2\text{O}_3$ ternary diagram (Buddington and Lindsley, 1964) showing major solid solution series in mole percent	73
Fig. 5.1 (b): $\text{Cr}^{3+} - \text{Fe}^{3+} + \text{Al}^{3+}$ diagram (after Stevens, 1944) plotted for the	73
Fig. 5.2 (a): Cr_2O_3 versus Al_2O_3 diagrams of spinel group	74
Fig.5.2 (b): TiO_2 versus Al_2O_3 variation in Cr-magnetite with respect to modern-day tectonic settings for Naga Ophiolites Belt at Phokpur	74

Fig.5.3 (a): $\text{Fe}^{2+}/\text{Fe}^{3+}$ versus Al_2O_3 variation diagram of Cr-magnetite from	75
Nagaland ophiolite suites	
Fig.5.3 (b) $\text{Cr}/(\text{Cr} + \text{Al})$ versus $\text{Mg}/(\text{Mg} + \text{Fe}^{2+})$ tectonic discrimination diagrams for chromites of Naga Ophiolites Belt at Phokpur, District Kiphire, Nagaland	75
Fig.5.4 (a): Photomicrographs shows chromite crystal altered at margin to Cr- magnetite	76
Fig.5.4 (b):BSE images of chromite grain; XY line shown in the figure is used for the EPMA line scan for different oxides as displayed in Figure. (C – F) X- Ray elemental maps for Fe, Cr, O and Si, respectively	76
Fig.5.5: EPMA line scans along the line X-Y (as shown in Figure 5.4 (b) for various oxides in the studied Cr-magnetite grain.....	77
Fig.5.6: Primitive mantle normalized enrichment pattern of Cr-magnetite ore from	83
Phokpur deposit. Primitive mantle values from Palme and O, Neill (2014) and elemental composition of magnetite is obtained from (Rengma and Singh, 2021).	
Fig.5.7: Mineral composition of chlorites from Phokpur magnetite ore samples from	84
NOB plotted in $\text{FeO-MgO-Al}_2\text{O}_3$, triangular for end-members of chlorite (Fleming and Fawcett,1976).	
Fig. 5.8: Mineral composition of chlorites from Phokpur magnetites ore samples from NOB. $\text{SiO}_2\text{-(MgO+FeO)-Al}_2\text{O}_3$ ternary diagram of chlorite end-members and substitution considered in chlorite solid solution model (Vidal et al., 2001).	85
Fig.5.9: Mineral composition of chlorites from Phokpur magnetite ore samples from	86
NOB plotted in projection field (R^{2+} -Si diagram)for chlorite compositions(after Wiewiora & Weiss 1990); Bourdelle and Cathelineau,2015).	
Fig.5.10: Correlation between MnO and NiO content of chlorite from the Phokpur	87
magnetite ore samples from NOB.	
Fig.5.11: Correlation between FeO_t and NiO content of chlorite from the Phokpur	87
magnetite ore samples from NOB.	
Fig.5.12: Correlation between SiO_2 and Cr_2O_3 content of chlorite from Phokpur	88
magnetite ore samples from NOB.	
Fig.5.13: Correlation between Al_2O_3 and Cr_2O_3 content of chlorite from Phokpur	88
magnetite ore samples from NOB.	
Fig.5.14 :Correlation between FeO_t and Cr_2O_3 content of chlorite from Phokpur	89
magnetite ore samples from NOB.	
Fig.5.15:Correlation between NiO and Cr_2O_3 content of chlorite from Phokpur	89
magnetite ore samples from NOB.	

CONTENTS

	Page Nos.
Declaration.....	i
Certificate of Supervisor	ii
Plagiarism-Free Undertaking	iii
Acknowledgementsiv
Particulars of the Candidate	v
Bio-data of the Candidate	vi
List of Tables	vii
List of Plates	viii
List of Figures	ix
 Chapter 1: Introduction	 1-20
1.1 General Aspects	1
1.2 Ophiolite in India	1
1.2.1 Ladakh Ophiolite Belt	2
(i) Spontang Ophiolite Complex	2
(ii) Nidar Ophiolite	3
(iii) Karzog Ophiolite	3
(iv) Dras Arc	3
1.2.2 Mayodia Ophiolite Belt, Arunachal Pradesh	5
1.2.3 Nagaland-Manipur Ophiolites	6
1.2.4 Andaman Ophiolites	9
1.3 Naga Ophiolite Belt	11
1.4 Location and Approach	13
1.5 Physiography and Drainage	14
1.6 Climate and Soil	15
1.7 Flora and Fauna	16
1.8 Inhabitants	16
1.9 Previous Works	16
1.10 Aims and Objective of Research	18

Chapter 2: Geological Setting	21-40
2.1 Regional Geology and Tectonics	21
2.2 Stratigraphy	23
2.2.1 Nimi Formation/ Naga Metamorphics	23
2.2.2 The Ophiolite Suite	24
2.2.3 Disang Formation	25
2.2.4 Jopi/ Phokphur Formation	25
2.2.5 Alluvium/Laterites	26
2.3 Mineralisations in Naga Ophiolite Belt	28
2.3.1 Chromite	29
2.3.2 Magnetite	30
2.3.3 Sulphide Mineralisation	33
2.3.4 Laterites	34
2.3.5 Late Felsic Intrusives/Late Tertiary Granitoids	34
2.4 Geology of the Study Area	35
2.4.1 Phokpur Magnetite Deposit	36
2.5 Traverses and Sample Collection	39
Chapter 3: Methodology and Instrumentation Techniques	41 - 45
3.1 Literature Survey	41
3.2 Geological Field Work	41
3.3 Laboratory Work	42
3.3.1 Preparation of polished thin sections	43
3.3.2 Preparation of powdered samples	43
3.4 Analytical Methods	44
3.4.1 Optical studies	44
3.4.2 Inductively coupled plasma - Optical Emission Spectroscopy (ICP-OES) ..	44
3.3.3 Electron Probe Micro Analysis	45
3.3.4 Petrochemical calculations and graphical diagrams	45
3.3.5 Software and Rockware	45
Chapter 4: Petrography and Geochemistry of Phokpur Magnetite	46-56
4.1 Introductory	46
4.2 Phokpur Magnetite	46
4.2.1 Ore Microscope studies	47
4.2.2 BSE Images of Magnetite Ores and their Textural Features	50
4.3 Paragenetic sequence of Phokpur Magnetite	51
4.4 Modal Mineralogy	52
4.5 Geochemistry of Phokpur Magnetite	53.

Chapter 5: Mineral Chemistry of Magnetite Ore	57-91
5.1 Introductory	57
5.2 Results	59
5.2.1 Electron Probe Micro Analysis	59
5.2.2 Mineral chemistry of magnetite ore samples	70
5.2.3. Mineral chemistry of chlorite	83
 Chapter 6: Genesis of Phokpur Magnetite Deposit	 92-99
6.1 Magnetite Historical information	92
6.2 Magnetite ore mineral: General Information	92
6.3 Transformation of ferrous hydroxide into magnetite.....	93
6.4 Earlier Views on the Genesis of Phokpur Magnetite Deposit	94
6.5 Discussion on the Genesis of Phokpur Magnetite Deposit	94
 Chapter 7: Summary and Conclusions	 100 - 108
7.1: Introduction	100
7.2 Geological Setting	101
7.3: Petrography and Geochemistry of Phokpur Magnetite	102
7.3.1: Ore microscopic studies	103
7.3.2 Modal Mineralogy	104
7.3.3: Geochemistry of Phokpur magnetite105
7.4: Mineral chemistry of Magnetite ore	105
7.5: Genesis of Phokpur magnetite deposit	107
 REFERENCES	 109-122

INTRODUCTION

1.1 General Aspects

Ophiolites are usually considered as remnants of the oceanic lithosphere (oceanic crust and upper mantle) tectonically emplaced/ obducted onto continental margins (Dewey and Bird, 1971; Coleman, 1977; Nicolas, 1989; Dilek et al., 1999) during continent–continent and arc-continent collisions (Dilek and Flower, 2003), ridge-trench interactions (Cloos, 1993; Lagabrielle et al., 2000), and/ or subduction-accretion events (Cawood et al., 2009). Though ophiolites can be formed in mid-oceanic ridge (MOR) as well as supra-subduction zone (SSZ) tectonic environments, Phanerozoic ophiolites are usually formed in the SSZ tectonic setting (Pearce et al., 1984; Dare et al., 2009; Pagé et al., 2009; Pal et al., 2014). A typical ophiolite sequence constitutes mantle peridotite with tectonite at the base followed subsequently by ultramafic-mafic cumulates, massive gabbro, sheeted dykes, pillow basalts, and deep sea pelagic sediments and chert at the top (Anonymous, 1972; Coleman, 1977). The mafic and ultramafic rocks of the ophiolite suite are very important to reconstruct the tectono-magmatic history of the oceanic lithosphere (Dilek and Furnes, 2011). Therefore, they have got much interest among the Earth Scientists of the world. They are the potential sites for exploration of various metallic deposits like copper sulphides, chromium bearing magnetite, podiform chromite etc. and constitute favorable locales for occurrences of precious metals like PGE and gold. Consequently, the ophiolite belts are being explored for their mineral wealth.

1.2 Ophiolites in India

In India, the Phanerozoic ophiolites mainly belong to Late Mesozoic to early Tertiary period. They are found in Ladakh, Arunachal Pradesh, Nagaland, Manipur and Andaman Islands, and represent the ancient ocean basins consumed by the process of

subduction. Further, these ophiolites of India are classified as Indus-Tsangpo Suture Zone (ITSZ) and Indo-Myanmar Range (IMR) ophiolites representing the collision of Indian and Asian plates. Ladakh ophiolite belt and the ophiolites of Arunachal Pradesh represent the ITSZ ophiolites, whereas the ophiolites of Nagaland, Manipur and Andaman represent IMR ophiolites. In contrast to the other above mentioned ophiolites of India, the Andaman Island ophiolite represents an area of active subduction (Geological Survey of India, 2015). A brief description of these ophiolites is given below:

1.2.1 Ladakh Ophiolite Belt: It consists mainly of Spontang, Nidar and Karzog ophiolite complexes of the South Ladakh, and Dras ophiolite sequences of North Ladakh within the expanse of the Himalayan belt and distance along ITSZ (Fig. 1.1). In the NW Himalayas (Ladakh-Zaskar area), the convergence of the Indian and Asian plate and closure of the Neo-Tethys Sea is marked by the presence of two distinct tectonic domains of ophiolites and related ophiolitic mélanges (Fig. 1.2). The first domain, i.e. Dras arc (associated with Ladakh batholith) is localized to the north of ITSZ. This ophiolitic unit represents the subduction of the Indian plate under the oceanic margin of the Asian plate. The second domain, the south Ladakh group, located to the south of ITSZ is represented by three ophiolites and ophiolite mélanges namely, (i) *Spontang ophiolite* consists of both crustal and mantle units, (ii) *Nidar ophiolite* consists mainly of crustal units, and (iii) the small *Karzog ophiolite* having abundant chromitite and gabbros.

(i) Spontang Ophiolite Complex: It represents almost the complete ophiolite sequence comprising mantle rocks (depleted harzburgites, dunites and little lherzolites) as well as crustal rocks (basalt, isotropic gabbros, layered gabbros etc.). The Spontang mafic sequence exhibiting N-MORB affinity is originated from a depleted upper mantle with little contribution from subduction-related fluids. MORB-type of Neo-Tethyan oceanic crust is associated with the earliest phase of subduction during Early Jurassic period with subsequent development of a younger intra-oceanic Spong island arc. The other side of the mafic sequence is characterized by the interplay of subduction-related melts with the upper mantle during the commencement of subduction in Early Cretaceous period (Jonnalagadda et al., 2022).

(ii) Nidar Ophiolite: It is located between the North Himalayan nappes and ITSZ in the Eastern Ladakh of NW Himalaya. The Nidar ophiolite is typically interpreted as a relic of an intra-oceanic arc (Mahéo et al., 2004) developed at around 140 Ma prior to the collision of Indian and Eurasian plates (Ahmad et al., 2008). The following rock types are present from top to bottom: various sedimentary rocks like conglomerates enriched in quartz and K-feldspar, and conglomerates with clasts of basalt and radiolarites with immediate contact of basaltic rocks. This compositional variation reflects different detrital sources, e.g. from the felsic part of the Ladakh batholith and the upper part of the ophiolite. Pillow lavas form the most abundant volcanic rocks located mainly on top of the layered gabbros, the main plutonic rocks of the Nidar Ophiolite. The further underlying mantle rocks are partially serpentinized harzburgites with irregular contacts of surrounding dunites. Clinopyroxenites, gabbro dykes and little chromitites are the minor rock types. Formation of the Nidar Ophiolite can be explained by the two main events:

- (i) Formation of oceanic crust recorded by the layered gabbros, underlying harzburgites and olivine basalts.
- (ii) Presence of intrusive complexes within the layered gabbros as well as in the mantle rocks, possibly related to the formation of an intra-oceanic arc.

(iii) Karzog Ophiolite: It is present near south of the Tso Morari dome within the core of a synform of Permian sediments. The Karzog ophiolite consists mainly of highly deformed and altered chromitites, serpentinites and minor gabbros. Due to the presence of abundant chromitites, the Karzog ophiolite is considered as a relic of a transition zone between the crust and the mantle. There is a contradiction in the age of the Karzog ophiolite. Fuchs and Linner (1996) proposed Permian whereas Berthelsen (1953) and de Sigoyer (1998) proposed Cretaceous to Eocene ages for this ophiolite. There is no absolute dating available for The Karzog ophiolite.

(iv) Dras Arc: In the NW Himalaya in India, there is a belt of basaltic-andesites with intercalation of arkose-dominated volcanoclastics of the Nindam Formation along the Indus Suture zone between India and Eurasia (Mahéo et al., 2004). Whether these rocks are formed in a forearc basin to the Eurasian margin or as part of an intra-oceanic island arc

system that collided with either India or Eurasia before final continental collision is debated. U-Pb dating of detrital zircons from the Nindam Formation yields the age of ~ 84 Ma to 125 Ma, corresponding with arc magmatism. The basal section of the Nindam Formation reveals the presence of arc-derived basaltic-andesite and tonalite clasts, plus ophiolitic components sourced from an adjacent accretionary complex. It is suggested that the Dras and Spong arcs are the same intraoceanic island arc system that developed as a result of subduction initiation along NNE-SSW transform faults perpendicular to the Indian and Eurasia continents.

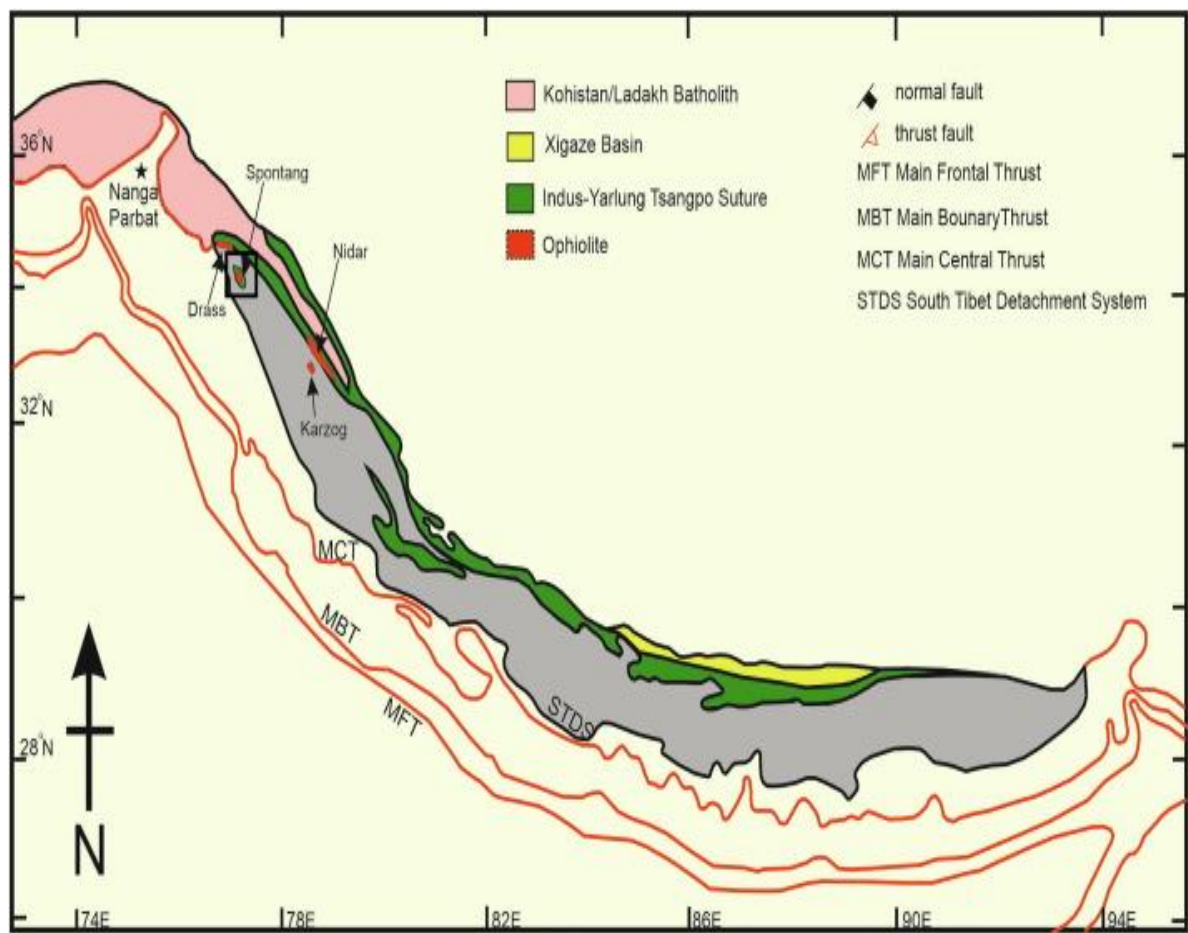


Fig.1.1: Regional geological map of the Himalayas (after Hébart et al., 2003) showing location of the South Ladakh (Spontang, Nidar and Karzog) and North Ladakh Ophiolite (Dras) sequences of Mahéo et al., 2004 (Jonnalagadda et al., 2022).

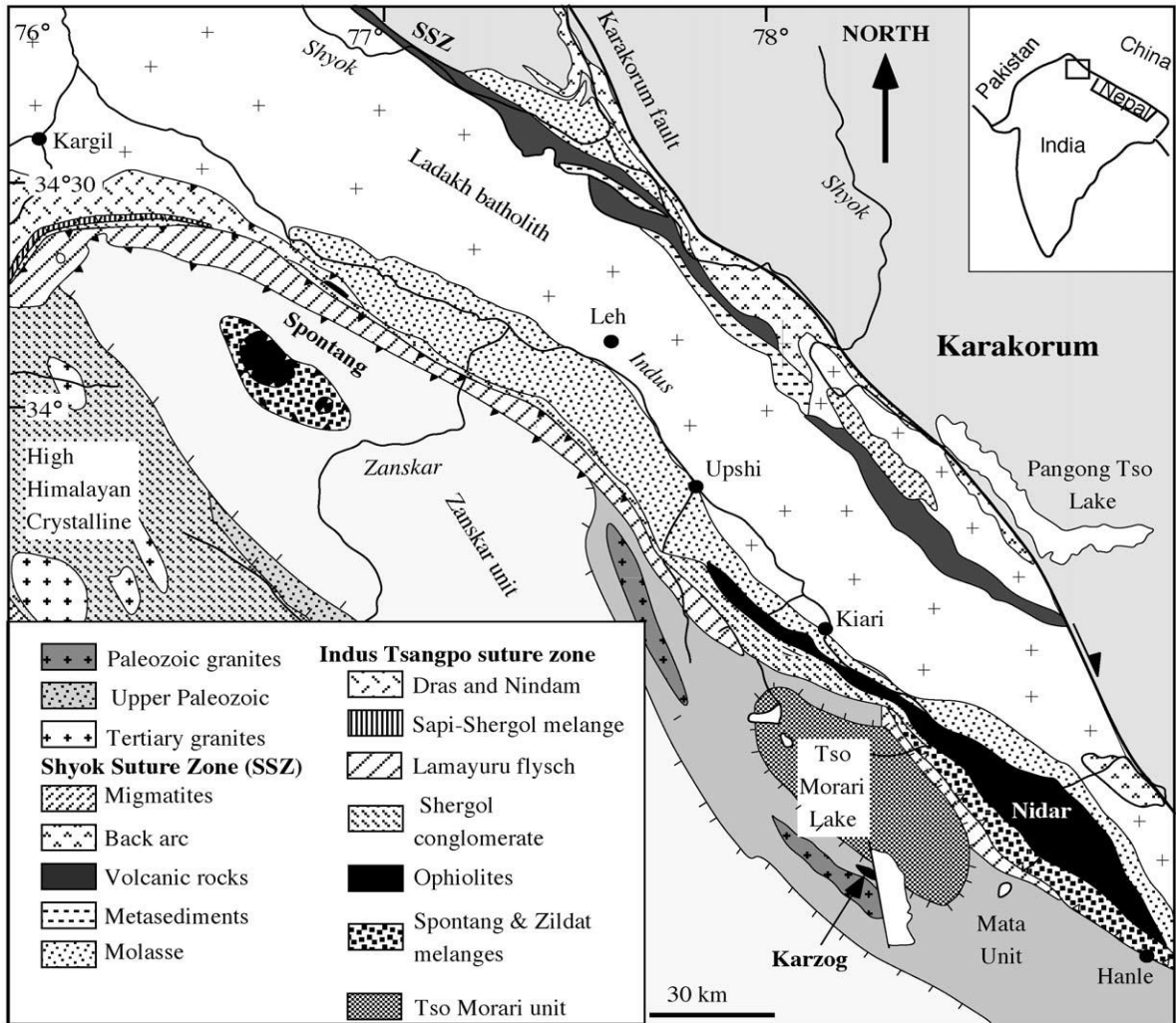


Fig.1.2: Geological map of Ladakh– Zaskar area (Mahéo et al., 2004).

1.2.2 Mayodia Ophiolite Belt, Arunachal Pradesh: The Mayodia ophiolite belt is located in Dibang Valley of Arunachal Pradesh and falls in the eastern extension of the ITSZ. It is represented by three litho-units, viz. peridotite tectonite, hornblendite (dyke) and amphibolite. The whole sequence is overlain by metabasalt cover inter-layered with metapelites of pelagic sediments. The basal peridotite is mainly wehrlite in nature. The hornblendite is represented by cumulus primary amphibole and occurs typically as intrusive dyke within the basal peridotite. The amphibolite is characterized by well developed gneissose banding. The pillow lava is represented by actinolite-chlorite-albite-epidote schist. According to Ghose et al. (2007), the Mayodia ophiolite suite was evolved

by the partial melting of a depleted mantle source having MORB affinity as a result of the collision Indian and Asian plates that commenced with the closing of Tethyan Ocean during Mesozoic and Early Tertiary.

1.2.3 Nagaland-Manipur Ophiolites

The Nagaland-Manipur ophiolites form a part of the Indo-Myanmar Range (IMR) comprising the Arakan Yoma, Chin and Naga Hills. They occur as rootless blocks having various dimensions along the eastern side of the Indian plate. The ophiolites have been emplaced by thrusting between the Indian plate and the Myanmar continental plate during Late Oligocene terminal collision (Acharyya et al., 1990; Sengupta et al., 1990; Acharyya, 2007). In the Nagaland-Manipur belt, the ophiolites occur as dismembered slabs in an accretionary prism overlying Eocene-Oligocene sediments.

On the basis of the structural features of the Nagaland-Manipur ophiolite belt, Bhattacharjee (1991) suggested that the subduction began during Cretaceous time and collision occurred in two stages. First between the subducting plate and an island arc, and second between the subducting plate and Myanmar plate. The ophiolites consist of diverse igneous, sedimentary and metamorphic rocks of which ultramafics are the main component. The ultramafics are interpreted as slices of oceanic crust and upper mantle obducted onto the Indian continental margin. The associated blue schist is indicative of subduction zone tectonics. The occurrences of ultramafics showing intrusive contacts and the presence of intermediate - acid volcanics suggest an island arc - continent type of collision along the Benioff Zone coincident with the ophiolite belt. There are two groups in the Indian side ophiolite belt of the IMR: (a) ophiolites of Naga- Manipur Hills, Arakan coast and Andaman Islands having mid-Eocene accretion history, and (b) ophiolites of Mt. Victoria and Chin Hills, Myanmar having an early Cretaceous accretion history (Mitchell 1993; Acharyya 2007).

In the Naga-Manipur Hills, volcanics of the ophiolite are closely associated with radiolarian cherts, and radiolarian and micro-foraminiferal limestone indicating late Jurassic to early Eocene age (Anon 1986; Acharyya et al. 1989).

Bhattacharjee (1991) summarized the tectonic history of the Indo-Myanmar orogenic belt in the following lines:

- (i) Introduction of the subduction zone during Cretaceous times; obduction of oceanic crust and upper mantle and intermixing with deep oceanic sediments.
- (ii) Deposition of the Disang sediments. Formation of an island arc separating the sedimentary basin into eastern and western sub-basins. The Barail sediments were deposited in both basins. The formation of the island arc was accompanied by plutonism and volcanism and by deformation and low grade metamorphism of the lower Disang sediments.
- (iii) Gradual shallowing of the basin consequent upon the collision of the island arc with the easterly subducted India plate.
- (iv) Continent-continent collision and rotation of the down-basin normal faults into low angle reverse faults (thrusts) along which the thrust sheets were piled up. The frontal areas of the thrust sheets were asymmetrically folded. This was followed by asymmetrical folding of the rocks of the foreland areas.
- (v) Formation of gravity faults and conjugate sets of strike-slip faults in the orogen and the foreland areas. The structures associated with the ophiolite belt are attributed first to the collision of the easterly subducting India plate with an island arc and subsequently with the Myanmar plate.

Distribution of ophiolite at the eastern margin of the Indian plate and location of Nagaland-Manipur ophiolite belt is shown in figure 1.3.

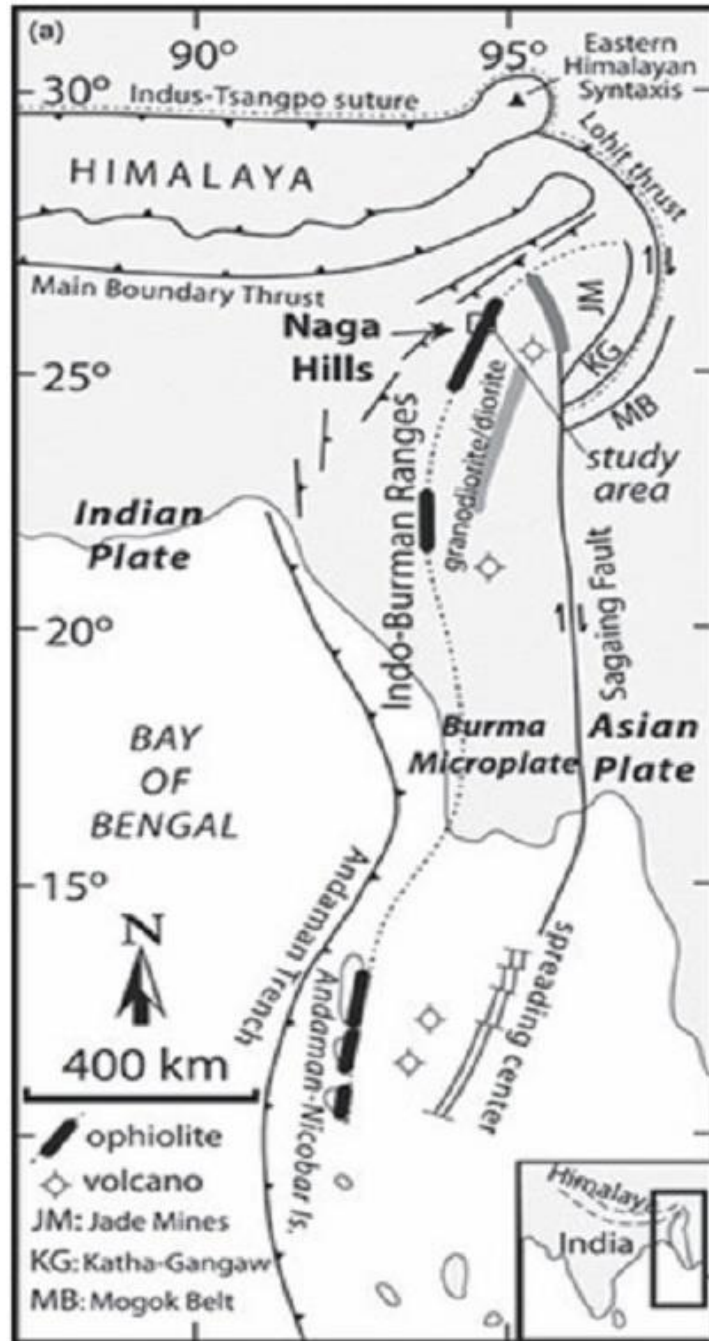


Fig.1.3: Distribution of ophiolite at the eastern margin of the Indian plate and location of Naga Hills (after Searle et al., 2007).

1.2.4 Andaman Ophiolites

The Andaman ophiolites are located to the south of the Nagaland-Manipur ophiolite belt and bear signatures of an active subduction tectonics, whereas the Nagaland-Manipur ophiolites represent a relic arc in a collision setting. Recently, a detailed study of the Andaman ophiolite has revealed evidence for (a) the existence of boninitic magmatic rocks, (b) melt–rock interaction, and (c) polygenetic MORB-SSZ tectonic setting (Pal, 2011). The Andaman stratigraphic succession comprises of four groups (Awasthi et al., 2015). They are: (i) the Cretaceous Ophiolite Group, (ii) the Eocene Mithakhari Group, (iii) the Oligocene Andaman Flysch Group, and (iv) the Mio–Pliocene Archipelago Group (Figure 1.4). The basement of the Andaman Islands is represented by the Ophiolite Group. It contains thrust blocks of supra-subduction zone ophiolite complexes and pelagic sediments (chert, limestone and shale). The U–Pb zircon dating of plagiogranites revealed that the age of these ophiolites could be at least 94 Ma (Pedersen et al., 2010; Sarma et al., 2010). The Mithakhari Group consists of polymict conglomerate, sandstone and shale. These rocks are identified as trench-slope deposits formed by the sediments derived from the volcanic arc and/or thrust blocks of ophiolites of the overriding plate. The Andaman Flysch represents siliciclastic turbidites whereas the Archipelago groups of rocks contain carbonate turbidites, both deposited in a forearc basin.

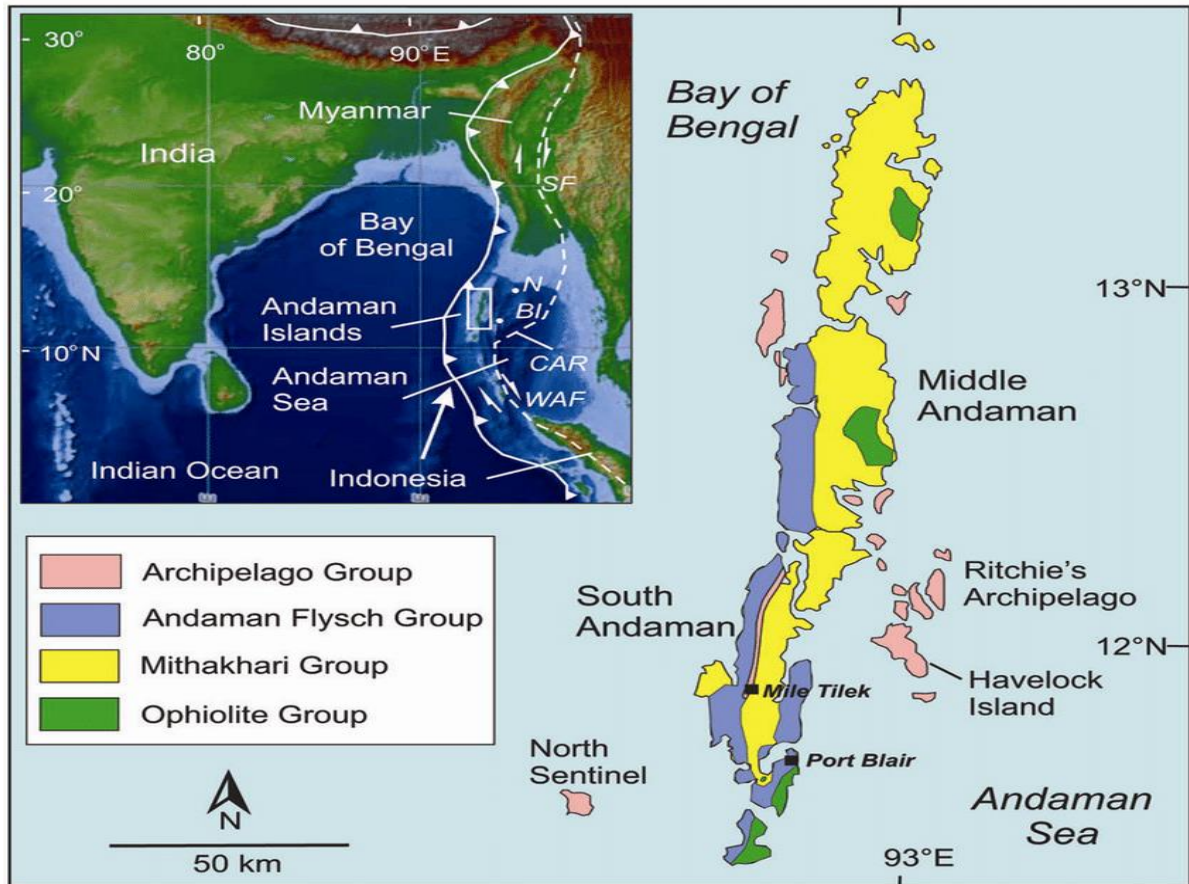


Fig.1.4: Geological map of the Andaman Islands (after Pal et al., 2003) showing distribution of various lithological rock units. (Inset) Location of the islands in Southeast Asia, the Andaman-Sumatran subduction zone, Central Andaman Ridge (CAR) and major faults in the region. Arrow shows the direction of the motion of the Indian plate. N (Narcondam), BI (Barren Island), SF (Sagaing Fault), WAF (West Andaman Fault).

Based on the map sourced from GeoMap App software (Singh, 2022), the regional tectonic setting of the Himalaya showing Tethyan ophiolite occurrences and their age of formation (white) is presented in the following figure 1.5.

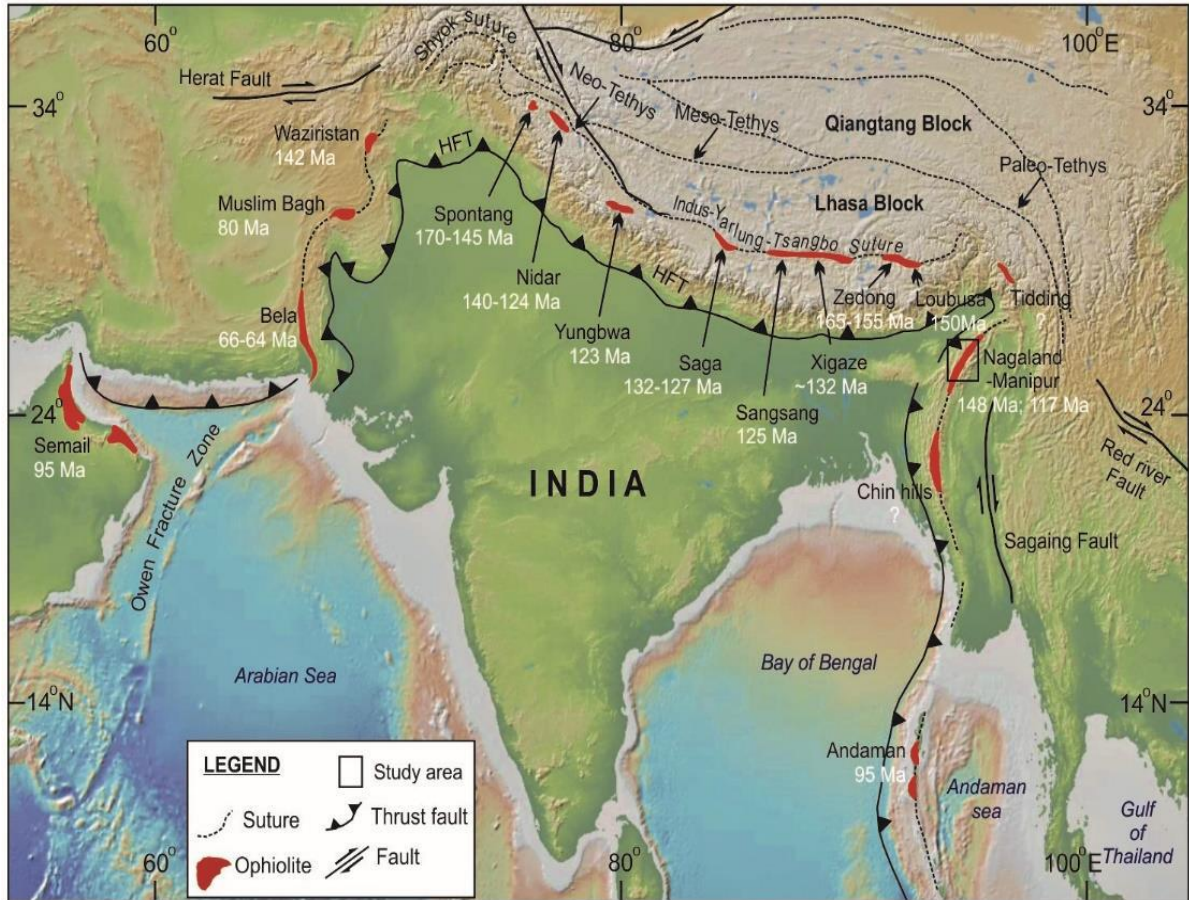


Fig.1.5: Regional tectonic setting of the Himalaya showing all Tethyan ophiolite occurrences and their age of formation (white).

The present study is a part of ophiolite belt in Nagaland, which is popularly known as Naga Ophiolite Belt. Therefore, a brief information on the Naga ophiolite belt is given in the present chapter. Further detailed description on its geology, tectonic settings and mineralisation potential has been given in Chapter 2.

1.3 Naga Ophiolite Belt: The Nagaland – Manipur ophiolite belt within India extends for about 200 km from Chokla (Nagaland) in the north to Moreh (Manipur) in the south with width ranging from 5 to 16 km. The part of the ophiolite belt within Nagaland extends for about 90 km and is termed as Naga Ophiolite Belt. It is placed between the Nimi Formation in the east and the Disang flysch in the west (Ghose, 1980; Acharyya et al., 1984; Singh et al., 1989). Various government and private exploration agencies have

done some work on the search of metals in this difficult terrain, and have indicated the possibilities of PGE and gold incidences (Rao et al., 2005; Ghose, 2014), but till date no promising mineral incidences have been discovered except the magnetite deposit.

Nickel (Ni) - cobalt (Co) - chromium (Cr) - bearing magnetite deposit associated with Naga Ophiolite Belt is a rare type of occurrence. The main deposit, popularly known as the Phokpur magnetite deposit, occurs at eastern-most part of the Nagaland. It is located at the Matungse Kein Hill, about 4 km east of Phokpur village in Kiphire district of Nagaland. A number of small magnetite incidences have also been reported at Phor, Ziphu, Mollen, Washello, Reguri, Molhe Peaks, Ghoos Camp in Meluri Subdivision of Phek district of Nagaland (Agrawal and Rao, 1978; Ghose, 1980; Chattopadhyay and Bhattacharya, 1986; Ghose and Goswami, 1986). Important amongst these are located on the western flank of Jopi-Mollen ridge where discontinuous slabs of bedded magnetite varying in thickness from 1 m to 9 m are occurring above the serpentinite bodies and are unconformably overlain by the rocks of 'Jopi Formation'.

The Phokpur magnetite deposit occurring in the northern part of the Naga Ophiolite Belt is exposed as a massive sheet like band over serpentinitised peridotite with almost a sharp contact and is overlain by Mio-Pliocene molassic sediments (Jopi Formation) with an unconformity. The ore body has been traced for a strike length of approximately 1 km (intermittently) in NNE-SSW direction with moderate to steep westerly dips. The thickness varies between 5 m to 15 m with an outcrop width of about 300 m along the dip direction (Majumdar et al., 1976). The ore body represents a low plunging (SSW) synformal warp truncated on its west and east by high angle faults giving the body a form of a 'horst' like block. The basal contact with the serpentinite body is marked with discrete grains of chromite (Ghose and Goswami, 1986).

Occurrence of such exceptionally large bodies of magnetite within ophiolite is a unique and rare petro-mineralogical phenomenon in such a geological set-up. The field relations of the magnetite in Nagaland have indicated a petro-tectonic control wherein such bodies have preferential emplacement along with peridotite-pyroxenite litho-assemblage, especially those in close proximity with hornblendite/ amphibolites.

With so much of iron deposits in other states of India, a small deposit of magnetite in Phokpur in Kiphire district of Nagaland may go unheard of except for its content of other strategic minerals like nickel, cobalt and chromite. Nickel and cobalt containing rocks/ores are vital, strategic and significance for any nation, as magnetite in Nagaland. These metals are indispensable for different industries like aerospace, special steels products, electroplating, etc. Our defense needs a lot of nickel and cobalt and their alloy products for the manufacture of superior military armaments. Most of the annual needs of nickel in India are met through import only. The Sukinda ultramafic complex of Orissa is the only significant source of these metals in the country. The chromite mine overburden contains nickel and cobalt, and efforts are being made continuously to recover these metals. In view of the scarcity of raw materials for nickel and cobalt in the country, every possible indigenous source of these metals should be exploited. In this context, the nickel bearing magnetite of Phokpur, Nagaland, in spite of its low nickel and cobalt content, can be considered a potential source of these metals of our country.

1.4 Location and Approach

The study area, popularly known as the Phokpur Magnetite Deposit, forms a part of Naga Ophiolite Belt along Indo-Myanmar border and is located at the Matungse Kein Hill, about 4 km east of Phokpur village in Kiphire district of Nagaland. It is located with coordinates latitudes N25°25'38" to 25°58'13" and longitudes E 94°32'53" to 95°02'56" in Survey of India toposheet No. 83 K/13 under the administrative sub-division of Pungro (SDO, Civil). Phokpur is about 60 km from Kiphire and is connected by unmetalled road. Kiphire is linked to Dimapur by state highways via Meluri- Pfuetero-Kohima (326 km); and also by Tuensang-Mokokchung-Mariani (340 km). Location map of the study area is shown in Fig. 1.6. The road from Phokpur to the magnetite deposit reaches the farthest village Thongsongyu on Indo-Myanmar border.

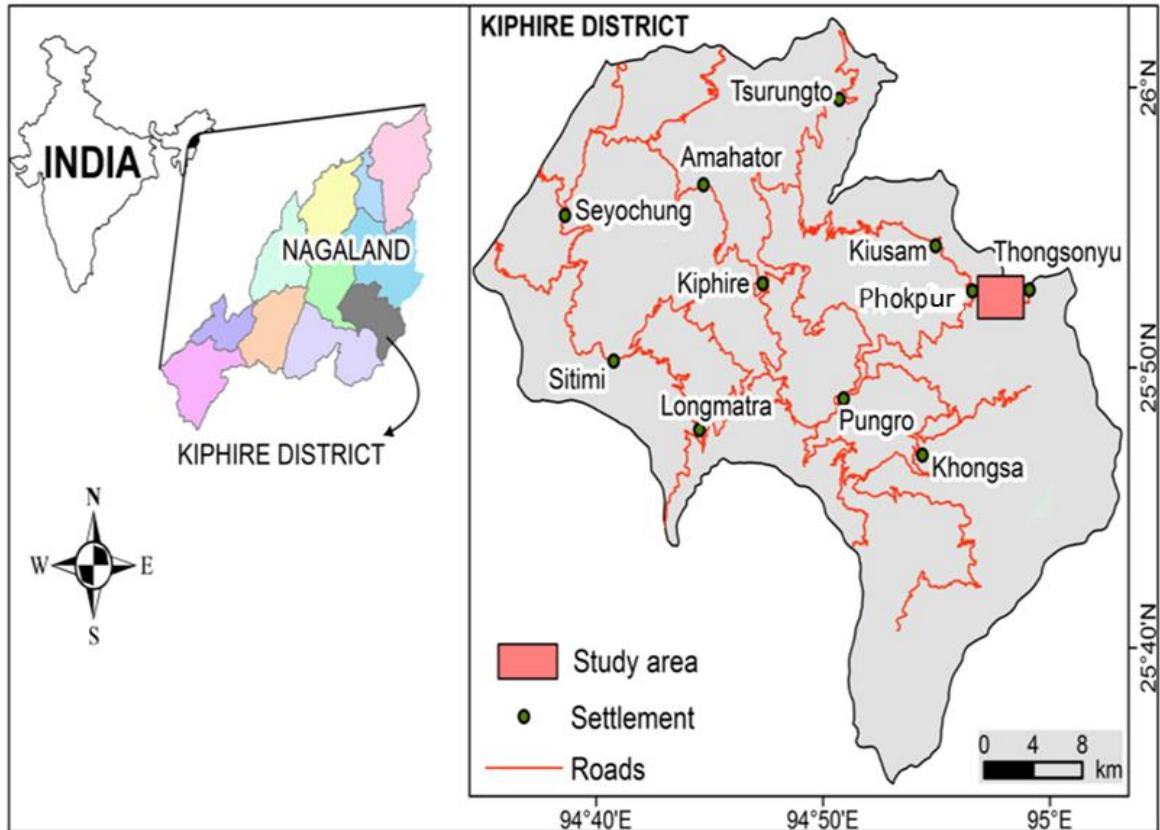


Fig. 1.6: Location map of the study area in the Kiphire district of Nagaland

1.5 Physiography and Drainage

Physiographically, the area depicts a panoramic and picturesque landscape of the surrounding hills and mountain ranges forming part of the Arakan- Yoma- Patkai mountain ranges of Nagaland (Plate I, Fig.1). The topography of the area is characterized by high rugged mountains ranges, deep gorges, parallel to sub-parallel ridges and V-shaped valleys trending NE. In Phokpur section, the Matungse Kein Hill, where the largest magnetite deposit occur (Plate I, Fig.2), has altitude of 1978 m and gain altitude toward the east one after another and reaches 3837 m at Saramati Peak in Indo-Myanmar border (Sharma, 1983). The major rivers in the area are Chokla River in NE having tributaries namely Tarare Nalla in the east and Pongsingde nalla in the west of Matungse Kein ridge/spur and Likhimro river in the SW, both drain into the Zungki river. The Zungki River flows N-S direction and joins Tizu in the south. In the Phor-Jopi section, the hills and mountain

ranges mountain ranges generally gain elevation toward the east culminating at Ngazipfu (2357 m) while the western boundary is controlled by Jopi- Zephuhu range. Zipuhuhu peak at an elevation of 2509 m is the highest elevation point which forms the source of many perennial streams. The ridge is almost dissected longitudinally by a number of streams and nallas draining the area.

Drainage system is structurally controlled with dentritic to sub-trellis pattern. The area is mostly within the catchment area of Tizu river, a major river of eastern Nagaland. The Tizu river originates in the upper Himalayan ranges at an elevation of about 2250 m and has a total length of about 165 km up to its confluence with Zungki. Layakti nalla, Khayakti nalla, Changsulizu nalla, Washelloti nalla and Yokhriti nalla are the major perennial streams draining the region. The Shakhatu Luku nalla with its tributaries is the main drainage system of the Waziho area. It flows northerly to join the Tizu. The Turati nalla and Chizati nalla are the two major streams draining Mimi. They flow in west-south-west direction forming deep gorges along their course.

1.6 Climate and Soil

The climate is sub-tropical with average annual rainfall of 1800 mm occurring over about 6 months from May to October and the potential evapo-transpiration at 1219 mm. This clearly indicates that there is a shortage of water for a considerable period from November to April. The region generally experiences warm summer varying from 20 °C to 30 °C and very cold winter with temperature often going below freezing point. The zungki-Tizu valley is often covered with clouds throughout the year.

The soils of the Kiphire district are derived from tertiary rocks belonging to Barail and Disang Groups. Though the district is small, but due to large variation in topography and climate, there is a wide variety of soil types prevailing in the district. Both alluvial and residual soils are found in the district. Recent alluvial (Entisol), Old alluvium (Oxizols and Ultisol) and Mountain valley soil (Entisol) are the main alluvial soil types. Under the residual soil, three different types- laterite soil (Oxizols and Ultisol); brown forest soils (Mollisols and Inceptisols) and podzolic soils (Spodosols) are the main soil types.

1.7 Flora and Fauna

The variation in height gives rise to the diversity in forest ranging from tropical evergreen to coniferous evergreen types. Bamboos are extensive in the low-lying tracts. Chesnuts, oaks, etc are commonly seen on the slopes above 1800 m and pine or chir forest generally above this height. Besides these, cane and thorny shrubs, spear grasses and ferns are frequently found. Generally vegetation cover is thick over sedimentary and volcanic terrain whereas the serpentinite and ultramafics terrains are thinly vegetated.

The practice of shifting cultivation has led to degradation of forests and the habitats of different animal's population. However, there are still large tracts of land under forest, which harbour a number of animal species such as barking deer, monkey, rodent, mithun, jungle cat, bear, wild boar, wild goat, snake, porcupine, squirrel, wild fowls, varieties of fishes etc.

1.8 Inhabitants

The Ophiolite areas are inhabited by tribal communities namely Pochury in Phek district and Yimkhiung, Sangtam and Sumi in Kiphire district. Each tribe has their own dialect, however, almost everyone can be communicated by Naga common dialect called Nagamese (originally from Assamese, Bengali, Hindi, and even English). The belief of the people is mostly Christianity though the traditional practices are preserved. The people are simple and hard working. The main occupation of the people is agriculture mostly jhum cultivation though terrace paddy cultivation is done in river valleys. The agro products are rice, maize, cabbage, beans, millet, squash, pumpkins, brinjal, king chilly, etc. The people in the area are also known for fruits cultivation of orange and apple. The population density in the area is very sparse.

1.9 Previous Works

With the inception of the State Directorate of Geology and Mining, Govt. of Nagaland in 1968, more emphasis was given to unravel the geology and mineral resources

of the eastern part of the state. In this endeavour, one of the most important mineral discovery of the multi-metal nickel-cobalt-chromium bearing magnetite deposit of Phokpur was made by the Directorate of Geology and Mining (DGM), Nagaland during geological traverse in the Ophiolite belt of Pungro-Thonoknyu areas (Agrawal & Rao, 1971) of the then Tuensang district (now in Kiphire district of Nagaland). Later Bhowmick et al. (1973) along with DGM, Nagaland took geological traverses which was followed by detailed geological and topographical mapping (1:1000/2000) by Majumdar and Pandey (1974), and Majumdar and Prabhakar (1976). The strategy of the investigation to know the economic feasibility and delineate the potential block, GSI drilled 17 boreholes in the north block from 1977-79 and estimated the magnetite reserve of 1.83 MT. Further, DGM, Nagaland started drilling from 1979 to 1984 where four GPPH boreholes and 15 boreholes were completed. However, DGM had located two more smaller magnetite bands below the main magnetite body northeast of the north block (drilled by GSI 1977-79) and was mapped in 1:2000 scale (Sharma, 1983). Besides, 7 additional boreholes were drilled in 1987-88. A total reserve of 2.966 MT of magnetite ore was estimated in the south block.

Ravikumar and Prabhakar (1977), on the basis of their investigation, reported the magnetite to be nickel-cobalt bearing. Ghose (1980) discussed the occurrence of chromite and magnetite in the Naga Ophiolite Belt. Later Ravi Kumar and Prabhakar (1981) estimated the net probable reserve to be 1.83 million tonnes in the North block while Sharma (1983) of the Directorate of Geology & Mining, Nagaland indicated the reserve to be 1.62 million tonnes in the south block. Chattopadhyay et al. (1983) have studied the litho-assemblages, structures, metamorphism, etc. of the ophiolite suite. The Phokpur magnetite has been reported to occur as sheet like body over the cumulate sequence of the ophiolites. It has further been found that nickel is associated with this magnetite body which is composed mainly of magnetite, chromite and silicate matrix. Ghose (1980), Venkataramana et al. (1984 and 1986), Ghosh and Goswamy (1986), Chattopadhyay and Bhattacharya (1986), Venkataramana and Bhattacharya (1989), and Singh et al. (1989) have investigated the mode of occurrence, petrography, geochemistry and origin of chromite, magnetite, and Ni-bearing laterites associated with the Naga Ophiolite Belt.

Ghose (1980) proposed that the nickel-rich Phokpur magnetite, a rare occurrence in the ophiolite, have been formed by increased activity of water in ultramafic cumulate zone on layered sequence favouring formation of amphibole in association with ore. Ghosh and Goswamy (1986) suggested that the magnetite was released by replacement of chromite during serpentinization of host dunite. Chattopadhyay and Bhattacharya (1986) opined that the magnetite are part of the cumulate sequence and has been formed by crystal fractionation and gravitational settling. Venkataramana and Bhattacharya (1989) based on geochemical and petrographic evidence suggested that the magnetites from the Naga Ophiolite Belt were a late magmatic crystalline phase of a Mg-rich magma undergoing crystallization under high P_{O_2} . They further proposed that based on the mineralogical and geochemical evidences, Ni in the laterite was derived from olivines in the underlying peridotite during weathering processes and concentrated in the goethite phase. Singh et al. (1989) stated that chromite, Ni-rich magnetite and sulphides form important recognizable primary ore minerals associated with the Naga ophiolites. But only magnetite was concentrated to form a small recognizable ore deposit near Phokpur village. They further observed that chromite is marked by podiform and lensoid bodies, sometimes arranged sub-parallel order in the early cumulus dunite besides rarely found in the harzburgite in association with dunite. Nayak et al. (2010) reported high concentrations of Ni, Cr and Co in Phokpur magnetite.

The Phokpur magnetite deposit, whether truly evolved by the replacement of earlier formed chromite during serpentinization of host dunite under the influence of hydrothermal fluid activity or represent intrusive equivalents of the massive flow is the subject matter of the present research work.

1.10 Aims and Objectives of Present Work

Ophiolite rocks have evoked as much interest for exploration geologist as for tectonic geologists. These have proved potential sites for several minerals deposits. Consequently, ophiolites are being explored throughout the world for this mineral wealth. Similarly the mineral exploration in Naga Ophiolite Belt has been carried on since the last

few decades. The occurrence of metallic and non-metallic mineral deposits in association with the ophiolite recorded till date are high grade limestone/marble, magnetite, nickel, cobalt, chromite, prospects of base metals (sulphides: Cu-Fe-Mo), decorative building stones, etc. which have make this belt attractive for detailed study and exploration.

The discovery of the Ni-Co-Cr bearing magnetite in the Naga Ophiolite Belt assumes particular significance since India is totally dependent on imports with reference to metals like nickel and cobalt. The multi-metallic magnetite ore of Nagaland, being unique reserve in the world, is a boon to the people of Nagaland.

Nickel and cobalt are the strategic metals in our country. Therefore, even a small deposit of nickel and cobalt bears an utmost importance in the national economy.

Therefore, the proposed research work entitled “Study of magnetite mineralization associated with Naga Ophiolite belt at Phokpur in Kiphire district of Nagaland.” has been undertaken to study a detailed and unified picture of the evolution of the Phokpur magnetite with the following objectives:

- Preparation of Geological Map of the study area to appreciate the orientation and extension of the mineralized body.
- To know the petrogenesis history as well as geological conditions responsible for the evolution of the Phokpur magnetite ore body.

To fulfill the above given aims and objectives the following steps have been carried out systematically:

- **Literature Survey:** Survey of pertinent literatures will be undertaken in order to gather available information about the local and regional geology of the study area, as well as details about metallogeny associated with ophiolites.

- **Field Observations**

- (i) Identification of the various litho units of the study area.
- (ii) Measurement of data on orientation of various litho-units of the area.
- (iii) Sample collections including representative samples of each litho-units of the study area.
- (iv) To study the field relationship among the various litho-units of the study area.

- **Laboratory Work**

- (i) Preparation of geological map of the study area to appreciate the orientation and extension of various litho units.
- (ii) Cleaning, numbering and megascopic studies of the collected rock samples. Preparing of thin sections for microscopic studies.
- (iii) Microscopic Studies:
 - (a) Detailed petrography and modal mineralogy of each litho-unit of the study area.
 - (b) Selection of representative samples for bulk-rock chemistry and mineral chemistry on the basis of detailed petrography.
- (iv) Bulk–Rock Chemistry (major elements) of the representative samples of the magnetite ores.
- (v) Mineral Chemistry (EPMA) of some important ore samples selected on the basis of detail ore petrography.

GEOLOGICAL SETTING

2.1 Regional Geology and Tectonics

The Naga Ophiolite Belt (NOB), along Indo-Myanmar border, forms a part of the Naga - Arakan Yoma flysch trough of Late Mesozoic to Eocene age. This N-S to NNE - SSW trending narrow arcuate Ophiolite Belt of Nagaland and Manipur extends approximately for 200 km from northeast of Chokla (Noklak district) in Nagaland to south of Moreh in Manipur (Fig. 2.1). It continues further south in Indo-Myanmar range, Chin and Arakan-Yoma to Andaman and Nicobar Group of islands. In Nagaland, it extends over 90 km in length and with varying widths ranging from 2-15 km, occupying an area of about 1000 sq km. The Ophiolite have tectonic contacts on either side with evidence of their transport into and onto the Disang flysch in the west and, in turn, have been over-ridden in places, by Nimi Formation/ Naga Metamorphics of possible Mesozoic age (Ghose et al., 2014) from the east. The contact between Ophiolite suite/sequence and Disang formation is marked by shearing, brecciation and silicification with occasional development of tight to isoclinal folds. The ophiolite sequence is unconformably overlain by the immature, mainly ophiolite derived, shallow marine to paralic, volcanoclastic Phokpur Formation possibly homotaxial with Barail Group of rocks (Ghose et al., 2014) in other parts of the Naga Hills.

Naga Hills are characterised by multiple deformations and fracturing (Acharyya et al., 1990). Structural studies reveal that there are three generation of folding within the mafic-ultramafic and the sedimentary rocks. The first generation folds, trending generally in N-S direction, have low plunging isoclinal folds with steeply dipping axial planes. Ophiolite suite was probably emplaced during the waning stages of the first generation of folding. The second generation of folds trends NE-SW and are moderately tight to open type dipping at moderate angles towards east and west. The third generation folds are transverse to the trend of orogenic belt. They are broad, open type, having WNW-ESE trend with steeply dipping axial planes towards SW and NE.

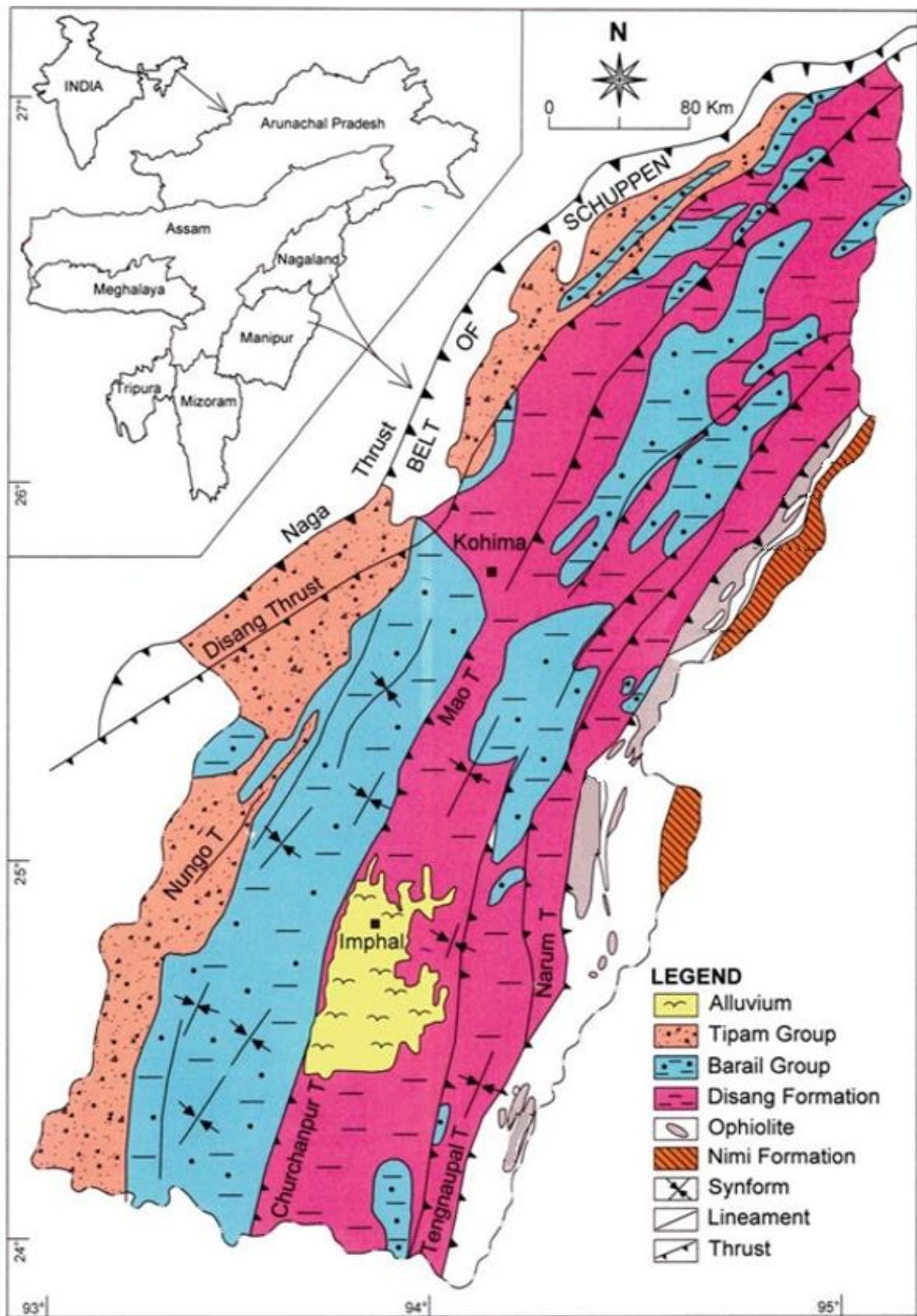


Fig.2.1 Simplified geological and tectonic map of Nagaland and Manipur states, India (modified after Ningthoujam et al., 2012; Ghose et al., 2014).

The studies of structural elements of the Ophiolite belt in Manipur show that the different tectonic slices of the Ophiolites are further modified by folding ((Acharyya et al., 1990; Sengupta, et al., 1987 and 1990)). These are mainly rootless bodies, which are repeated on the surface due to regional, open upright folds. The dips of the tectonic contacts of the Ophiolite are clearly visible in most of the exposures and are conformable with the dips in adjacent sediments. They have usually changing attitudes, compatible with the geometry of the major folds and appear like a multilayered stack of ophiolite slices on Disang group, co-folded with the Disang formation during a later deformation history. The macrofracture system includes mainly faults viz. longitudinal and transverse. The longitudinal faults trend NNE-SSW to NE-SW dipping towards east or west. They are mostly high angle reverse faults. The major transverse faults trend NW-SE, and are of wrench fault type. They account for the major off-set of the lithological makeup of the Ophiolite belt.

2.2 Stratigraphy

Geological setting of the Naga Ophiolite Belt is very complex with various constraints such as mountainous terrain, outcrops exposed close to the international boundary with Myanmar, lack of infrastructure, high monsoon rain, thick vegetation and soil cover and dismembered lithology. The salient geological features of different rock types in each tectono-stratigraphic group their inter-relationships are shown in Table 2.1 and the details are presented below.

2.2.1 Nimi Formation/ Naga Metamorphics

Nimi Formation (after its type locality at Nimi village) comprises of thick sequence of low-grade regionally metamorphosed rocks which crops out as a linear overthrust belt along the Indo-Myanmar border (Agrawal and Ghose, 1986). The rocks usually retain the relict sedimentary clastic texture which is totally obliterated in the Naga Metamorphics. The dominant rock units of this Formation are phyllite, feldspathic quartzite, marble, limestone, quartz-sericite schist. The Nimi Formation has not yielded any fossil remains as yet but they are lithologically and homotaxially similar to the Pansat beds (Brunnschweiler, 1966). He considered the Nimi Formation/ Naga Metamorphics as Pre-Mesozoic age.

2.2.2 The Ophiolite Suite

The Ophiolite suite occurs as a long arcuate linear belt between Nimi Formation in the east and Disang Flysch sediments in the west and unconformably overlain by Jopi Formation in Phek District and Phokpur Formation in Kiphire District. It represents the Nagaland Ophiolite Suite which extends about 90 km in length and 2-15 km in breadth. It comprises of highly dismembered litho-units represented by peridotites (tectonites), mafic-ultramafic cumulates, mafic-volcanics, meta-basics etc., mixed with rare dykes, minor felsic intrusive and oceanic sediments such as chert, greywacke, limestones. The ultramafics are the predominant rock type and exposed along the entire length of the ophiolite belt. Peridotite, dunite and pyroxenite are the main ultramafic rock-types. In most of the cases, these ultramafics are altered to serpentinites. The mafic cumulates are primarily a gabbroic complex and can be grouped into (i) low level gabbro displaying layering and (ii) high level gabbro exhibit-massive and rare banding. Cumulates are characterized by features like cyclic, cryptic or rhythmic layering with variation in the thickness of individual layers and grain size from bottom to top.

The ultramafics are interpreted as slices of oceanic crust and upper mantle obducted onto the continental margin. The ophiolite slices along with sub-ophiolitic blue-schists are emplaced within the Eocene-Oligocene sediments, possibly along an active continental margin (Acharyya, 2007). Chatterjee and Ghose (2010) indicated that the eclogites of Naga ophiolite formed near the top of the subducting crust during the convergence between India and Eurasia (Acharyya, 2007). From the fossil evidence of radiolarian assemblages in ophiolite chert (near Salumi), the age of Naga Ophiolite Belt (Ziphu Formation) has been assigned from Upper Jurassic to Eocene age (Baxter et al., 2011).

The Naga Ophiolite Belt contains economically important chromite and magnetite deposits with minor nickel and cobalt contents. The magnetite bodies are associated with the cumulate ultramafic rock. The magnetite bodies at Phokpur and Thongsongyu villages are the biggest magnetite deposits in the ophiolite. At Phor in Phek district of Nagaland, the magnetite/hematite deposit also occupies an extensive area compare to the other parts of the Naga Ophiolite Belt.

2.2.3 Disang Formation (Flysch)

It represents a folded sequence comprising slate (including graphitic slate), phyllite, siltstone and fine-grained sandstone, having thickness around 3000 m, exposed to west of the ophiolite suite. The rocks of the Disang Formation show NNW–SSE trending ridges and valleys with a rhythmic alternation of shale/slate and siltstone. Near the axial planes of folds and faults, the shale-siltstone rock sequence is replaced by phyllite and quartzite. The shallow water depositional structures like ripple marks, sole marks and cross bedding are the common features of the rocks, but at places graded bedding are also present (Agrawal and Ghose 1986; Ghose et al., 2014).

The Disang sediments exhibit tight folds, drags and multi-generation quartz veins close to contact of the ophiolite. These, together with the occurrence of tectonic slivers of serpentinites and its intermixing with sediments (Vidyadharan et al., 1986), give unequivocal evidence of their emplacement along the deep fractures of basin/continental margin. Despite their large thickness, fossils are rare in the Disang sediments. A limited number of bivalves, gastropods and foraminifera are reported that suggests an Upper Cretaceous-Eocene age of their deposition (Acharyya et al., 1986).

Molluscan biozones in the Disang sediments from Manipur reflect an age of Paleocene to Upper Eocene (Lukram and Kachhara 2010). The turbidite sequences of the Disang Formation grade into coarse shallow marine to fluviatile sediments represented by conglomerate, grit, sandstone and coal streaks of overlying Barail Group. The Disang and Barail sediments were deposited in the distal shelf and on the continental margin, respectively, in an epicontinental sea (Vidyadharan et al., 1989).

2.2.4 Jopi/ Phokphur Formation

Jopi Formation is a young and immature sedimentary litho-sequence unconformably overlying the ophiolites at different topographic levels. It comprises of thick pile of alternating and repeated sequence of polymictic conglomerate-grit-pebbly and cobbly sandstone, sub-greywacke and shale. The conglomerate, forming the basal horizon, contains angular to sub-rounded boulders, cobbles and pebbles of mafic and ultramafic rocks embedded in a reworked tuffaceous to siliceous cement. The succession grades upward into grit, lithic greywacke, siltstone, sandstone and shale. The plant fossils reported from the sequence suggest them to be of Late Eocene –

Oligocene age and could be possibly homotaxial with Barail Group of rocks in the western part of Naga Hills (Chattopadhyay et al., 1983; Ghose et al., 2014).

The Jopi Formation, near Phokpur, is known as Phokphur Formation (Miocene-Pliocene) by the Geological Survey of India (Vidyadharan et al., 1986, Singh et al., 1989). Phokphur Formation is a thick sequence of tuffs and agglomerates inter-layered in volcanic and volcanoclastic sediments, exposed infolded with the ophiolites in the Phokpur Section. The sequence comprises of red, green, massive tuffs, tuffaceous shales and agglomerates. The agglomerates contain fragments of various metamorphic rocks and volcanic bombs of basaltic compositions. These volcanogenic sediments are quite distinct from the sequence of conglomerates, sandstones and shales in Phokpur section.

2.2.5 Alluvium/Laterites

Thin, isolated and scattered laterite cappings are preserved in favourable locations over both the metamorphic and cumulate ultramafics in the area (Phor and Sutsu). High level terrace deposits composed of boulder-conglomerate and sand (Tizu River).

The litho-stratigraphy succession of east part of Nagaland (NHO) (modified after Agrawal and Ghose (1986) and Ghose et al. (2014) is shown in Table 2.1.

Table 2.1: Lithostratigraphic Succession of Eastern part of Nagaland (modified after Agrawal and Ghose, 1986; Ghose et al., 2014)

Age	Formation	Lithology
Recent to sub-recent	Alluvium and high level terraces	Laterites and alluvium
Miocene-Pliocene	Jopi/Phokphur Formation (Homotaxial to Barail)	Ophiolite derived younger sedimentary cover of repeated sequence of polymictic conglomerates, grits, sub- greywacke, sandstone and tuffaceous shale.
-----unconformity-----		
Late Cretaceous	Disang Flysch	Disang Flysch
	Ophiolite Complex	Ophiolite Complex
	Tectonic contact	
to		
Eocene		
-----Tectonic contact-----		
Mesozoic?	Nimi formation /Naga Metamorphics	phyllite, schist, limestone and Quartzite with occasional serpentinite intrusion.

2.3 Mineralisations in Naga Ophiolite Belt

In Naga Ophiolite Belt, broadly two distinct metallogenic events can be envisaged: (i) an earlier Late Cretaceous to Eocene pre-orogenic syngenetic podiform chromite deposit (with traces of Ni, Co, Au and PGE) in cumulate peridotite and serpentinite, and a later (ii) Late Palaeogene syn- to late-orogenic, syngenetic to epigenetic disseminated and vein-type copper-molybdenum sulfides associated with mafic volcanics/ late felsic intrusives. In addition, serpentinitisation and metasomatism (secondary processes) have also resulted in the formation of Ni-Co-Cr-bearing magnetite deposits (Agrawal and Ghose, 1989; Ghose et al., 2014). Occurrence of these mineralisations is shown in Fig.2.2.

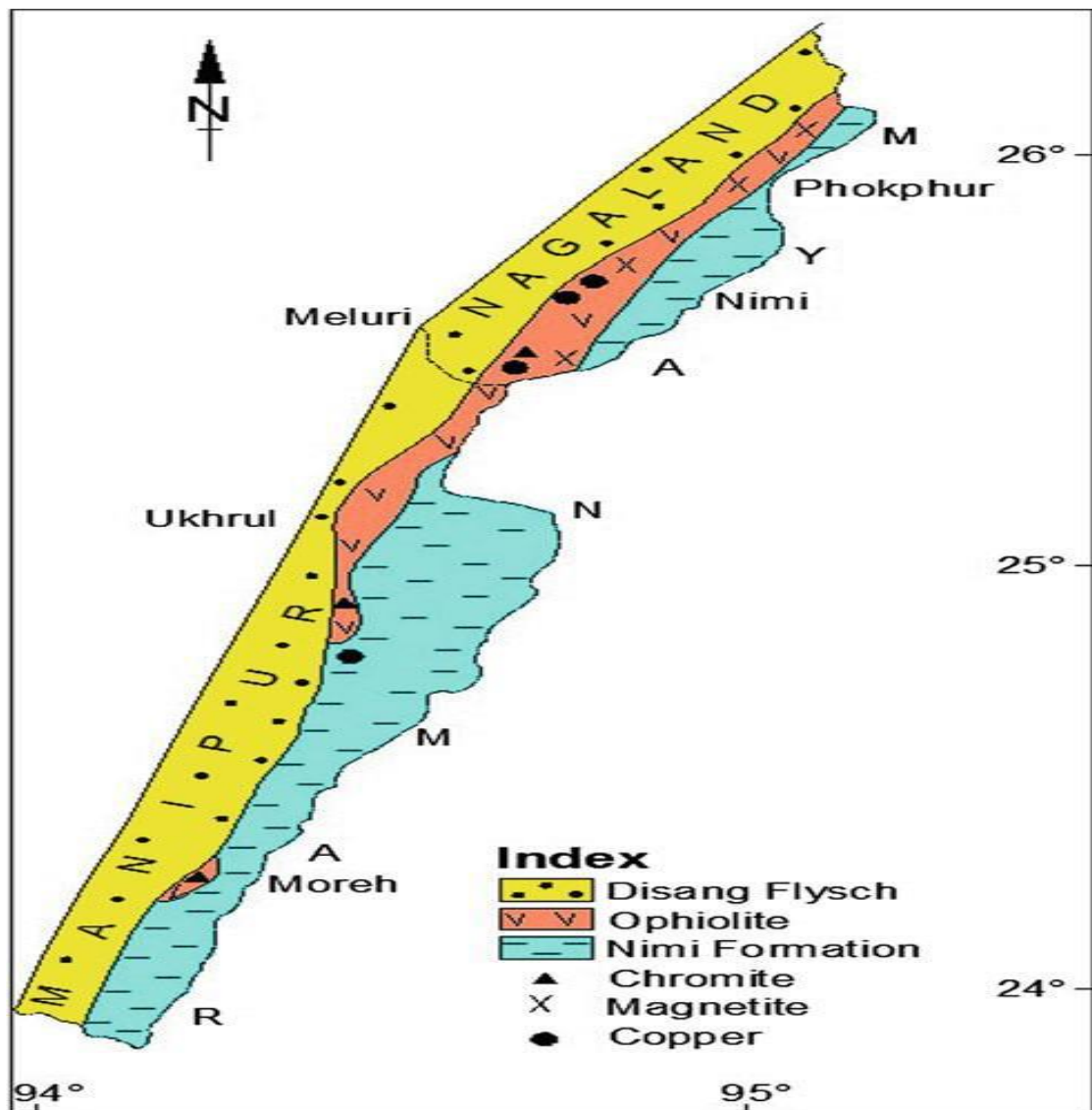


Fig. 2.2: Naga-Manipur Ophiolite Belt showing occurrence of chromite, nickeliferous magnetite and base metals (Ghose et al., 2014)

The formation of minor talc, steatite, magnesite, brucite and chrysolite asbestos may also be related to this metallogenic phase. Development of localized gossans and minor laterite including nickeliferous soil profile over the ultramafics could be associated with some Tertiary metallogenic episode though its development is insignificant. Several occurrences of magnetite are recorded in Naga Hills Ophiolite, however it is restricted to Nagaland, and more chromite deposits occur in Manipur side of the Ophiolite. Brief descriptions of the number of metallogenic events recorded in the Naga ophiolite belt by various workers (Agrawal and Rao, 1971 and 1972; Ghose, 1980; Singh and Ghose, 1981; Venkataramana et al., 1984; Ghose and Shrivastava, 1986; Venkataramana and Bhattacharya, 1989) are given below.

2.3.1 Chromite

Though there is occurrence of chromite in the Naga Ophiolite Belt, extensive exploration has not been undertaken. The places where chromites have been reported are Satuza, Reguri, Ziphu, Molen, Laluri, Washello, Phor in Phek district, and Wui, Kenjong in Noklak district. The chromite occurs as:

- (i) Minor disseminations of chromite within tectonized peridotite and cumulate ultramafics
- (ii) As chromitite in form of segregated lenses, pods, tabular slices and lenticular bodies usually within tectonized peridotite

(i) Disseminated chromite: Accessory chromite, which forms about 5% by volume in the tectonized peridotite, occurs as fractured anhedral and elongated grain with corroded grain margin between serpentinized olivine and bastitised pyroxene grains. Occasionally they occur as inclusion within serpentinized olivine. At places the chromite grains are stretched and fractured; the fracture plane being filled by serpentine and talc. In the cumulate ultramafics accessory chromite occurs as subhedral to euhedral grains in the olivine and pyroxene grain boundaries.

(ii) Chromitite: Chromite bodies with 60-90% chromites and rest serpentine occur as lenses, pods, tabular slices and lenticular bodies of restricted lateral extent within tectonized peridotite. These bodies vary in length from 1m to over 5m and in width from 1 to 3m. The chromite bodies generally have steep dips, 70-90° and plunge 15 to 20° toward north or south. The contact between the ore bodies and the enclosing host

rock is sharp and often highly sheared. At places chromite is polished smooth and marked by slickenside, which suggest their emplacement in solid state. The chromite bodies are classified into three types:

- (a) **Massive ore bodies:** Massive chromitite occur as pods, lenses and streaks with serpentized dunite and harzburgite and comprised up to 90% of interlocked anhedral chromite and serpentine. Under reflected light the rock comprises of anhedral to subhedral chromite grains, which at places are highly fractured and granulated. Chromites rarely occur as idiomorphic grains within a silicate gangue of serpentine. At places chromite grains show annealing texture. Deposits of these types occur in Reguri, Laluri, Washello, Ziphu, Satuza.
- (b) **Granular ore:** Granular chromitite occurs as lensoid masses within serpentized harzburgite. The coarse grained rock comprises between 50 to 80% coarse granular chromite forming a net-texture, the inner-granular space being occupied by serpentized olivine and bastitised pyroxene. Rarely, they show orbicular texture in which oval shape clots of serpentine are surrounded by beads of granular chromite. Granular ore occur in Molen.
- (c) **Nodular ores:** Nodular ores occur as lensoid and lobular bodies within serpentized harzburgite and comprises of sub rounded to ellipsoidal masses rich in chromite embedded in serpentinite matrix. The individual nodule varies in size from 10mm to 20mm across and is either separated from one another or juxtaposed. At places the nodules are deformed and have an incipient alignment of their long axis. Nodular ores occur in Reguri.

2.3.2 Magnetite

In addition to the Phokpur magnetite deposit (the study area) in Kiphire district (described later), a number of small iron incidences have also been reported in Phek district of Nagaland (Agrawal and Rao, 1978; Ghose, 1980; Chattopadhyay and Bhattacharya, 1986; Ghose and Goswami, 1986; Agrawal and Ghose, 1989; Venkataramana and Bhattacharya, 1989; Singh et al. 1989; DGM-Nagaland, 2015). A brief introduction on the occurrence and geology of these small iron incidences located at various parts of the Naga Ophiolite Belt is given below:

(a) Phor Hematite Mineralization, Phek District

Phor hematite/ magnetite deposit is situated at 7 km south of Phor village along Phor-Laluri Mineral Road junction. It is connected by Mineral Road and can be found in the toposheet No. 83 K/14 with co-ordinates N25°43'38.9" and E94°49'04".

The geology of the area consists of spillite and ultramafic rocks. The magnetite rock extends from north toward south for about 120 m. The deposit is divided by approached road in the middle. The north block is associated with volcanic and the south block is associated with ultramafics. The volcanic are hard, compact and massive and brownish to greenish in colour. The attitude of the volcanic shows N20°W dipping toward south. The ultramafics are altered, sheared and crushed into fragments. The ultramafic rocks also show the presence of platinum group of metals mineralisations.

(b) Reguri Chromatic-Magnetite Deposit, Phek District

The village is located in the toposheet No. 83 K/10 with coordinates N25°32'11.3" and E94°39'34". The chrome-magnetite mineralization in the Govt. middle school area is dark grey to dark brown in colour covering an area of about 200 sq m. The deposit is epigenetic in origin as the minerals are formed due to concentration and segregations of chrome-magnetite in the altered ultramafic rocks.

The rocks comprises of ophiolite suite of rocks such as mafic, ultramafics, serpentinite, quartzite, limestone shale and sandstone. The ultramafic is the dominant rock type but are highly sheared, fractured and altered to serpentinite ultramafics. The deposit in this area may be for academic interest and do not show any prospect of exploration.

(c) Thewati Deposit, Phek District

Thewati is situated 75 km east of Waziho village in Phek district and accessible by Mineral Road. The village is located in the toposheet No. 83 K/14 with coordinates N25°31'51.4" and E94° 46'49.8". The village is situated geologically on the ultramafic terrain.

The rocks of the area comprises of ophiolite suite of rocks such as mafic, ultramafics, serpentinite, blue schist, quartzite and Jopi Formation sandstone.

The ultramafics constitute the dominant rock types of the area. They are highly sheared, fractured and altered to serpentinitised ultramafics and the persisted olivine nodules in the weathered ultramafics spread in the surrounding area. The ultramafics occupied at the bottom and quartzite covers from the village area to the Molen Post. The area around 3 km south-east of Thewati village is covered with quartzite rocks, where transported boulders and pebbles of chromite and hematite are found.

Mafic rocks of green brown and altered types are found at 2 km east of Thewati village. Mafic rocks of normal basalt are found at the base and brownish altered at the top. Multi-metals of Cu (malachite), Fe (magnetite/hematite), Cr (chromite) etc. are found as disseminated grains in the basalt usually in fracture veins and rings of pillows.

(d) Washelo Deposit, Phek District

Float ores of small to large dimension of magnetite are seen NNE of Washelo village which are scattered at the contact of cumulate ultramafics and overlying sedimentary cover. No in-situ exposure could be located. Chrome-magnetite is also reported in SW of Washelo, NW of Washelo and Metsidi area. It occurs as floats deposit.

(e) Hematite Deposit at S.P. Camp, Phek District

The hematite incidences are found at 300 m east of S.P. Camp and about 7 km east of Thewati village showing the coordinates of N25°29'47.5" and E94°46'05". The hematite is cherry red in colour, hard and high sp. gravity. The hematite occurs within the quartzite below the conglomerate of the Jopi Formation. The hematite incidences trend almost parallel to the Jopi Formation. It is exposed for about 10 m along foot-track, and further it appeared as gone inside the hill.

Hematite boulders also occur in Ghoos camp area, 3 km away from SP camp, on the way to Molhe Pass. It is located at coordinates 25°29'46.0" and 94°46'03.3". The hematite boulders intermittently continue to the east of Methapani nallah. The trend of Methapani nallah is N-S. Another hematite bodies are exposed near the foot track to Molhe pass. Its location is N25°29'46.4" and E94°45'05.8".

(f) Molen Post, Phek District

Molen Post is located at the international boundary of India (Nagaland) and Myanmar with coordinates N25°28'53.2" and E94°46'22.2". The area is occupied by quartzitic and ultramafic rocks with incidences of multi-metal mineralisations like chrome-magnetite, hematite, copper and cobalt etc. Floats of chromatic-magnetite are also found in the area. The tectonic activities in the area can be seen at the Molen Post where the plate movements took place. Here the ophiolite formation is prominently overlain by the sediments of Jopi Formation.

(g) Zee-lake/T-lake, Phek District

The Z-lake is located on the top of the international boundary of India (Nagaland) and Myanmar having the coordinates N25°28'34" and E94°47'06". The place is also a good site for geo-tourism spot. The lake is covered with ice almost throughout the year. Geologically, the lake is lying on the quartzite rock. Chrome-magnetite, hematite etc., occurring as segregated minerals, are found within the ultramafic rocks. The main rock type is quartzite. Dunite is also found about 600 m south of Zee-lake.

(h) Molen Village, Phek District

Molen is a small village in Phek district. The village is known for rich mineral resources like limestone, semi-precious stone, dimensional stones and chrome-magnetite etc. The village is located at the contact of the ophiolite and sedimentary rocks. The ophiolite rocks consist of basalt, pillow basalt, spillite basalt, chert, ultramafics, serpentinite and limestone. Basaltic rocks are brownish to yellowish brown in colour and weathered and altered at places. The ultramafic rock occupied a big area covering an area of about 4-5 sq km extending from 4 km west of the village to 3 km east of the village along the foot-tract of Waziho-Molen and foot-path from Molen village to the field.

2.3.3 Sulphide Mineralisation

A number of syngenetic sulphide minerals incidences occur with the cherts, volcanics, occasionally with serpentinite, gabbro, igneous breccia and late felsic intrusives almost throughout the ophiolite belt (Fig. 2.2). Iron and copper-bearing sulfides, for examples, pyrite, chalcopyrite, chalcocite, bornite, arsenopyrite and

sphalerite together with azurite and malachite (the copper carbonates) are commonly observed as veins, disseminations and fracture filling. Fe-Mn oxides (hematite, goethite and pyrolusite) and quartz are usually observed in gossan (Ghosh and Goswami 1986; Agrawal and Ghose, 1989). They are synchronous with the formation of mafics/ultramafics of the ophiolite belt and formed due to interaction of basalt and sea water at the accretionary ridge of the ocean crust.

The late felsic intrusion (I-type granite) was responsible for the second phase of disseminated and vein-type copper-molybdenum sulphide epigenetic mineralisation during collision/ post-collision period. This was caused by concentration of copper and molybdenum during their migration of the hydrothermal fluids through pre-existing fractures and shear zones in the volcanics. The felsic intrusion originated in the contact aureole of a spreading centre by the partial melting of oceanic basalt (Ghose and Chatterjee, 2011).

2.3.4 Laterites

Thin cappings of isolated and scattered laterites are developed usually at undissected topography and gentle slope over serpentinised peridotites and cumulate ultramafics under favourable warm and dry climate between elevations of 1200 and 1800 m (Agrawal and Ghose, 1989). They comprises mainly of goethite or garnierite with high Ni contents (Ghosh and Goswami 1986). The best preserved sections of laterite are exposed between Purr and Sutsu on the southern side of the Tizu River. They are up to 10 sq m in size with thickness ranging between 3 cm and <2 m. These laterite profiles are divided into four zones from bottom to top: (i) bed rock, (ii) granular goethite-limonite zone, (iii) pisolitic goethite and cryptocrystalline quartz zone, and (d) top soil (5-20 cm) with laterite granules (Venkataramana et al., 1986).

2.3.5 Late Felsic Intrusives/Late Tertiary Granitoids

Minor intrusions of felsic/ granitoids composition and variable thickness cut through the cumulate sequences and the volcanics (Fig. 2.3) of the Naga Ophiolite Belt (Ghose and Chatterjee 2011). Mineralogically, they vary in composition from quartz porphyry to granite and granodiorite. These late granitic rocks are distinguished from the plagiogranites of layered cumulates by the abundance of modal quartz and presence of potash feldspar. These late felsic granitoids were emplaced and controlled by two

macro-fractures, trending N–S to NE–SW and E–W in the central part of Naga Ophiolite Belt. The copper-molybdenum mineralisation in Zipu and Lacham are found to be associated with these late intrusives.

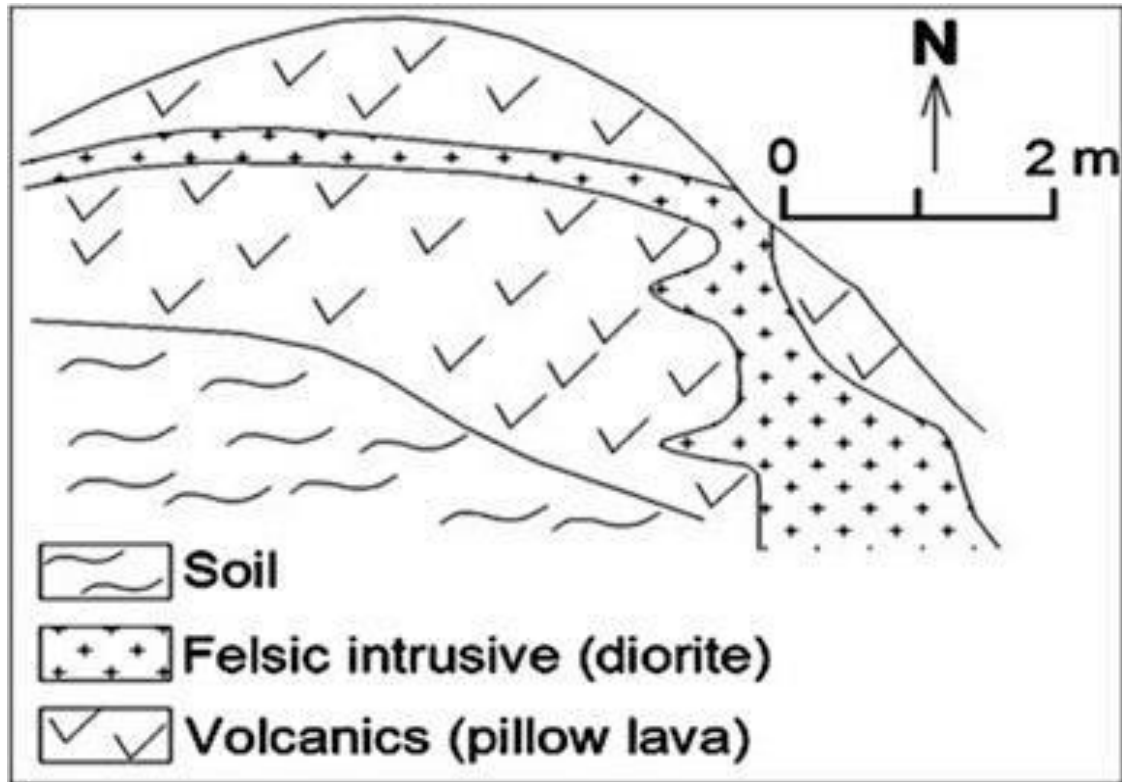


Fig. 2.3: Schematic diagram showing the late felsic granite cut-across pillow lava at Salumi in Kiphire district of Nagaland (Ghose et al., 2014).

2.4 Geology of the Study Area

The rocks of the ophiolite belt of the study area occur as steeply dipping tectonic slices, and are brought in juxtaposition against the sediments of the Disang Group. Within the ophiolite belt, various members occur as faulted slices. They are not preserved in sequential order and are highly dismembered. The meta-ultramafites show tectonic fabrics defined by parallelism of serpentine grains. Planar structure in the meta-volcanics is defined by parallel alignment of amphibole, chlorite and epidote. Variable trends are seen in these secondary planar structures and the layering in the associated cumulates. Slices of the ophiolites of varying dimensions are arranged in NE-SW to N-S trending en-echelon patterns with parallel to sub-parallel tectonic interrelation. The salient features of the main rock types of the study area are as follows (Ghose and Goswami, 1986):

The host rock of the Phokpur magnetite deposit is a serpentinitised dunite composed mainly of olivine with a subordinate amount of chromite and hypersthene. The olivine is usually traversed by anastomosing veinlets of antigorite and lizardite. Fine/ dusty grains of secondary magnetite are frequently observed within the olivine. The secondary magnetites are also developed along fractures and grains boundaries of chromite. The serpentinitised dunite grades into a compact laminated serpentinite mass interspersed with fine/ dusty grains of magnetite. They further grade into the bands of magnetite ore.

The magnetite ore forms thin bandings alternately comprised of (a) coarse magnetite with patches of relict chromite, (b) fine skeletal grains of magnetite within silicate matrix disseminated with corroded chromite grains, and (c) silicate matrix with diffused chromite grains characterized by reaction rims of ferrochromite. The relics of primary layering of the parent rock is reflected by the gross linear arrangement of chromite grains as well as the development of magnetite along to such laminations. The silicate matrix includes aggregates and flakes mainly of antigorite and lizardite with minor brownish yellow bowlingite and patches of green garnierite.

2.4.1 Phokpur Magnetite Deposit

The best studied magnetite ore body in the Naga Ophiolite Belt is located 4 km east of Phokpur village occur in the form of sheet-like magnetite body. The strike length of the Phokpur magnetite body is about 1 km along NNE-SSW to N-S direction with a 30° to 40° westerly dip (Plate II, Fig.1). The Phokpur magnetite body, the largest among other magnetite occurrences, in the Naga ophiolite belt is exposed along the inner rim of a broad synformal structure (Molhe-Jopi-Zipu-Phokphur ridge) forming the basin floor of an unconformably overlying Mio-Pliocene younger paralic sediments (Jopi/Phokphur Formation) concealing the magnetite bodies beneath them. The ore is usually hard, massive, compact, and jointed (Plate II, Fig. 2 and Plate III, Fig. 1). At places, the ore is highly fractured/ fragmented (Plate III, Fig. 2) showing cataclastic effects (Majumdar and Prabhakar, 1975; Sen et al.1979; Agrawal and Ghose, 1989; Singh et al., 1989). The geological map of the study area is shown in figure 2.4.

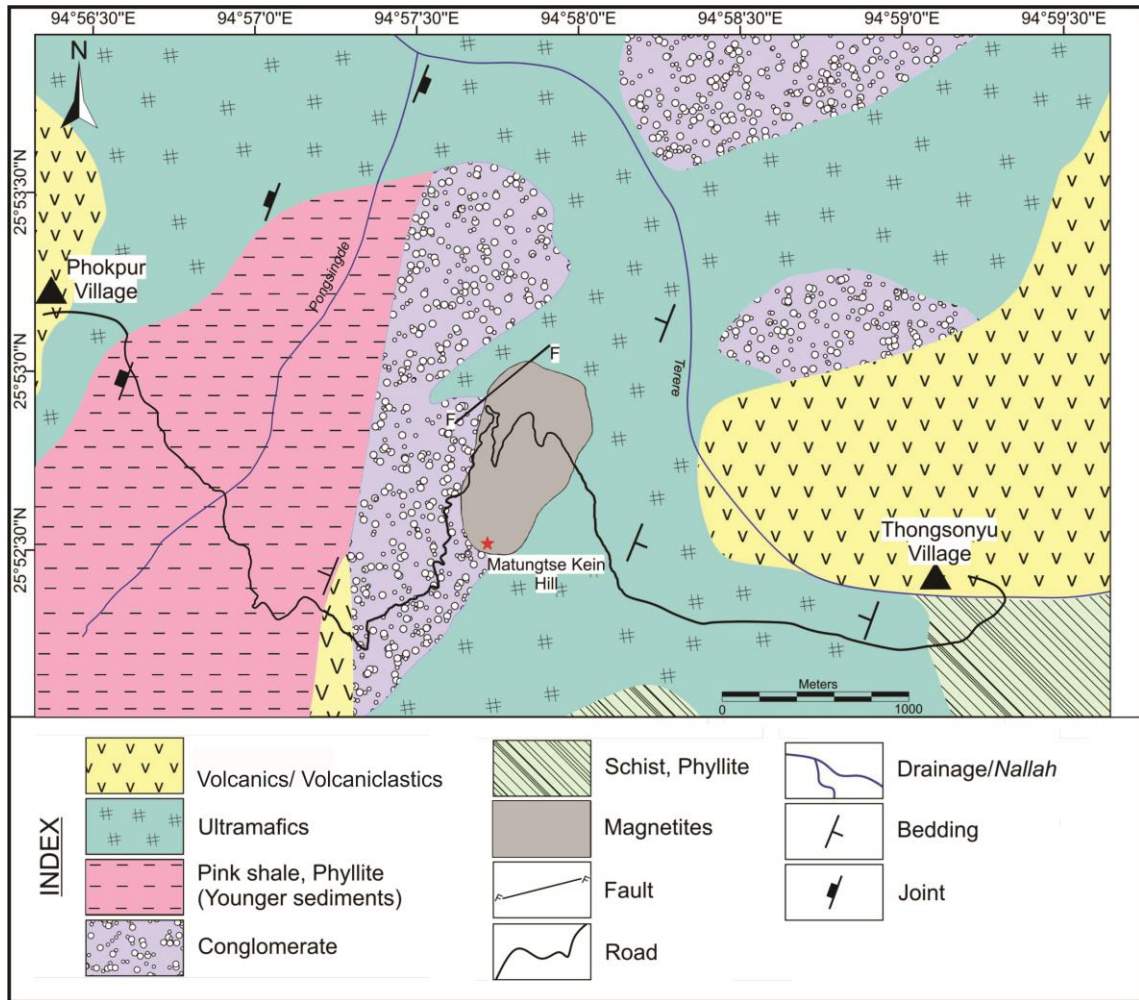


Fig. 2.4: Geological map of the Phokpur magnetite deposit

The thickness of the ore body varies from 5 to 15 m and usually thins out towards the south. The average thickness of the ore body is about 8 m with an average outcrop width of about 300 m. From the hilltop, the magnetite band extends down to a maximum inclined distance of about 600 m with ground slope 30° west. The ore body in general show swelling and pinching both along the strike and dip direction. Slickensides and groove lineation present in the synformal warp of magnetite suggesting scale sliding. (Agrawal and Rao, 1972 and 1978; Bhowmick et al., 1973; Majumdar et al., 1976; Venkataramana and Bhattacharya, 1989). It is underlain by cumulate ultramafic basement of serpentinised dunite and pyroxenite (Fig. 2.5). The contact is generally sharp and at places gradational being marked by gradual decrease in magnetite content from the underlying ultramafics (Chattopadhyay and Bhattacharyya, 1986). At places it is observed that serpentinised dunite with magnetite

disseminations grade into bands of magnetite ore (Ghosh and Goswami, 1986). A thin layer of chromite with inter-granular magnetite (up to 1.0 cm in thickness) also occurs at the base of the magnetite layer (Fig. 2.6, Ghose et al., 2014).

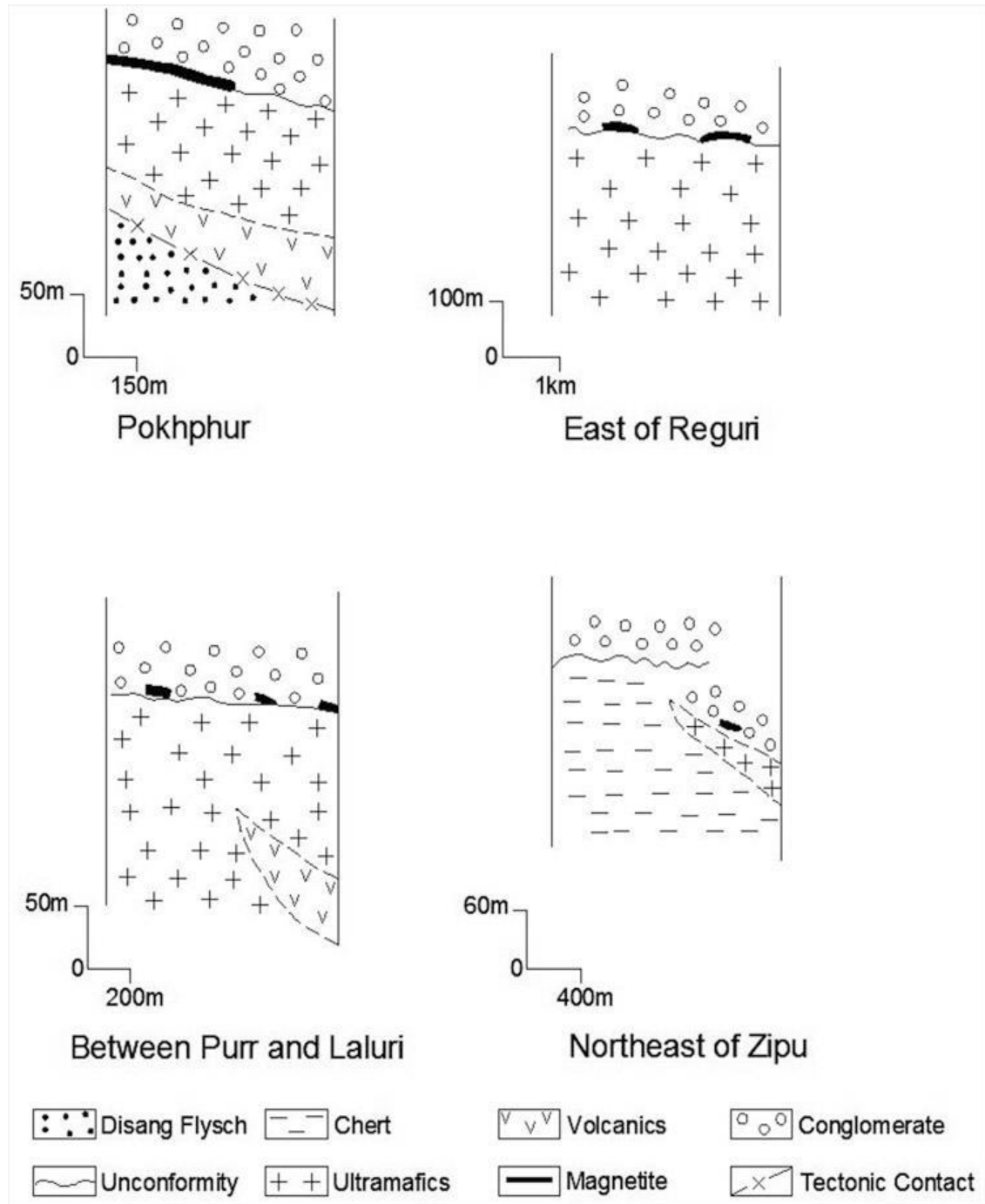


Fig.2.5: Schematic diagrams showing occurrence of nickeliferous magnetite in the Naga ophiolite belt (Ghose et al., 2014)

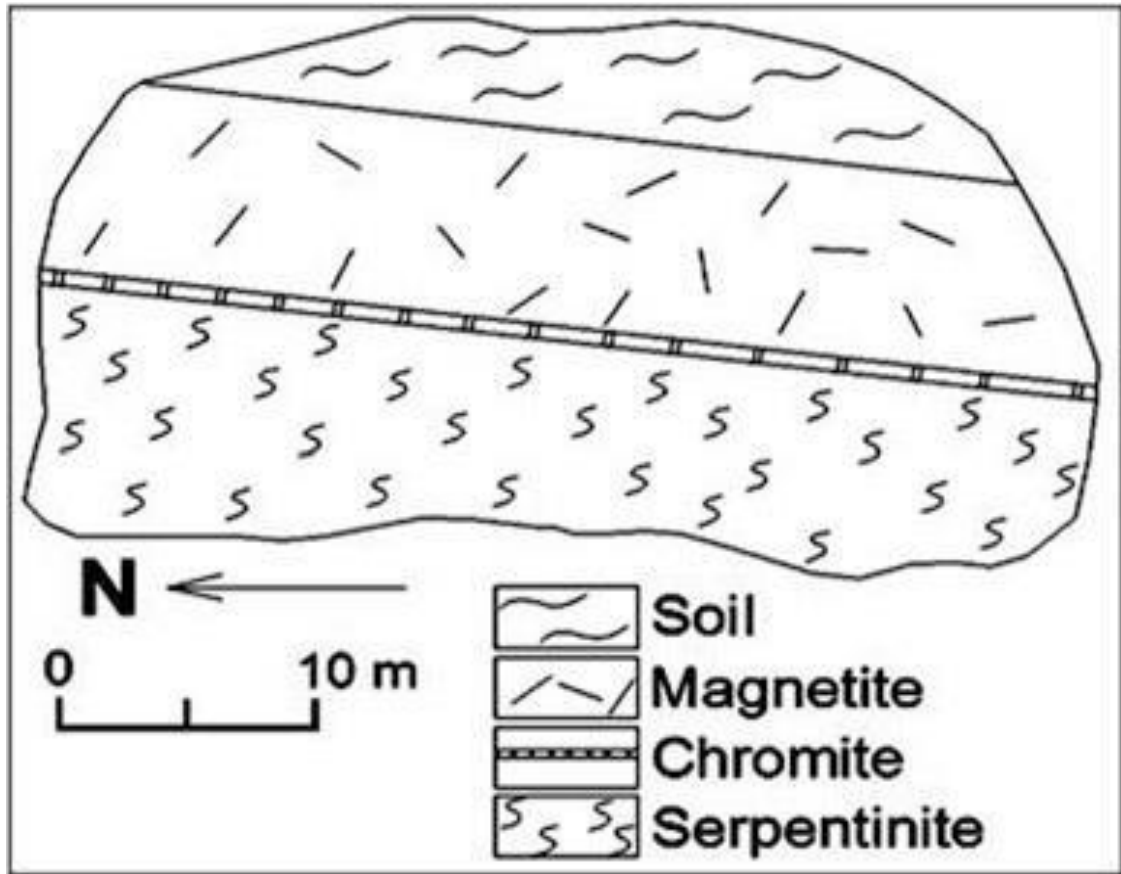


Fig.2.6: Lamination of chromite with inter-granular magnetite in nickeliferous magnetite at Matungsekien Ridge, Phokpur magnetite deposit (Ghose et al., 2014)

2.5 Traverses and Sample Collections

The geological field work of the study area of Phokpur magnetite deposit was carried out to understand the ore and host rock relationship as well as to collect the representative samples of the magnetite for their ore petrography, ore geochemistry and mineral chemistry. The locations of collected and studied ore samples along the planned traverses are shown in Fig. 2.7.

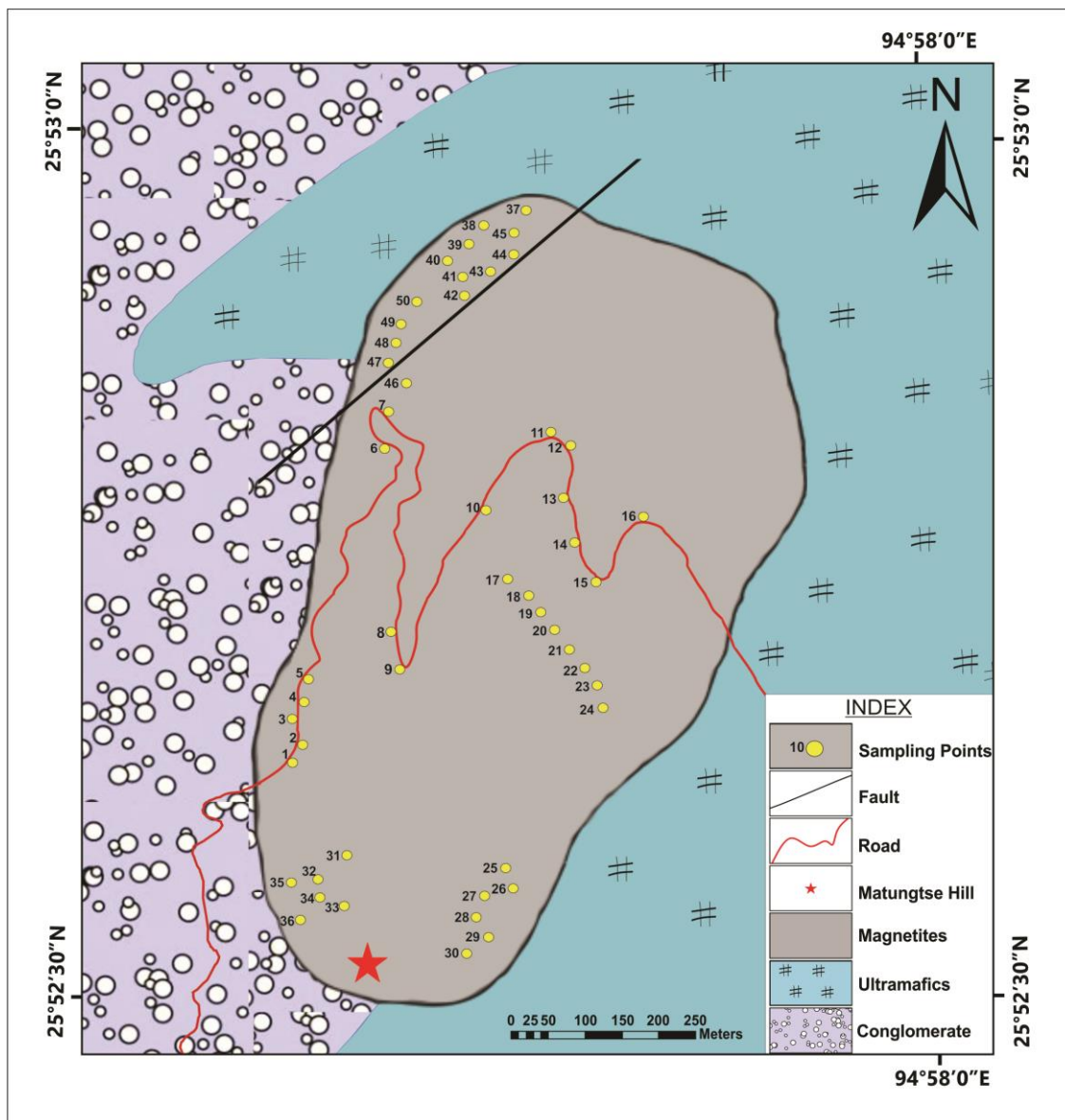


Fig. 2.7: Geological map showing the locations of collected ore samples.

METHODOLOGY AND INSTRUMENTATION TECHNIQUES

In the present study, various field and laboratory techniques have been employed to decipher the physico-chemical conditions and tectono-magmatic processes responsible for the formation of Phokpur magnetite deposit. The methodology and instrumentation techniques used are described in this chapter. However, the details of advanced petrological and geochemical methods are described in relevant chapters.

3.1 Literature Survey

A survey of the pertinent literatures including study of existing field reports and maps, published works in the national and international journals of repute has been carried out in order to study the available information about the local and regional geology of the study area as well as total geological environments responsible for the formation of magnetite deposits associated with subduction-obduction/collision tectonic regime. This includes a coherent understanding of all the events (mineralogical, tectonic and geochemical) involved in the evolution of magnetite deposits in different tectonic settings.

3.2 Geological Field Work

Geology is a field science, and therefore geological field work is inevitable for carrying out research in the field of geology. During the course of the present research work, three phases of geological field work were carried out. The first phase of the field work was carried out during 5th to 18th April 2015. During this phase, fifty representative ore samples were collected for laboratory investigation. The second phase of the field work was carried out during 20th to 24th November 2017 along with the supervisor Prof. Santosh Kumar Singh for verification of the first phase of geological field work as well as further collection of ore samples. The third and final phase of field work was carried out during 7th to 11th November 2018 to delineate the magnetite ore body and other lithological units on the geological map of the study area.

During the geological field works, traverses were made along and across the road cutting of the Phokpur magnetite deposit. The path of traverse and sample location area was traced and marked through GPS. Field data were collected with the help of traditional geological tools (toposheet of the study area, Brunton compass, hand lens, measuring tape, hammer and note book etc.) Field photographs of the important geological features observed at various locations of the study area were also taken for documentation.

3.3 Laboratory Work

The laboratory works adopted in the present study include:

- (i) Megascopic study of the collected ore samples and selection of samples for their petrographic studies.
- (ii) Preparation of polished thin sections of the selected ore samples of the study area.
- (iii) Detailed petrography (ore microscopy) of the prepared polished ore thin sections.
- (iv) Selection of the representative samples for the bulk ore chemistry and electron probe micro analysis on the basis of detailed petrography.
- (v) Preparation of powders of the 10 selected bulk magnetite ore samples for their geochemical (radical) analyses.

The polished thin sections of the representative samples of the Phokpur magnetite ores were prepared at the Department of Geology, Presidency University, Kolkata as well as at the Department of Geology, Nagaland University, Kohima Campus Meriema. The chemical analyses of 10 magnetite ore powder samples were carried out at MER Division of the CSIR - National Metallurgical Laboratory, Jamshedpur for estimation of Fe radical by NML/ANC/Fe-Ore-1 method, and Cr, Ni, Co, Ti, V radicals by using Inductively Coupled Plasma - Optical Emission Spectroscopy (ICP-OES) instrumentation technique. Further, the Electron Probe Micro-Analyses (EPMA) of 400 points of the important ore minerals/ silicate minerals present in the 4 selected polished thin sections of Phokpur magnetite ore samples were carried out at the EPMA Laboratory of the Department of Geology, Banaras Hindu University, Varanasi to measure their elemental concentration in oxide forms. It is a versatile tool for geological material and can be utilized for identification of a particular mineral phase as well as to make out the quantitative difference in composition from the core to rim in a minute grain.

3.3.1 Preparation of polished thin sections

Standard polished thin section of the magnetite ore samples were prepared for EPMA analysis. Thin polished section should be of 45 mm in length, 25 mm in width and 1 mm thick. It should be epoxy mounted. The solid blocks should be 25 mm in diameter (inner circle) and should not be more than 15 mm thick. It must be perfectly mounted either in Bakelite or in PVC. After finishing with 1000 mesh carborundum powder, polishing is started with chrome oxide for about 30 minutes.

During polishing, sample is checked intermittently. The sample is then polished with 6-micron diamond paste for 20 minutes followed by polishing with a 3-micron diamond paste for 20 minutes and 1-micron diamond paste for another 20 minutes. The sample is finally polished with ¼ micron diamond paste for 5 minutes. It must be noted that after each stage of polishing the slide, it is washed thoroughly using a separate cloth for each stage.

3.3.2 Preparation of powdered samples

The sequence for powdering of ore samples for chemical analysis is given below:

1. Coarse grained fractions of < 1 mm size are obtained from each ore sample by hammering in a steel mortar.
2. The coarse powder is then homogenized by coning-quartering method of bulk sample; about 200 gm of sample is separated for analysis.
3. The separated sample is grinded by using pulveriser until a smooth powdery feel (200 mesh) is attained.
4. The powder sample is further coned and quartered by choosing the required amount in gram.
5. Finally, 20 g of each powdered sample is weighed using an electronic balance for sending them to National Metallurgical Laboratory, Jamshedpur for their chemical analyses.

While preparing the powder samples, precaution was taken as much as possible to avoid contamination after processing each successive sample. After every sample is crushed and grinded, the steel and agate mortar is thoroughly cleaned by isopropyl alcohol.

3.4 Analytical Methods

3.4.1 Optical studies

Polished ore thin sections of 20 magnetite ore samples were prepared and optical studies were carried out at the Department of Geology, Nagaland University using a Leica (Leitz) DM LP HC Research Polarizing Microscope (TL & RL). Detailed petrographic properties of each ore minerals and their textural relationships etc. were studied under reflected light microscopy depending upon the objectives of the study. Reaction textures and zoning provide useful information on the petrogenesis and evolution of ore/ rock bodies. Therefore, textural features of petrogenetic significance from the selected polished ore thin sections were photographed. Unidentified phases, zoned grains, accessory minerals and minute inclusions were carefully studied and marked for EPMA analysis. Modal mineral analyses of the ten representative polished ore thin sections were also carried out by visual interpretation.

3.4.2 Inductively coupled plasma - Optical Emission Spectroscopy (ICP-OES)

It is an analytical technique used to determine the trace elements in a sample. It involves the principle that the atoms and ions can absorb energy to move electrons from the ground state to an excited state. In this method, the source of that energy is heat from argon plasma that operates at 10,000 Kelvin.

As an electron returns from a higher energy level to a lower energy level (usually the ground state) it emits light of a very specific wavelength. The type of atom or ion, and the energy levels the electron is moving between, determines the wavelength of the emitted light. The amount of light released at each wavelength is proportional to the number of atoms or ions making the transition. The Beer Lambert law describes the relationship between light intensity and concentration of the element.

3.4.3 Electron probe micro analysis (EPMA)

Electron probe micro analysis is a micro analytical technique which is able to image or analyze materials. Its impact on the study of geological and planetary materials has been tremendous. The basic principal involved in EPMA is, an electron beam is applied on a polished solid surface of the sample causing the emission of characteristic X-Rays, which in Wavelength Dispersive Spectrometers (WDS) are diffracting by crystal involving the principle of Bragg's Law ($n = 2d \sin$). Each atomic element emits specific and identical wavelengths of X-rays that are focussed onto a detector where they are counted. From the intensity of the characteristic X-rays the concentration atomic element in the sample are calculated, and proper matrix corrections are applied. The details of the analytical procedure are given in the concerned chapter.

3.5 Petrochemical calculations and graphical diagrams

The chemical data thus obtained through the various analytical methods described above have been processed through a number of petrochemical calculations and their graphical representations including various triangular discrimination diagrams as well as spidergram of major oxides and elements (radicals) of the analyzed samples. They are of great significance in restructuring the tectonic environment involved during the formation of the Phokpur magnetite deposit.

3.6 Software and Rockware

Variety of software was used to handle the mineral and whole-rock geochemical database. The EPMA worksheet was used for calculating the end members of the spinel group members. Geochemical database were also processed for various purposes using spreadsheet (MS Excel 2007). Table, text etc are processed and edited on MS Word 2007. Geological map and some figures were digitized using Surfer 8.0 version. The figures generated from the chemical data by using different software were also cross-checked manually following the principles of programme theories.

PETROGRAPHY AND GEOCHEMISTRY OF PHOKPUR MAGNETITE

4.1 Introductory

Ore petrography (megascopic and ore microscopic studies) provides most valuable petrogenetic information of ores, as primary ore minerals as well as their alteration products are very significant to infer the geological processes involved in their formation. The textural features of ores/rocks are a record of ores/rocks forming processes. Minerals preserve cryptic messages in their texture, relations with other associated minerals in the ores. Thus the petrography reveals the type of operative geological processes and the paragenetic sequences. Modal abundance of minerals constituting the ores and their textural relationships can be used for process mineralogy and mineral beneficiation to remove the gangue and get the concentrate of the ores which are directly used to extract the metal by the process of extractive metallurgy.

4.2 Phokpur Magnetite

Phokpur magnetite ore samples are usually massive, hard and compact. The selected representative Phokpur magnetite ore samples (hand specimens) were cut and polished for their megascopic studies. The megascopic studies (with aid of 10 X Hand Lens) of the polished surface of the ore samples reveal that magnetite and silicate matrix are the main constituents of the ore. Various mode of occurrences of the ore minerals within the magnetite ore observed are: (i) anhedral magnetite grains (gray) within dark gray to black silicate matrix (Plate 4, Fig.1), (ii) randomly oriented magnetite grains (gray) within grayish black silicate matrix (Plate 4, Fig.2); (iii) elongated magnetite grains (gray) oriented in a linear pattern (like banding) within grayish black silicate matrix (Plate 4, Fig.3); (iv) poorly oriented magnetite grains/ patches (gray) within grayish black silicate matrix (Plate 4, Fig.4). The silicate matrix of the ore is occupied by the highly weathered

aphanitic and fine aggregates of silicates as well as fine and disseminated grains of the ore minerals including secondary hematite and goethite.

Mohapatra et al. (1995) reported that the silicate matrix consists mainly of microlites of chlorites containing some Cr and Ni, most probably derived from the host serpentinites, which was confirmed in the electron probe micro analyses presented and discussed in Chapter 5. The magnetite is usually dispersed in the silicate matrix and, at places, martitised along grain boundaries and fractures. Thin partings of silicates and hydrated iron oxides are usually present within the ore. The hydrated iron oxides might have formed due to weathering of magnetite grains. Coexistence of magnetite and chromite is observed where magnetite replaces chromite.

4.2.1 Ore Microscopic Studies

Textures of ore/ rock forming minerals, their reaction products, accessory minerals and minute inclusions are of paramount significance and provide useful information on the genesis and evolution the ore/ rock body. Therefore, ore microscopic studies of the 20 polished thin sections of the Phokpur magnetite samples were carried out using a Leica (Leitz) DM LP HC Research Polarizing Microscope (TL & RL) at the Department of Geology, Nagaland University, Kohima Campus Meriema. The various optical properties of each mineral, such as colour, habit, textures, relationship with other minerals etc. were studied under plane-polarized light as well as between cross polars. The textural features of petrogenetic importance from each polished ore thin section were photographed. Unidentified phases and zoned mineral grains were also studied and marked for further analysis. After petrographic studies, the polished ore thin sections were carbon coated for better conductivity during electron probe micro-analysis of the various ore/silicate minerals present in magnetite. The thickness of coating may be around 20 nm.

The ore microscopic (reflected light) studies of the polished thin sections of the Phokpur magnetite ore samples reveal that magnetite and chromite are the main ore mineral phases. In addition, hematite and goethite are also observed as secondary minerals. The details of the various ore mineral constituents and their textures are described below

(abbreviations of minerals adopted from the Canadian Mineralogist list of symbols for rock- and ore-forming minerals, 2018).

Magnetite: It occurs as irregular (anhedral) to skeletal (rarely euhedral) grains within the silicates matrix (mainly chlorite) in Phokpur magnetite ore samples (Figs. of the Plate V and Plate VI). Smaller grains of chlorite are usually present as inclusions within magnetite and chromite ore minerals (Plate V, Figs. 1 and 2). In reflected light magnetite appears as a light gray (with low reflectance) to grayish-white (medium reflectance) colour mineral depending upon its chemical composition (chrome-magnetite and magnetite, respectively). Usually it is observed as metasomatic replacement of chromite (dark gray) by grayish-white magnetite through light-gray chrome-magnetite with gradational to sharp contacts leaving the relics of primary mineral chromite (Plate VI, Fig. 1 and Plate VII, Fig. 1). At places, dendritic grains of magnetite are also observed (Plate VI, Fig. 2) reflecting the flowage of the magnetite along weak planes due to pressure and remobilization. A large elongated chrome-magnetite grain along with fragmented and oriented smaller grains of chromite (Plate VIII, Fig.1) also indicates the influence of directed pressure. Martitization of magnetite is also observed giving rise to the formation of hematite along grain boundaries and fractures (Plate VII, Fig.1). Fine grains of magnetite present within silicate matrix also show martitization (Plate VI, Fig. 1). Martitization is a secondary process and took place in two stages in Phokpur Magnetite deposit (Singh et al., 1989): (a) Initially with the formation of maghemite along incipient cracks forming net textures and finally changing into martite; and (b) martitization took place directly along fractures forming a replacement ore texture.

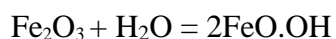
Chromite: It occurs as euhedral to anhedral, sub-rounded to elliptical highly corroded grains and often replaced by magnetite along the grain boundaries and fracture planes (Plate VIII, Fig.2 and Figs. of the Plates IX to XII). The fracture planes in chromite are infilled by magnetite. Compositional transformation of dark grey chromite to dull white magnetite (showing higher reflectance) along the margin and cracks of chromite crystal is very well observed. Chromite altered to chrome-magnetite (rather lower reflectance than magnetite) at margin is also frequently observed. Octahedral chromite grains are frequently observed within the matrix of magnetite and chlorite. Chromite is showing alteration from

margin. Chlorite is often present as small inclusions within chromite. Discrete and altered chromite grains oriented in one direction (Plate IX, Figs. 1 and 2) and showing pull apart texture (Thayer, 1969) indicate the pronounced role of directed pressure and tectonism in the evolution of magnetite deposit of the study area. Deformational cracks filled with interstitial chlorite are also observed within euhedral chromite grains. It appears that magnetite is formed by replacement of earlier formed chromite by overgrowth of magnetite on chromite. Two types of replacement have been observed: (a) change of chromite to ferrochromite along grain margins with successive reaction rims of ferrochromite. Subsequently, the ferrochromite rims are replaced or veined by magnetite in various habits/ shapes; (b) Chromite is directly replaced by magnetite without the formation of ferrochromite.

The replacement took place along the weak planes of the earlier formed chromite. At places, the chromite grain is almost totally replaced by magnetite leaving only relict islands of primary minerals (Plate VI, Fig.1). The replacement starts initially from the grain boundaries/ fractures, gradually advances towards the core of primary chromite minerals forming net and branching textures (Plate X, Fig.2 and Plate XI, Fig.2).

Hematite: It is observed as a grayish-white (high reflectance, anisotropic) secondary mineral formed by the process of martitization of magnetite usually at the contact of grain boundaries and fracture planes of chromite (Plate X, Fig.2 and Plate XII, Fig.1) forming an irregular pattern. It is also observed as smaller disseminated grains in the silicate matrix.

Goethite: It occurs usually as veins along fracture within magnetite (Plate VII, Fig. 2) and silicate matrix (Plate XI, Fig. 1 and Plate XII, Fig. 2). In reflected light microscopy, it shows blue-gray colour, poor bireflectance, distinct anisotropism and brownish-yellow to reddish-brown internal reflection. The formation of goethite along fractures in martitised-magnetite may be explained by the following reaction:



This reflects that the fractures developed in the magnetite served as passages for the water to enter and react with hematite to form the hydrated iron oxide mineral (goethite) in due course of time.

4.2.2 BSE Images of Magnetite Ores and their Textural Features

Detailed textural studies of the Back Scattered Electrons (BSE) Images of the Phokpur magnetite ore samples obtained from high resolution scanning electron microscope attached with the electron probe micro analyzer reveal that magnetite and chromite, occurs as composite as well as discrete ore mineral phases, are the main constituents of the ore body (Figs. of the Plates XIII to XVII). The magnetites are usually observed as anhedral (irregular) to subhedral, deformed, elongated and oriented grains within the silicate matrix (Plate VI, Fig. 1 and Fig. 2). The chromite grains are generally observed as anhedral to subhedral as well as rounded to elliptical in form. Most of the chromite grains (including isolated chromite grains) are zoned to contain outer rims of magnetite. It shows a typical replacement texture where chromite grains are being replaced by magnetite along their grain boundaries and fracture planes/ partings (Figs. of Plates XIV and XV).

Size of the magnetite grains varies usually from 20 to 500 microns and size of the chromite grains varies from 10 microns to more than 2 mm. Ore minerals are fractured in nature with indications of deformational activities after the formation of chromite and magnetite grains. Usually the fractures are occupied by goethite and maghemite. They are also filled with secondary silicate matrix composed mainly of chlorite and serpentine, which also served as the major constituents of the magnetite ore body. Magnetite grains also display conspicuous rims of maghemite/goethite (Plate XVII, Fig.1) which indicates secondary alteration and deposition of oxidized iron from the diffusion process possibly combined with martitization (Davis et al., 1968).

Ferrochromite/maghemite and martite/goethite are observed as the common alteration products along fractures in chromite and magnetite respectively. Chromite is corroded and replaced by magnetite and the fracture planes in chromite are infilled by magnetite (Plates XV, Fig.2). In general, the opaque grains are corroded and at places show highly sutured margins.

The detailed textural and mineralogical studies (ore microscopy and BSE Images) the Phokpur magnetite ore samples show fracturing of the individual chromite grains under stress. Ore bodies affected by shearing/faulting and subsequent deformation reflect cataclastic texture where the chromite grains are shattered into smaller to fine fragments of highly irregular shape. Some of the chromite grains are observed to be rounded and corroded and rimmed by chrome-magnetite/ magnetite. The rounding of the chromite

grains may be due to the metasomatic resorption caused by reaction between early formed chromite crystals and later introduced iron-rich fluid.

Zoning texture is common in chromite grains of Phokpur magnetite ores. This may be due to metasomatic alteration of the chromite grains. Two types of alteration products are possible: (i) the iron-rich high reflecting phase, and (ii) the Mg and Al-rich low reflecting phase. In the Phokpur magnetite ore samples, the chromite grains alter to a high reflecting phase of magnetite with an intermediate phase of ferro-chromite having medium reflectance. The high reflecting magnetite phase is almost devoid of chromium. The intermediate phase with medium reflectivity between magnetite and chromite shows a decrease in chromium and magnesium content but slightly increase in iron and aluminium. These altered mineral phases show gradational to sharp contact. This zonal texture may be related to the alteration of chromite during serpentinization of the host dunites/ peridotites/ pyroxenites of the study area.

4.3 Paragenetic Sequence of Phokpur Magnetite

The mineral paragenetic sequence of the Phokpur magnetite ore deposit has been recognized mainly based on the degree of crystallinity, mineral inclusions and textural relationships. Most of the minerals in Phokpur magnetite have been crystallized during alteration of the pre-existing ultramafic rocks (Agrawal & Ghose, 1989). On the basis of the detailed textural and mineralogical studies of the Phokpur magnetite ore samples, the paragenetic sequence is shown in the following Table 4.1.

Table 4.1: Paragenetic sequence of Phokpur magnetite based on textural relationship

Time	—————→
Mineral	Primary Secondary
Chromite	—————▼—————
Magnetite	—————
Chlorite- Serpentine	—————
Hematite	—————
Goethite	—————

4.4 Modal Mineralogy

Phokpur magnetite ore body is highly altered and occurs in very irregular form. Therefore, it's quantitative (modal analysis) estimation was very difficult. Hence, modal mineral analyses of the ten representative samples of the Phokpur magnetite deposit were carried out by visual assessment and the obtained results are presented in Tables 4.2. Magnetite constitutes about 40 to 55% proportion (average 45%) whereas chromite constitutes about 8 to 15% proportion (average 10%) of the studied ore samples. Hematite and goethite, etc. constitutes an average proportion of 7%. Remaining part of the ore is occupied by the highly weathered aphanitic silicate matrix (average 38%) containing disseminated grains of chromite and magnetite as well as fine aggregates of silicate matrix (the microlites of chlorites and serpentinites).

Table 4.2: Modal percentage of minerals of the Phokpur magnetite ore Samples

Sr. No.	Sample No.	Minerals in percentage			
		Magnetite	Chromite	Chlorite-silicate matrix	Hematite and goethite, etc*.
1	OG 01	45	10	40	5
2	OG 02	55	5	35	5
3	OG 05	45	10	38	7
4	OG 10	40	12	40	8
5	OG 13	40	15	35	10
6	OG 16	45	5	40	10
7	OG 20	40	10	42	8
8	OG 25	55	8	30	7
9	OG 36	40	15	40	5
10	OG 42	45	10	40	5
Average		45	10	38	7

* Other unidentified iron oxides

4.5 Geochemistry of Phokpur Magnetite

The chemical analyses of the 10 samples from the Phokpur magnetite ores was carried out in National Metallurgical Laboratory, Jamshedpur, Jharkhand by using ICP-OES instrumentation technique and the results are shown in Table 4.3. It can be observed that the concentration of nickel in the magnetite ore ranges from 0.14 to 0.91 % with an average concentration of 0.49 %, and the concentration of chromium ranges from 1.33 to 3.79 % with an average concentration of 2.38%. The iron content ranges from 40.51 to 55.95% with an average concentration of 50.54%. Cobalt (average 0.04%), titanium (average 0.56%), and vanadium (average 0.02%) have been reported in very small amount in the magnetite ore samples, though titanium and vanadium are usually rich in magnetites of magmatic origin.

Table 4.3: Chemical Analyses of Phokpur Magnetite Ore Samples (in %)

Radicals → Sample Nos. ↓	Ni	Cr	Co	Ti	V	Fe
OG 01	0.65	2.37	0.03	0.26	0.01	55.95
OG 02	0.26	2.38	0.008	0.79	0.019	47.58
OG 05	0.14	1.33	0.01	1.77	0.06	40.51
OG 10	0.44	3.79	0.02	0.10	0.008	51.63
OG 13	0.55	3.11	0.01	0.50	0.021	54.66
OG 16	0.91	3.16	0.13	0.10	0.011	54.66
OG 20	0.52	1.87	0.03	0.36	0.013	49.39
OG 25	0.38	1.69	0.04	0.52	0.016	54.70
OG 36	0.31	2.15	0.012	0.79	0.017	45.91
OG 42	0.76	13.90	0.14	0.43	0.011	50.42
Average	0.49	2.38	0.04	0.56	0.02	50.54

Nickel (Ni), cobalt (Co) and chromium (Cr) values of the Phokpur magnetite ore samples were plotted in Duran et al. (2020) diagram to understand the petrological environment prevailed during the evolution of Phokpur magnetite deposit (Fig.4.1: a and b). When the Ni versus Co values are plotted in figure 4.1(a), most of the points fall in the magmatic field. This reflects the involvement of magma in the formation of Phokpur magnetite deposit. Again to understand the nature of magma, when the Co versus Cr values are plotted in figure 4.1(b), all the points fall between primitive magma and evolved magma. This indicates that the formation of the Phokpur magnetite deposit took place in a transitional environment between primitive and evolved magma during magmatic differentiation within the ultramafic/ mafic domain. The magmatic differentiation might have produced the iron-rich fluids during the transition stage between primitive mantle to evolved magma. These iron-rich fluids reacted with the earlier formed chromite grains and probably responsible for the metasomatic replacement of chromium as well as addition of iron in various proportions in the Phokpur magnetite ore deposit.

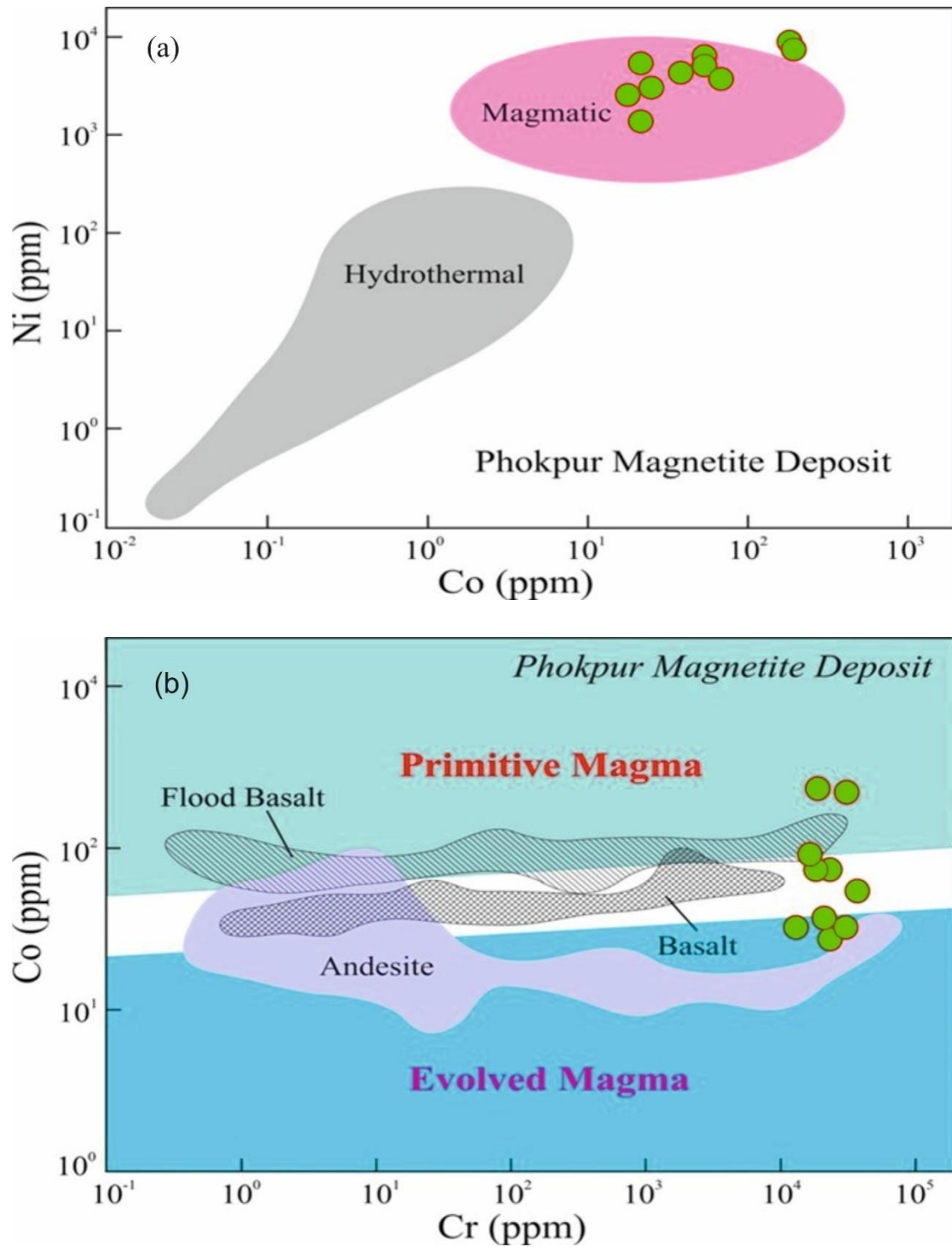


Figure 4.1: Binary diagram of (a) Ni versus Co and (b) Co versus Cr plotted for Phokpur Magnetite ore samples from NOB (after Duran et al., 2020).

Magnetite is an illustrious petrogenetic indicator and occurs in various ore deposits, which contains several discriminator elements that display systematic variations (Nadoll et al., 2014). Trace elements in magnetite provide a tool to understand the processes that aid discrimination based on their different environments of formation, which helps to understand petrogenetic and provenance studies in the exploration of ore deposits (Dare et al., 2014; Eliopoulos et al., 2019). Generally, magnetite related to mafic-ultramafic complex, hydrothermal deposits, granodiorite-porphyry and ophiolites are known for their low Cr, Ni, and Co content (Devaraju et al., 2014; Lopez-Garcia et al., 2016; Mavrogonatos et al., 2019). But, the Phokpur magnetite ore deposit associated with Naga Ophiolite belt are characterized by slightly higher Ni and Co contents (Fig. 4.2). Magnetite trace element compositions have capability to be powerful tool in exploration of economic mineral deposit (Pisiak et al., 2017).

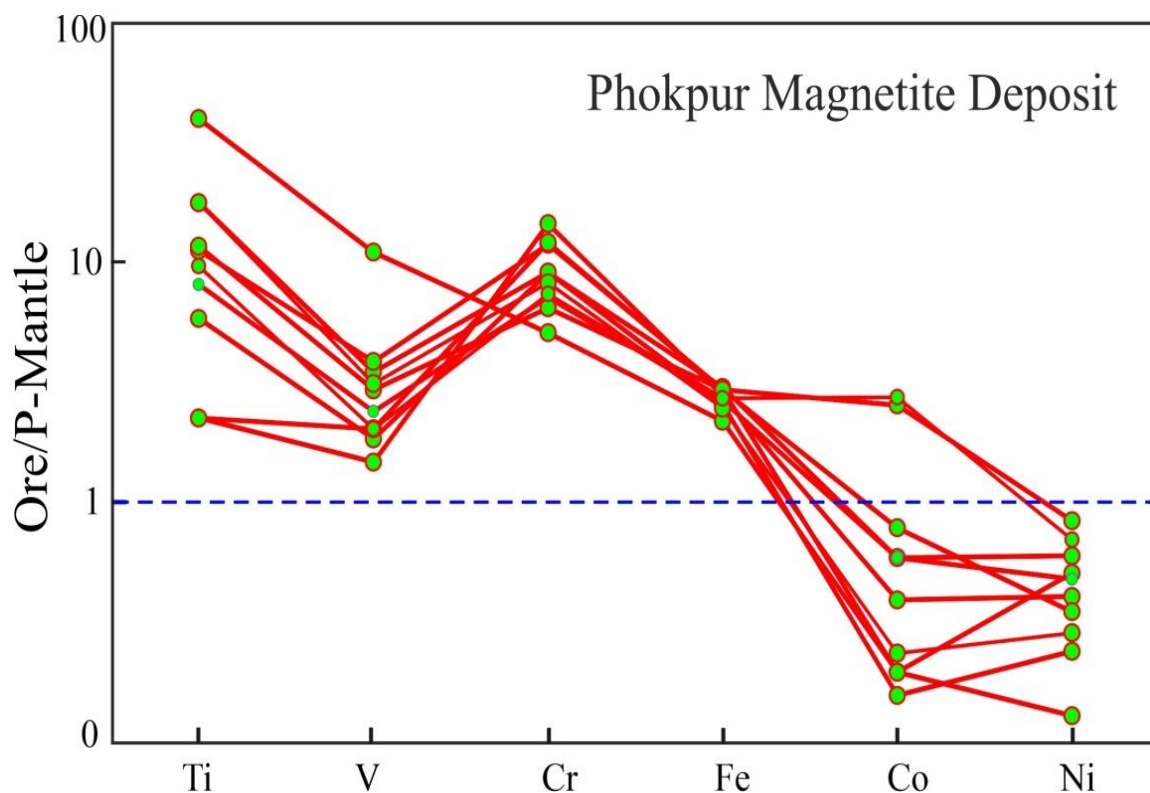


Figure 4.2.: Primitive mantle normalized enrichment pattern of chrome-magnetite ore samples from Phokpur deposit, NOB. Primitive mantle values from Palme and O, Neill (2014).

MINERAL CHEMISTRY OF MAGNETITE ORE

5.1 Introductory

Electron probe micro analyses (EPMA) of magnetite, chromite and chlorite from the four selected ore samples of the Phokpur Magnetite (OG/4, OG/19, OG/25 and OG/36) were carried out to know their mineral chemistry. These sample numbers in the EPMA tables are shown as 1-TP, 2-TP, 5-TP and 36-TP, respectively. The results of representative analysis of magnetite, chromite and chlorite, etc. along with their cation calculation for individual sites are presented in the form of tables at their respective places. Structural formula of magnetite and chromite has been calculated on the basis of 32 combined oxygens. Structural formula of chlorite has been calculated based on 28 atoms of combined oxygen.

Analytical Methods

The experimental work was carried out on the Electron Probe Micro Analyzer (EPMA) CAMECA SXFive instrument at DST-SERB National Facility, Department of Geology (Centre of Advanced Study), Institute of Science, Banaras Hindu University. Polished thin section was coated with 20 nm thin layer of carbon for electron probe micro analyses using LEICA-EM ACE200 instrument. The CAMECA SXFive instrument was operated by SXFive Software at a voltage of 15 kV and current 10 nA with a LaB6 source in the electron gun for generation of electron beam. Natural silicate mineral andradite as internal standard used to verify positions of crystals (SP1-TAP, SP2-LiF, SP3-LPET, SP4-LTAP and SP5-PET) with respect to corresponding wavelength dispersive (WD) spectrometers (SP#) in CAMECA SX-Five instrument. The following X-ray lines were used in the analyses: F-K α , Na-K α , Mg-K α , Al-K α , Si-K α , P-K α , Cl-K α , K-K α , Ca-K α , Ti-K α , Cr-K α , Mn-K α and Fe-K α . Natural mineral standards: fluorite, halite, apatite, periclase, corundum, wollastonite, orthoclase, rutile, chromite, rhodonite and hematite standard supplied by CAMECA-AMETEK used for routine calibration, X-ray elemental

mapping and quantification. Point analysis is measured on the sample mounted on a glass slide (size: 46 mm × 25 mm × 1 mm) in the form of a thin section. Routine calibration, acquisition, quantification and data processing were carried out using SxSAB version 6.1 and SX-Results softwares of CAMECA. The precision of the analysis is better than 1% for major element oxides and 5% for trace elements from the repeated analysis of standards. Analysis was carried out after a check that I_{Xstd}/I_{std} was 1.00 ± 0.01 for each element, where I_{Xstd} was intensity of the analyzed standard and I_{std} the intensity of the same standard monitored after each element calibration. BHU-EPMA (CAMECA-SXFive) calibration setting for common silicate minerals phases (olivine, mica, pyroxene, amphibole, spinel, garnet, feldspoids and feldspar) (Pandey et al., 2017a,b,c; Pandey et al., 2019; Chauhan et al., 2020). The details of X-ray lines used in the analyses are given in Table 5.1.

Table 5.1: X-ray lines used in the analyses along with their counting statistics with respect to natural and synthetic standards

At. No.	Element & X-ray	Crystal	Peak Time (ns)	Bckgd (-ve)	Bckgd (+ve)	Standard	Composition	Standard Intensity (cps/nA)
9	F- $K\alpha$	TAP	10	-500	+500	Fluorite	CaF ₂	15.671
11	Na- $K\alpha$	TAP	10	-500	+500	Albite	NaAlSi ₃ O ₈	387.505
12	Mg- $K\alpha$	TAP	10	-500	+500	Periclase	MgO	896.505
13	Al- $K\alpha$	TAP	10	-500	+500	Corundum	Al ₂ O ₃	1053.184
14	Si- $K\alpha$,	TAP	10	-500	+500	Wollastonite	CaSiO ₃	464.060
15	P- $K\alpha$	PET	10	-500	+500	Apatite	Ca ₅ (PO ₄) ₃ (F,Cl,OH)	73.845
16	S- $K\alpha$	PET	10	-500	+500	Pyrite	FeS ₂	169.995
17	Cl- $K\alpha$	PET	10	-500	+500	Halite	NaCl	176.506
19	K- $K\alpha$	PET	10	-500	+500	Orthoclase	KAlSi ₃ O ₈	69.222
20	Ca- $K\alpha$	PET	10	-500	+500	Diopside	CaMgSi ₂ O ₆	354.887
22	Ti- $K\alpha$,	LIF	10	-500	+500	Rutile	TiO ₂	58.679
24	Cr- $K\alpha$	LIF	10	-500	+500	Chromite	Cr ₂ O ₃	81.590
25	Mn- $K\alpha$	LIF	10	-500	+500	Rhodonite	MnSiO ₃	36.529
26	Fe- $K\alpha$	LIF	10	-500	+500	Hematite	Fe ₂ O ₃	79.794
28	Ni- $K\alpha$	LIF	10	-500	+500	Nickle	Ni	92.643
38	Sr- La	TAP	10	-500	+500	Celestine	SrSO ₄	359.136
39	Y- La	TAP	10	-500	+500	Y-Glass	Y-Ca-Al-Si	272.395
40	Zr- La	TAP	10	-500	+500	Zircon	ZrSiO ₄	293.294
41	Nb- La	PET	10	-500	+500	Niobium	Nb	106.480
56	Ba- La	PET	10	-500	+500	Barite	BaSO ₄	20.277

5.2 Results

5.2.1 Electron probe micro analysis

Electron probe micro analysis (EPMA) of selected ore samples from Phokpur magnetite ore body was carried out for their spinel group minerals and results are presented in Tables 5.2 to 5.5. Apart from the samples displayed in Plates XIII to XVII, several grains with evident of chromiferous cores were also selected for chemical analysis. *Fe³⁺ in ore minerals were calculated on the basis of stoichiometry, i.e., 32 oxygens.* Standard deviations, mainly those for major elements involved in the transformation from chromite to magnetite, were significantly large (Della Giusta et al., 2011). The compositional variations from chromite to magnetite is observed because change in chemistry of all the grains studied from core to rim.

In addition, the EPMA of the silicates which are present in substantial amount as matrix within Phokpur magnetite samples (as already mentioned in chapter 4) was also carried out to study their mineralogy. The analytical results of the mineral grains of the silicate matrix are presented in Tables 5.6.

Table 5.2: Representative EPMA analyses of magnetite grains from the Phokpur magnetite ore samples of Naga Ophiolite Belt

Sample Nos.→ Wt% Oxide↓	1-TP	1-TP	1-TP	1-TP	1-TP	1-TP	1-TP	1-TP
Point#	7 / 1	8 / 1	9 / 1	11 / 1	25 / 1	26 / 1	27 / 1	28 / 1
SiO ₂	1.12	1.30	1.20	1.13	0.81	1.23	0.66	1.42
TiO ₂	0.04	0.02	0.00	0.00	0.37	0.02	0.10	0.05
Al ₂ O ₃	0.41	0.27	0.28	0.18	0.77	0.57	0.48	0.55
Cr ₂ O ₃	1.32	0.90	0.56	0.16	1.28	0.66	1.29	1.90
V ₂ O ₃	0.00	0.00	0.00	0.00	0.00	0.00	0.00	0.00
Fe ₂ O ₃	61.41	61.25	61.87	64.47	62.05	53.77	62.83	59.30
FeO	31.11	31.10	30.92	31.68	31.45	27.65	30.76	31.06
MnO	0.06	0.13	0.10	0.22	0.13	0.12	0.13	0.20
MgO	0.06	0.02	0.05	0.01	0.02	0.03	0.03	0.05
CaO	0.02	0.03	0.05	0.01	0.04	0.04	0.02	0.07
ZnO	0.00	0.00	0.00	0.00	0.00	0.00	0.00	0.00
TOTAL	95.55	95.02	95.03	97.86	96.91	84.09	96.29	94.60
Mineral Formula Calculated Based on 32 Oxygen Basis								
Si	0.36	0.42	0.39	0.35	0.25	0.44	0.21	0.46
Ti	0.01	0.01	0.00	0.00	0.09	0.01	0.02	0.01
Al	0.15	0.10	0.11	0.07	0.29	0.24	0.18	0.21
Cr	0.33	0.23	0.14	0.04	0.32	0.19	0.32	0.48
V	0.00	0.00	0.00	0.00	0.00	0.00	0.00	0.00
Fe(iii)	14.78	14.83	14.98	15.18	14.71	14.67	15.03	14.37
Fe(ii)	8.32	8.37	8.32	8.29	8.29	8.38	8.18	8.37
Mn	0.02	0.04	0.03	0.06	0.04	0.04	0.04	0.05
Mg	0.03	0.01	0.02	0.00	0.01	0.02	0.01	0.02
Ca	0.01	0.01	0.02	0.00	0.01	0.01	0.01	0.02
Zn	0.00	0.00	0.00	0.00	0.00	0.00	0.00	0.00
TOTAL	24.00	24.00	24.00	24.00	24.00	24.00	24.00	24.00
Fe/Fe+Mg	1.00	1.00	1.00	1.00	1.00	1.00	1.00	1.00
Cr/Cr+Al	0.69	0.69	0.57	0.37	0.53	0.44	0.64	0.70
Fe(ii)	8.32	8.37	8.32	8.29	8.29	8.38	8.18	8.37
Fe(iii)	14.78	14.83	14.98	15.18	14.71	14.67	15.03	14.37
Fe ₂ /(Fe ₂ +Fe ₃)	0.36	0.36	0.36	0.35	0.36	0.36	0.35	0.37
Fe ₃ /(Fe ₃ +Fe ₂)	0.64	0.64	0.64	0.65	0.64	0.64	0.65	0.63

Table 5.2: Contd-----

Sample No.→ Wt% Oxide↓	1-TP	1-TP	1-TP	1-TP	1-TP	1-TP	1-TP	1-TP
Point#	29 / 1	30 / 1	33 / 1	34 / 1	47 / 1	50 / 1	51 / 1	52 / 1
SiO ₂	1.13	1.10	1.78	1.15	0.00	0.94	0.54	0.40
TiO ₂	0.03	0.08	0.00	0.04	0.00	0.00	0.08	0.12
Al ₂ O ₃	0.60	0.22	0.97	0.25	0.80	0.32	0.41	0.25
Cr ₂ O ₃	0.94	0.89	1.19	1.48	0.00	0.64	0.36	1.42
V ₂ O ₃	0.00	0.00	0.00	0.00	0.00	0.00	0.00	0.00
Fe ₂ O ₃	62.95	62.65	60.27	60.64	64.62	64.12	65.96	65.28
FeO	31.71	31.31	32.27	30.71	29.34	31.37	31.51	31.13
MnO	0.19	0.22	0.24	0.22	0.29	0.15	0.00	0.12
MgO	0.00	0.00	0.03	0.00	0.00	0.06	0.01	0.02
CaO	0.03	0.01	0.05	0.05	0.00	0.00	0.03	0.08
ZnO	0.00	0.00	0.00	0.00	0.00	0.00	0.00	0.00
TOTAL	97.59	96.48	96.79	94.55	95.05	97.59	98.90	98.82
Mineral Formula Calculated Based on 32 Oxygen Basis								
Si	0.35	0.35	0.56	0.37	0.00	0.29	0.17	0.12
Ti	0.01	0.02	0.00	0.01	0.00	0.00	0.02	0.03
Al	0.22	0.08	0.36	0.10	0.30	0.12	0.15	0.09
Cr	0.23	0.22	0.30	0.38	0.00	0.16	0.09	0.35
V	0.00	0.00	0.00	0.00	0.00	0.00	0.00	0.00
Fe(iii)	14.82	14.96	14.23	14.76	15.70	15.14	15.39	15.26
Fe(ii)	8.30	8.31	8.47	8.31	7.92	8.23	8.17	8.09
Mn	0.05	0.06	0.06	0.06	0.08	0.04	0.00	0.03
Mg	0.00	0.00	0.01	0.00	0.00	0.03	0.00	0.01
Ca	0.01	0.00	0.02	0.02	0.00	0.00	0.01	0.03
Zn	0.00	0.00	0.00	0.00	0.00	0.00	0.00	0.00
TOTAL	24.00	24.00	24.00	24.00	24.00	24.00	24.00	24.00
Fe/Fe+Mg	1.00	1.00	1.00	1.00	1.00	1.00	1.00	1.00
Cr/Cr+Al	0.51	0.73	0.45	0.80	0.00	0.57	0.38	0.79
Fe(ii)	8.30	8.31	8.47	8.31	7.92	8.23	8.17	8.09
Fe(iii)	14.82	14.96	14.23	14.76	15.70	15.14	15.39	15.26
Fe ₂ /(Fe ₂ +Fe ₃)	0.36	0.36	0.37	0.36	0.34	0.35	0.35	0.35
Fe ₃ /(Fe ₃ +Fe ₂)	0.64	0.64	0.63	0.64	0.66	0.65	0.65	0.65

Table 5.2: Contd-----

Sample No.→ Wt% Oxide↓	1-TP	1-TP	1-TP	2-TP	2-TP	2-TP	2-TP	5-TP
Point#	63 / 1	65 / 1	66 / 1	85 / 1	88 / 1	91 / 1	92 / 1	110 / 1
SiO ₂	1.66	1.11	0.81	1.10	0.83	0.00	1.67	1.52
TiO ₂	0.00	0.54	0.09	0.71	0.36	0.54	0.11	4.63
Al ₂ O ₃	0.92	1.98	0.51	1.51	1.11	1.09	0.48	1.77
Cr ₂ O ₃	1.07	1.48	1.00	1.32	1.94	0.65	1.10	1.89
V ₂ O ₃	0.00	0.00	0.00	0.00	0.00	0.00	0.00	0.00
Fe ₂ O ₃	60.63	58.73	64.88	61.27	63.39	65.04	58.57	49.11
FeO	31.95	31.50	31.58	32.60	32.29	31.18	31.03	36.06
MnO	0.26	0.36	0.25	0.39	0.17	0.10	0.11	0.00
MgO	0.06	0.13	0.12	0.00	0.12	0.01	0.06	0.05
CaO	0.06	0.03	0.05	0.13	0.14	0.01	0.12	0.04
ZnO	0.00	0.00	0.00	0.00	0.00	0.00	0.00	0.00
TOTAL	96.61	95.85	99.29	99.03	100.35	98.61	93.24	95.07
Mineral Formula Calculated Based on 32 Oxygen Basis								
Si	0.52	0.35	0.25	0.34	0.25	0.00	0.55	0.48
Ti	0.00	0.13	0.02	0.16	0.08	0.13	0.03	1.10
Al	0.34	0.73	0.18	0.55	0.40	0.40	0.18	0.66
Cr	0.27	0.37	0.24	0.32	0.46	0.16	0.28	0.47
V	0.00	0.00	0.00	0.00	0.00	0.00	0.00	0.00
Fe(iii)	14.35	13.94	15.03	14.13	14.47	15.19	14.39	11.70
Fe(ii)	8.40	8.31	8.13	8.36	8.19	8.09	8.47	9.55
Mn	0.07	0.10	0.07	0.10	0.04	0.03	0.03	0.00
Mg	0.03	0.06	0.06	0.00	0.05	0.00	0.03	0.02
Ca	0.02	0.01	0.02	0.04	0.05	0.00	0.04	0.01
Zn	0.00	0.00	0.00	0.00	0.00	0.00	0.00	0.00
TOTAL	24.00	24.00	24.00	24.00	24.00	24.00	24.00	24.00
Fe/Fe+Mg	1.00	1.00	1.00	1.00	1.00	1.00	1.00	1.00
Cr/Cr+Al	0.44	0.33	0.57	0.37	0.54	0.29	0.61	0.42
Fe(ii)	8.40	8.31	8.13	8.36	8.19	8.09	8.47	9.55
Fe(iii)	14.35	13.94	15.03	14.13	14.47	15.19	14.39	11.70
Fe ₂ /(Fe ₂ +Fe ₃)	0.37	0.37	0.35	0.37	0.36	0.35	0.37	0.45
Fe ₃ /(Fe ₃ +Fe ₂)	0.63	0.63	0.65	0.63	0.64	0.65	0.63	0.55

Table 5.3: Representative EPMA analyses of chrome-magnetite grains from the Phokpur magnetite ore samples of Naga Ophiolite Belt

Sample No.→ Wt% Oxide↓	1-TP	1-TP	1-TP	1-TP	1-TP	1-TP	1-TP	1-TP
Point#	10 / 1	12 / 1	13 / 1	14 / 1	15 / 1	40 / 1	46 / 1	49 / 1
SiO ₂	1.21	0.79	1.79	0.79	1.34	0.66	0.46	0.00
TiO ₂	0.11	0.11	0.11	0.06	0.05	0.12	0.45	0.00
Al ₂ O ₃	0.35	0.31	1.82	0.23	0.67	0.45	5.54	10.80
Cr ₂ O ₃	2.32	2.88	3.29	2.36	3.04	2.40	15.52	10.83
V ₂ O ₃	0.00	0.00	0.00	0.00	0.00	0.00	0.00	0.00
Fe ₂ O ₃	59.05	47.21	56.23	58.89	57.50	62.81	46.69	30.04
FeO	30.66	24.49	31.81	29.45	30.40	31.14	29.96	22.08
MnO	0.22	0.34	0.47	0.16	0.43	0.23	0.71	0.35
MgO	0.05	0.00	0.16	0.05	0.10	0.05	1.93	2.14
CaO	0.04	0.05	0.05	0.06	0.04	0.04	0.03	0.00
ZnO	0.00	0.00	0.00	0.00	0.00	0.00	0.00	0.00
TOTAL	94.02	76.19	95.72	92.05	93.56	97.90	101.29	76.23
Mineral Formula Calculated Based on 32 Oxygen Basis								
Si	0.39	0.32	0.56	0.26	0.43	0.21	0.13	0.00
Ti	0.03	0.03	0.03	0.02	0.01	0.03	0.10	0.00
Al	0.14	0.15	0.68	0.09	0.26	0.17	1.88	4.64
Cr	0.59	0.91	0.82	0.62	0.78	0.59	3.54	3.12
V	0.00	0.00	0.00	0.00	0.00	0.00	0.00	0.00
Fe(iii)	14.43	14.24	13.32	14.73	14.07	14.77	10.12	8.24
Fe(ii)	8.32	8.21	8.38	8.19	8.26	8.14	7.22	6.73
Mn	0.06	0.12	0.12	0.05	0.12	0.06	0.17	0.11
Mg	0.02	0.00	0.07	0.02	0.05	0.02	0.83	1.16
Ca	0.01	0.02	0.02	0.02	0.01	0.01	0.01	0.00
Zn	0.00	0.00	0.00	0.00	0.00	0.00	0.00	0.00
TOTAL	24.00	24.00	24.00	24.00	24.00	24.00	24.00	24.00
Fe/Fe+Mg	1.00	1.00	1.00	1.00	1.00	1.00	0.95	0.93
Cr/Cr+Al	0.81	0.86	0.55	0.87	0.75	0.78	0.65	0.40
Fe(ii)	8.32	8.21	8.38	8.19	8.26	8.14	7.22	6.73
Fe(iii)	14.43	14.24	13.32	14.73	14.07	14.77	10.12	8.24
Fe ²⁺ /(Fe ²⁺ +Fe ³⁺)	0.37	0.37	0.39	0.36	0.37	0.36	0.42	0.45
Fe ³⁺ /(Fe ³⁺ +Fe ²⁺)	0.63	0.63	0.61	0.64	0.63	0.64	0.58	0.55

Table 5.3: Contd-----

Sample No.→ Wt% Oxide↓	1-TP	1-TP	1-TP	2-TP	2-TP	2-TP	2-TP	2-TP
Point#	53 / 1	57 / 1	58 / 1	77 / 1	78 / 1	83 / 1	86 / 1	89 / 1
SiO ₂	0.00	3.04	0.90	1.41	1.58	0.72	0.95	1.02
TiO ₂	0.67	0.11	0.03	0.98	0.47	0.36	0.54	0.62
Al ₂ O ₃	0.27	4.55	0.45	1.16	2.40	1.22	1.15	0.89
Cr ₂ O ₃	24.55	10.17	2.36	6.30	7.47	2.04	2.12	2.58
V ₂ O ₃	0.00	0.00	0.00	0.00	0.00	0.00	0.00	0.00
Fe ₂ O ₃	41.86	43.63	62.06	52.51	51.89	61.45	62.38	58.27
FeO	29.31	31.80	31.20	31.92	32.49	31.29	32.75	31.44
MnO	0.41	1.29	0.20	0.43	0.29	0.13	0.10	0.00
MgO	1.18	1.09	0.05	0.07	0.04	0.08	0.09	0.03
CaO	0.02	0.05	0.06	0.06	0.27	0.22	0.08	0.10
ZnO	0.00	0.00	0.00	0.00	0.00	0.00	0.00	0.00
TOTAL	98.27	95.74	97.30	94.83	96.90	97.51	100.17	94.96
Mineral Formula Calculated Based on 32 Oxygen Basis								
Si	0.00	0.93	0.28	0.45	0.49	0.23	0.29	0.33
Ti	0.16	0.02	0.01	0.24	0.11	0.08	0.12	0.15
Al	0.10	1.64	0.17	0.43	0.88	0.45	0.41	0.34
Cr	5.94	2.45	0.58	1.59	1.83	0.50	0.51	0.65
V	0.00	0.00	0.00	0.00	0.00	0.00	0.00	0.00
Fe(iii)	9.65	10.01	14.67	12.61	12.10	14.43	14.26	14.05
Fe(ii)	7.50	8.11	8.19	8.52	8.42	8.17	8.32	8.43
Mn	0.11	0.33	0.05	0.12	0.08	0.03	0.03	0.00
Mg	0.54	0.50	0.02	0.03	0.02	0.04	0.04	0.02
Ca	0.01	0.02	0.02	0.02	0.09	0.07	0.03	0.03
Zn	0.00	0.00	0.00	0.00	0.00	0.00	0.00	0.00
TOTAL	24.00	24.00	24.00	24.00	24.00	24.00	24.00	24.00
Fe/Fe+Mg	0.97	0.97	1.00	1.00	1.00	1.00	1.00	1.00
Cr/Cr+Al	0.98	0.60	0.78	0.79	0.68	0.53	0.55	0.66
Fe(ii)	7.50	8.11	8.19	8.52	8.42	8.17	8.32	8.43
Fe(iii)	9.65	10.01	14.67	12.61	12.10	14.43	14.26	14.05
Fe ₂ /(Fe ₂ +Fe ₃)	0.44	0.45	0.36	0.40	0.41	0.36	0.37	0.37
Fe ₃ /(Fe ₃ +Fe ₂)	0.56	0.55	0.64	0.60	0.59	0.64	0.63	0.63

Table 5.3: Contd-----

Sample No.→ Wt% Oxide↓	2-TP	2-TP	5-TP	5-TP	5-TP
Point#	95 / 1	100 / 1	103 / 1	107 / 1	112 / 1
SiO ₂	0.81	1.98	1.45	1.39	0.88
TiO ₂	0.20	0.85	4.30	2.70	1.52
Al ₂ O ₃	0.64	2.06	8.52	7.05	1.06
Cr ₂ O ₃	2.49	2.99	8.08	12.15	2.77
V ₂ O ₃	0.00	0.00	0.00	0.00	0.00
Fe ₂ O ₃	62.01	55.70	26.45	26.29	57.16
FeO	31.52	33.85	32.70	30.54	32.46
MnO	0.13	0.03	0.00	0.00	0.00
MgO	0.01	0.12	0.11	0.07	0.02
CaO	0.13	0.09	0.03	0.05	0.08
ZnO	0.00	0.00	0.00	0.00	0.00
TOTAL	97.96	97.68	81.65	80.25	95.93
Mineral Formula Calculated Based on 32 Oxygen Basis					
Si	0.25	0.61	0.51	0.50	0.28
Ti	0.05	0.20	1.13	0.73	0.36
Al	0.24	0.75	3.52	2.99	0.40
Cr	0.61	0.73	2.24	3.45	0.69
V	0.00	0.00	0.00	0.00	0.00
Fe(iii)	14.55	12.91	6.97	7.11	13.63
Fe(ii)	8.22	8.72	9.57	9.17	8.60
Mn	0.03	0.01	0.00	0.00	0.00
Mg	0.00	0.06	0.06	0.04	0.01
Ca	0.04	0.03	0.01	0.02	0.03
Zn	0.00	0.00	0.00	0.00	0.00
TOTAL	24.00	24.00	24.00	24.00	24.00
Fe/Fe+Mg	1.00	1.00	1.00	1.00	1.00
Cr/Cr+Al	0.72	0.49	0.39	0.54	0.64
Fe(ii)	8.22	8.72	9.57	9.17	8.60
Fe(iii)	14.55	12.91	6.97	7.11	13.63
Fe ²⁺ /(Fe ²⁺ +Fe ³⁺)	0.36	0.40	0.58	0.56	0.39
Fe ³⁺ /(Fe ³⁺ +Fe ²⁺)	0.64	0.60	0.42	0.44	0.61

Table 5.4: Representative EPMA analyses of chromite grains from the Phokpur magnetite ore samples of Naga Ophiolite Belt

Sample No.→ Wt% Oxide↓	1-TP	1-TP	1-TP	1-TP	1-TP	1-TP	1-TP	1-TP
Point#	21 / 1	22 / 1	31 / 1	32 / 1	35 / 1	36 / 1	37 / 1	38 / 1
SiO ₂	0.33	0.00	0.00	0.00	0.00	0.03	0.16	0.24
TiO ₂	0.37	0.32	0.27	0.23	0.64	0.56	0.32	0.36
Al ₂ O ₃	13.03	10.55	26.31	23.50	1.85	2.35	9.27	11.17
Cr ₂ O ₃	26.36	40.37	35.10	36.66	30.57	31.72	29.22	33.77
V ₂ O ₃	0.00	0.00	0.00	0.00	0.00	0.00	0.00	0.00
Fe ₂ O ₃	26.42	10.20	5.00	0.00	35.22	32.29	28.22	9.30
FeO	28.58	22.72	23.16	9.89	28.04	27.80	27.88	22.11
MnO	0.48	0.40	0.34	0.35	0.56	0.42	0.68	0.41
MgO	3.31	4.80	8.06	7.84	2.32	2.25	3.04	3.78
CaO	0.02	0.00	0.00	0.00	0.01	0.02	0.01	0.00
ZnO	0.00	0.00	0.00	0.00	0.00	0.00	0.00	0.00
TOTAL	98.89	89.36	98.24	78.48	99.21	97.45	98.81	81.15
Mineral Formula Calculated Based on 32 Oxygen Basis								
Si	0.09	0.00	0.00	0.00	0.00	0.01	0.05	0.08
Ti	0.08	0.07	0.05	0.05	0.14	0.13	0.07	0.09
Al	4.29	3.79	7.89	8.62	0.65	0.84	3.12	4.40
Cr	5.82	9.73	7.05	9.02	7.19	7.56	6.59	8.92
V	0.00	0.00	0.00	0.00	0.00	0.00	0.00	0.00
Fe(iii)	5.55	2.34	0.96	0.00	7.88	7.33	6.06	2.34
Fe(ii)	6.67	5.79	4.92	2.58	6.97	7.01	6.65	6.18
Mn	0.11	0.10	0.07	0.09	0.14	0.11	0.17	0.12
Mg	1.38	2.18	3.05	3.64	1.03	1.01	1.29	1.88
Ca	0.00	0.00	0.00	0.00	0.00	0.01	0.00	0.00
Zn	0.00	0.00	0.00	0.00	0.00	0.00	0.00	0.00
TOTAL	24.00	24.00	24.00	24.00	24.00	24.00	24.00	24.00
Fe/Fe+Mg	0.90	0.79	0.66	0.41	0.94	0.93	0.91	0.82
Cr/Cr+Al	0.58	0.72	0.47	0.51	0.92	0.90	0.68	0.67
Fe(ii)	6.67	5.79	4.92	4.32	6.97	7.01	6.65	6.18
Fe(iii)	5.55	2.34	0.96	-1.75	7.88	7.33	6.06	2.34
Fe ²⁺ /(Fe ²⁺ +Fe ³⁺)	0.55	0.71	0.84	1.68	0.47	0.49	0.52	0.73
Fe ³⁺ /(Fe ³⁺ +Fe ²⁺)	0.45	0.29	0.16	-0.68	0.53	0.51	0.48	0.27

Table 5.4: Contd-----

Sample No.→ Wt% Oxide↓	1-TP	1-TP	1-TP	1-TP	1-TP	1-TP	1-TP	1-TP
Point#	39 / 1	41 / 1	42 / 1	44 / 1	45 / 1	54 / 1	55 / 1	56 / 1
SiO ₂	0.00	0.12	0.00	0.00	0.00	0.00	0.00	0.00
TiO ₂	0.41	0.58	0.40	0.37	0.40	0.47	0.33	0.40
Al ₂ O ₃	10.87	11.51	10.69	11.75	11.58	12.68	13.70	10.69
Cr ₂ O ₃	38.55	31.61	38.14	36.91	37.48	41.03	40.73	34.66
V ₂ O ₃	0.00	0.00	0.00	0.00	0.00	0.00	0.00	0.00
Fe ₂ O ₃	16.60	21.62	16.51	17.54	19.17	12.53	12.15	23.26
FeO	26.16	27.38	23.86	26.34	24.21	24.89	25.38	24.61
MnO	0.37	0.54	0.34	0.24	0.28	0.51	0.46	0.47
MgO	4.24	3.46	5.33	4.32	6.02	5.27	5.11	5.61
CaO	0.00	0.00	0.00	0.01	0.00	0.01	0.00	0.00
ZnO	0.00	0.00	0.00	0.00	0.00	0.00	0.00	0.00
TOTAL	97.20	96.82	95.26	97.48	99.14	97.38	97.85	99.70
Mineral Formula Calculated Based on 32 Oxygen Basis								
Si	0.00	0.03	0.00	0.00	0.00	0.00	0.00	0.00
Ti	0.09	0.12	0.09	0.08	0.08	0.10	0.07	0.08
Al	3.64	3.88	3.61	3.90	3.74	4.16	4.45	3.47
Cr	8.65	7.15	8.65	8.22	8.13	9.02	8.89	7.55
V	0.00	0.00	0.00	0.00	0.00	0.00	0.00	0.00
Fe(iii)	3.54	4.66	3.56	3.72	3.96	2.62	2.52	4.82
Fe(ii)	6.21	6.55	5.72	6.21	5.56	5.79	5.86	5.67
Mn	0.09	0.13	0.08	0.06	0.07	0.12	0.11	0.11
Mg	1.79	1.47	2.28	1.81	2.46	2.19	2.10	2.30
Ca	0.00	0.00	0.00	0.00	0.00	0.00	0.00	0.00
Zn	0.00	0.00	0.00	0.00	0.00	0.00	0.00	0.00
TOTAL	24.00	24.00	24.00	24.00	24.00	24.00	24.00	24.00
Fe/Fe+Mg	0.84	0.88	0.80	0.85	0.79	0.79	0.80	0.82
Cr/Cr+Al	0.70	0.65	0.71	0.68	0.68	0.68	0.67	0.69
Fe(ii)	6.21	6.55	5.72	6.21	5.56	5.79	5.86	5.67
Fe(iii)	3.54	4.66	3.56	3.72	3.96	2.62	2.52	4.82
Fe ₂ /(Fe ₂ +Fe ₃)	0.64	0.58	0.62	0.63	0.58	0.69	0.70	0.54
Fe ₃ /(Fe ₃ +Fe ₂)	0.36	0.42	0.38	0.37	0.42	0.31	0.30	0.46

Table 5.4: Contd-----

Sample No.→ Wt% Oxide↓	1-TP	1-TP	1-TP	1-TP	1-TP	1-TP	1-TP	1-TP	1-TP
Point#	59 / 1	60 / 1	61 / 1	64 / 1	67 / 1	68 / 1	69 / 1	71 / 1	72 / 1
SiO ₂	0.29	0.00	0.00	0.00	0.01	0.00	0.00	0.00	0.00
TiO ₂	0.25	0.46	0.41	0.96	0.55	0.62	0.24	0.30	0.55
Al ₂ O ₃	8.06	10.27	11.21	12.63	16.87	15.65	17.72	12.19	4.88
Cr ₂ O ₃	28.44	33.23	33.09	37.96	34.67	34.38	39.86	46.39	32.32
V ₂ O ₃	0.00	0.00	0.00	0.00	0.00	0.00	0.00	0.00	0.00
Fe ₂ O ₃	30.56	24.66	24.69	15.61	14.30	16.64	7.54	8.93	30.83
FeO	29.38	23.79	24.40	26.20	26.85	24.76	26.49	25.66	27.44
MnO	0.23	0.32	0.38	0.58	0.52	0.36	0.42	0.48	0.57
MgO	2.46	6.03	5.95	4.94	4.68	6.03	4.61	5.00	3.12
CaO	0.02	0.00	0.00	0.00	0.00	0.00	0.02	0.01	0.00
ZnO	0.00	0.00	0.00	0.00	0.00	0.00	0.00	0.00	0.00
TOTAL	99.67	98.76	100.13	98.88	98.45	98.45	96.89	98.97	99.72
Mineral Formula Calculated Based on 32 Oxygen Basis									
Si	0.08	0.00	0.00	0.00	0.00	0.00	0.00	0.00	0.00
Ti	0.05	0.10	0.08	0.20	0.11	0.13	0.05	0.06	0.12
Al	2.72	3.36	3.61	4.10	5.40	5.00	5.72	3.95	1.66
Cr	6.43	7.29	7.15	8.27	7.45	7.36	8.63	10.08	7.39
V	0.00	0.00	0.00	0.00	0.00	0.00	0.00	0.00	0.00
Fe(iii)	6.58	5.15	5.07	3.24	2.92	3.39	1.55	1.85	6.71
Fe(ii)	7.03	5.52	5.57	6.03	6.10	5.61	6.06	5.90	6.64
Mn	0.06	0.08	0.09	0.14	0.12	0.08	0.10	0.11	0.14
Mg	1.05	2.49	2.42	2.03	1.90	2.43	1.88	2.05	1.35
Ca	0.01	0.00	0.00	0.00	0.00	0.00	0.01	0.00	0.00
Zn	0.00	0.00	0.00	0.00	0.00	0.00	0.00	0.00	0.00
TOTAL	24.00	24.00	24.00	24.00	24.00	24.00	24.00	24.00	24.00
Fe/Fe+Mg	0.93	0.81	0.81	0.82	0.83	0.79	0.80	0.79	0.91
Cr/Cr+Al	0.70	0.68	0.66	0.67	0.58	0.60	0.60	0.72	0.82
Fe(ii)	7.03	5.52	5.57	6.03	6.10	5.61	6.06	5.90	6.64
Fe(iii)	6.58	5.15	5.07	3.24	2.92	3.39	1.55	1.85	6.71
Fe ₂ /(Fe ₂ +Fe ₃)	0.52	0.52	0.52	0.65	0.68	0.62	0.80	0.76	0.50
Fe ₃ /(Fe ₃ +Fe ₂)	0.48	0.48	0.48	0.35	0.32	0.38	0.20	0.24	0.50

Table 5.4: Contd-----

Sample No.→ Wt% Oxide↓	1-TP	1-TP	2-TP	2-TP	2-TP	2-TP	2-TP	5-TP	5-TP
Point#	74/1	75/1	76 /1	81 /1	82/1	84 /1	90/1	104 /1	106/1
SiO ₂	0.00	0.00	0.03	0.00	0.03	0.01	0.00	0.00	0.00
TiO ₂	0.29	0.38	0.43	0.38	0.24	0.42	0.52	0.41	0.39
Al ₂ O ₃	11.19	10.50	18.66	11.95	12.83	13.82	14.15	11.21	12.66
Cr ₂ O ₃	43.68	38.07	34.64	42.21	43.37	43.42	40.00	46.32	41.86
V ₂ O ₃	0.00	0.00	0.00	0.00	0.00	0.00	0.00	0.00	0.00
Fe ₂ O ₃	13.13	19.57	14.36	12.39	10.12	9.03	13.14	10.79	13.93
FeO	24.49	23.51	21.14	25.43	24.42	24.63	24.88	23.11	23.76
MnO	0.39	0.32	0.25	0.36	0.33	0.33	0.43	0.00	0.00
MgO	5.65	6.19	8.66	4.95	5.52	5.68	5.84	6.87	6.68
CaO	0.00	0.00	0.00	0.01	0.00	0.00	0.00	0.02	0.01
ZnO	0.00	0.00	0.00	0.00	0.00	0.00	0.00	0.00	0.00
TOTAL	98.81	98.55	98.16	97.68	96.86	97.33	98.96	98.73	99.29
Mineral Formula Calculated Based on 32 Oxygen Basis									
Si	0.00	0.00	0.01	0.00	0.01	0.00	0.00	0.00	0.00
Ti	0.06	0.08	0.09	0.08	0.05	0.09	0.11	0.08	0.08
Al	3.63	3.43	5.78	3.93	4.21	4.49	4.52	3.61	4.04
Cr	9.52	8.34	7.20	9.31	9.55	9.46	8.58	10.01	8.96
V	0.00	0.00	0.00	0.00	0.00	0.00	0.00	0.00	0.00
Fe(iii)	2.72	4.08	2.84	2.60	2.12	1.87	2.68	2.22	2.84
Fe(ii)	5.65	5.45	4.65	5.93	5.69	5.68	5.64	5.28	5.38
Mn	0.09	0.08	0.05	0.09	0.08	0.08	0.10	0.00	0.00
Mg	2.32	2.56	3.39	2.06	2.29	2.33	2.36	2.80	2.70
Ca	0.00	0.00	0.00	0.00	0.00	0.00	0.00	0.01	0.00
Zn	0.00	0.00	0.00	0.00	0.00	0.00	0.00	0.00	0.00
TOTAL	24.00	24.00	24.00	24.00	24.00	24.00	24.0	24.00	24.00
Fe/Fe+Mg	0.78	0.79	0.69	0.81	0.77	0.76	0.78	0.73	0.75
Cr/Cr+Al	0.72	0.71	0.55	0.70	0.69	0.68	0.65	0.73	0.69
Fe(ii)	5.65	5.45	4.65	5.93	5.69	5.68	5.64	5.28	5.38
Fe(iii)	2.72	4.08	2.84	2.60	2.12	1.87	2.68	2.22	2.84
Fe ₂ /(Fe ₂ +Fe ₃)	0.67	0.57	0.62	0.70	0.73	0.75	0.68	0.70	0.65
Fe ₃ /(Fe ₃ +Fe ₂)	0.33	0.43	0.38	0.30	0.27	0.25	0.32	0.30	0.35

5.2.2 Mineral chemistry of magnetite ore samples

In this section, results of the EPMA of the opaque minerals (mainly magnetite, chrome-magnetite and chromite) present in different textural forms within Phokpur magnetite ore samples are discussed. Composition of spinel group minerals can be used as an important petrogenetic indicator which may help in discriminating tectonic setting (Kamanetsky et al., 2001). Study of the spinel group minerals from different host rocks/ores is also indicators of the physical and chemical conditions of subsolidus re-equilibration (Tan and Liu, 2016). Therefore, the mineral chemistry of Phokpur magnetite has also been studied to find out the various physico-chemical and tectonic environments responsible for its formation.

Under magmatic conditions, ilmenite and hematite form a complete rhombohedral solid solution series. Likewise, magnetite and ulvospinel also form a complete solid solution series, called the spinel series. Coexisting compositions depend on temperature and the fugacity (similar to partial pressure) of oxygen. Hence, iron and titanium contents of the iron ores (oxides) are very helpful to calculate the temperature and oxygen fugacity of the ore formation. Minerals that allow for determination of the temperature of formation of minerals are referred to as a geothermometer. Therefore, the example called the Iron-titanium oxide geothermometer. When the EPMA compositions of the Phokpur magnetite ore samples are plotted in the FeO-Fe₂O₃-TiO₂ ternary diagram (Fig. 5.1a, after Buddington and Lindsley, 1964), almost all points fall along the wustite-magnetite solid solution line. The wustite-magnetite formation is rare in nature stems most probably required low oxygen fugacity, moderate temperature (around 600°C) and low-silica environment, however, composition of wustite changes with temperature in the FeO-Fe₃O₄ system (Darken and Gurry, 1945; Myers and Eugster, 1983). The textural relationships of the minerals suggest that the Phokpur magnetite may have formed slightly later than chromite, can be both interstitial (Wang et al., 2008), which explains the unusual association of chromite with Phokpur magnetite in the NOB.

Compositional variations for wide range of mafic-ultramafic rocks derived from variable tectonic settings have been obtained from global spinel database (Barnes and

Roeder, 2001). Phokpur magnetite contains significant quantity of aluminium, which are classified in Cr-Al-Fe³⁺ ternary discrimination diagram (Fig. 5.1b, after Stevens, 1944). This also reflects that the Phokpur magnetite was formed from Al-chromite according to the following stages: Al-chromite (initial stage) → Fe-chromite (intermediate stage) → Cr-magnetite (final stage).

The composition of spinel group mineral (chromite) from Nuasahi-Sukinda deposit exhibits high Cr# (0.75 - 0.87; Mondal et al., 2006), and the primary composition of the chromite from the Nuggihalli schist belt also exhibits high Cr# (0.78 - 0.86; Mukherjee et al., 2010). Composition of the magnetite samples from Phokpur deposit exhibit extended range of Cr-number (0.47 - 0.92). In order to decipher the nature of the magnetite from Phokpur deposit, various discrimination diagrams are plotted. Cr₂O₃ vs. Al₂O₃ variation diagram plotted for Phokpur chrome-magnetite (Fig. 5.2a) shows that most of the samples fall in the stratiform chromitite field and some of them fall away from this field. According to Dick and Bullen (1984), chromian spinel with low Cr# (<0.60) is derived from oceanic crust whereas high Cr# (>0.60) belongs to volcanic arcs, stratiform complexes and oceanic plateau basalts. The compositional variation of Phokpur magnetite ore samples plotted in Al₂O₃ vs. TiO₂ diagrams (Fig. 5.2b) indicates that most of the points are associated to volcanic-arc with some contributions from MORB lineage. This may be emphasized here that the composition of spinel mineral from volcanic-arc and MORB trends is coincident with pronounced changes in the mantle petrological-geochemical characteristics and conditions of mantle melting (Kamanetsky et al., 2001). Further clarification about the tectonic setting is inferred from Cr₂O₃ vs. Al₂O₃ diagram (Fig. 5.2a) and found that they exhibit an arc-cumulate affinity, which is further substantiated from Al₂O₃ vs. TiO₂ diagrams (Fig. 5.2b). Some of the podiform chromite deposits show deformation as well as relict cumulus texture that may indicate disrupted stratiform layers (Thayer, 1969; Jackson and Thayer, 1972).

Compositional variation in Fe²⁺/Fe³⁺ versus Al₂O₃ diagram shows that the magnetite composition from Phokpur deposit falls exclusively in supra-subduction zone (SSZ) peridotites (Fig. 5.3a). Petrogenetic regeneration of magma in the SSZ conditions

suggests that they were formed during the early stages of subduction. Authentication from the SSZ sources suggests that the early formed magma was derived in response to the intra-oceanic subduction emerged in the partial melting of the hydrated oceanic lithosphere in the mantle wedge (Pearce et al., 1984; Stern and Bloomer, 1992). This led to the development of Fe-rich hydrothermal fluid responsible for the massive metasomatic replacement of Cr^{3+} by Fe^{3+} along grain boundaries and cracks of the pre-existing chromite and ultimately the formation of Phokpur magnetite deposit in the NOB.

Photomicrograph of a chromite phenocryst from Phokpur magnetite ore deposit (Fig. 5.4 A) shows development of Fe-oxide rims surrounding the grain boundary. BSE image (Fig. 5.4B) displays very fine thread like features of iron oxides developed around the chromite phenocryst, which most plausibly related to secondary processes of iron oxide precipitation. The EPMA generated X-ray elemental maps of Fe, Cr, O and Si for the chromite phenocryst from Phokpur magnetite ore sample reveal minor variation in Si, which concentration is slightly elevated at rims in the grain boundary regions. Most other elements display significant compositional variation (Fig. 5.4 C-F). The relatively strong intensity of the elemental variation makes it more complicated to interpret complex patterns of developed due to remobilization of elements during secondary processes. Specially, X-ray maps of Fe and O displays similar enrichment pattern in the chromite phenocryst.

The EPMA line scans along X-Y profile for the phenocryst shown in Fig. 5.5 displays significant compositional variations in FeO^t and Cr_2O_3 (Table 5.5). Along the X-Y profile, FeO^t is depleted inside the phenocryst whereas Cr_2O_3 is enriched. At the grain boundary of the chromite phenocrysts, high enrichment of FeO^t is observed which indicates development of magnetite rims around the chromite phenocryst in the Phokpur magnetite ore deposit.

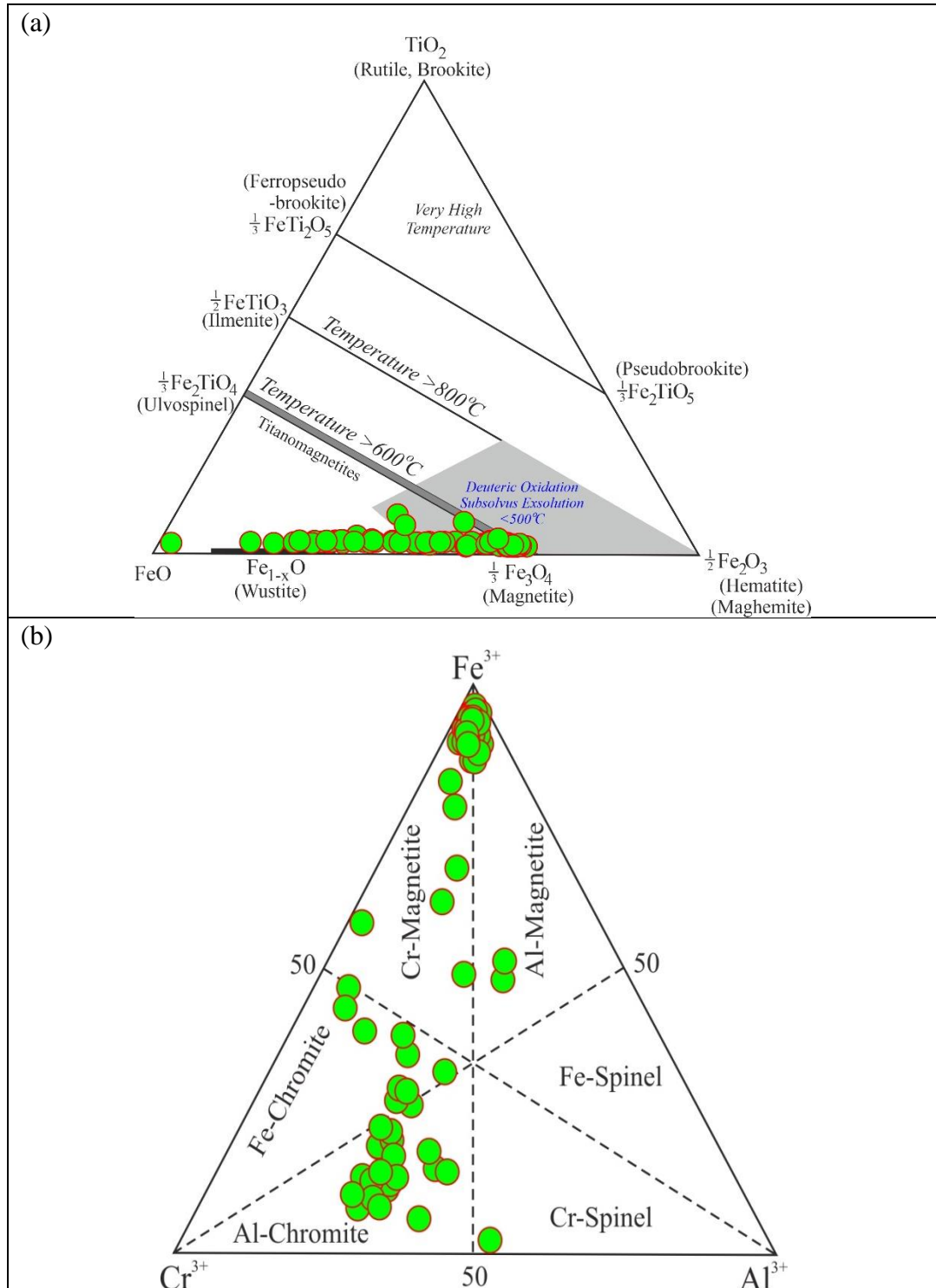


Fig. 5.1: (a) Composition of spinel group minerals plotted in TiO₂-FeO-Fe₂O₃ ternary diagram (Buddington and Lindsley, 1964) showing major solid solution series in mole percent. (b) Cr³⁺ – Fe³⁺ + Al³⁺ diagram (after Stevens, 1944) plotted for the Phokpur magnetite.

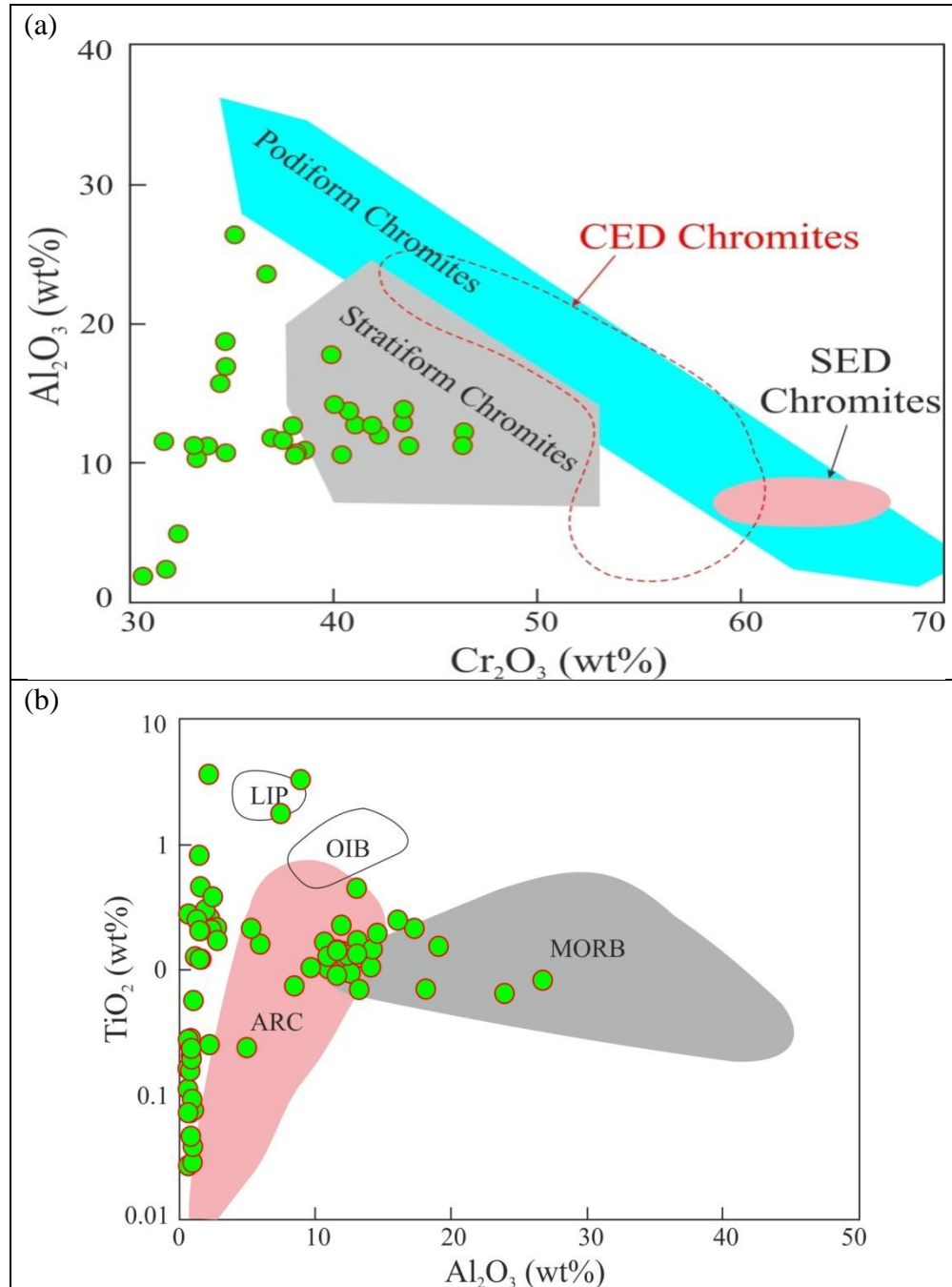


Figure 5.2: (a) Cr_2O_3 versus Al_2O_3 diagrams of spinel group. Compositional fields of podiform chromitites from the central (CED) and southern (SED) parts of the Eastern Desert of Egypt (after Ahmed et al., 2001) are given for comparison. The podiform and stratiform fields are from Bonavia et al. (1993). (b) Al_2O_3 versus TiO_2 variation in Cr-magnetite with respect to modern-day tectonic settings for Naga Ophiolites Belt at Phokpur, District Kiphire, Nagaland; different fields are from Kamenetsky et al. (2001).

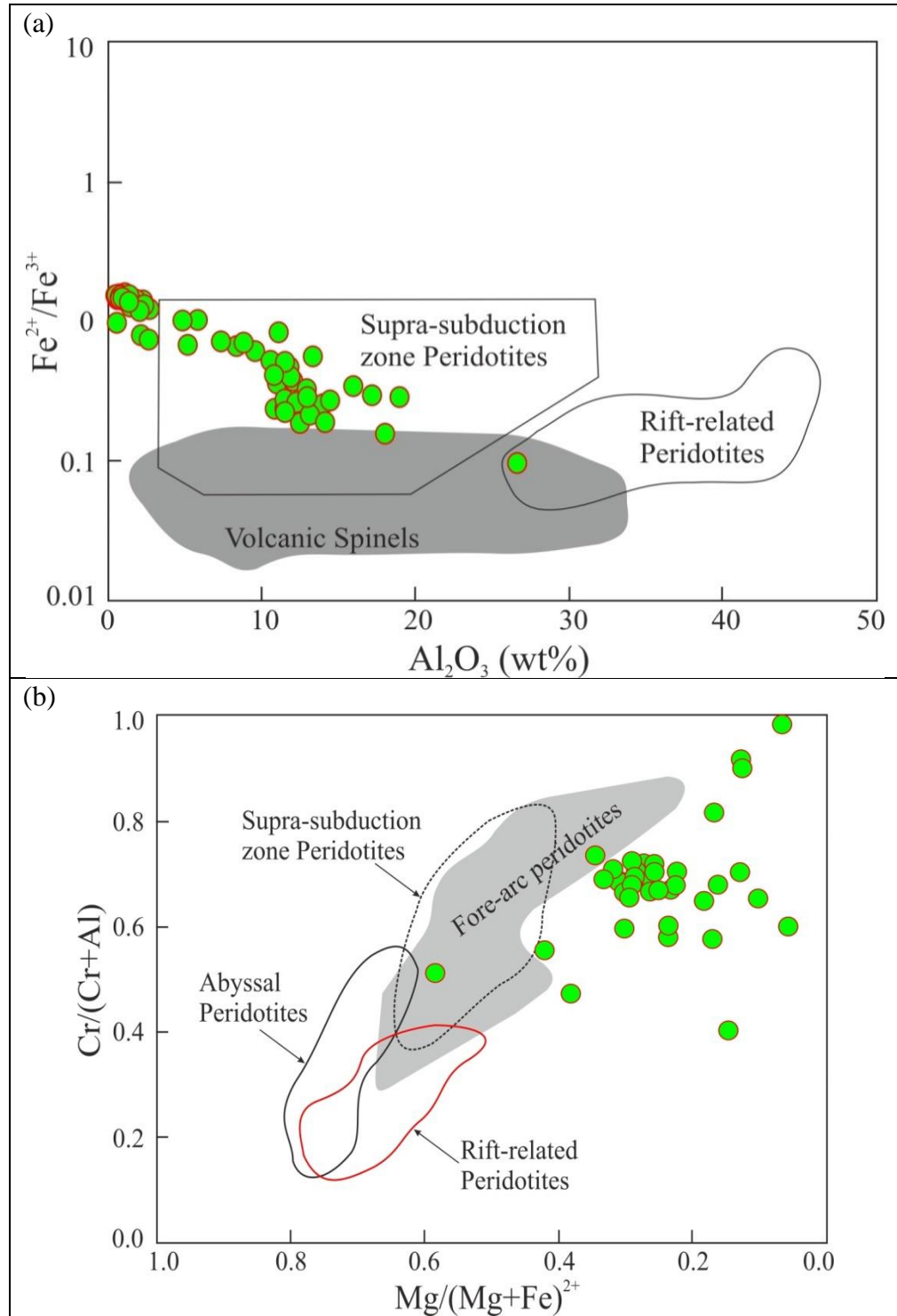


Figure 5.3: (a) $\text{Fe}^{2+}/\text{Fe}^{3+}$ versus Al_2O_3 variation diagram of Cr-magnetite from Nagaland ophiolite suites. Different fields are from Kamenetsky et al. (2001). (b) $\text{Cr}/(\text{Cr} + \text{Al})$ versus $\text{Mg}/(\text{Mg} + \text{Fe}^{2+})$ tectonic discrimination diagrams for chromites of Naga Ophiolites Belt at Phokpur, District Kiphire, Nagaland (Tamura and Arai, 2006).

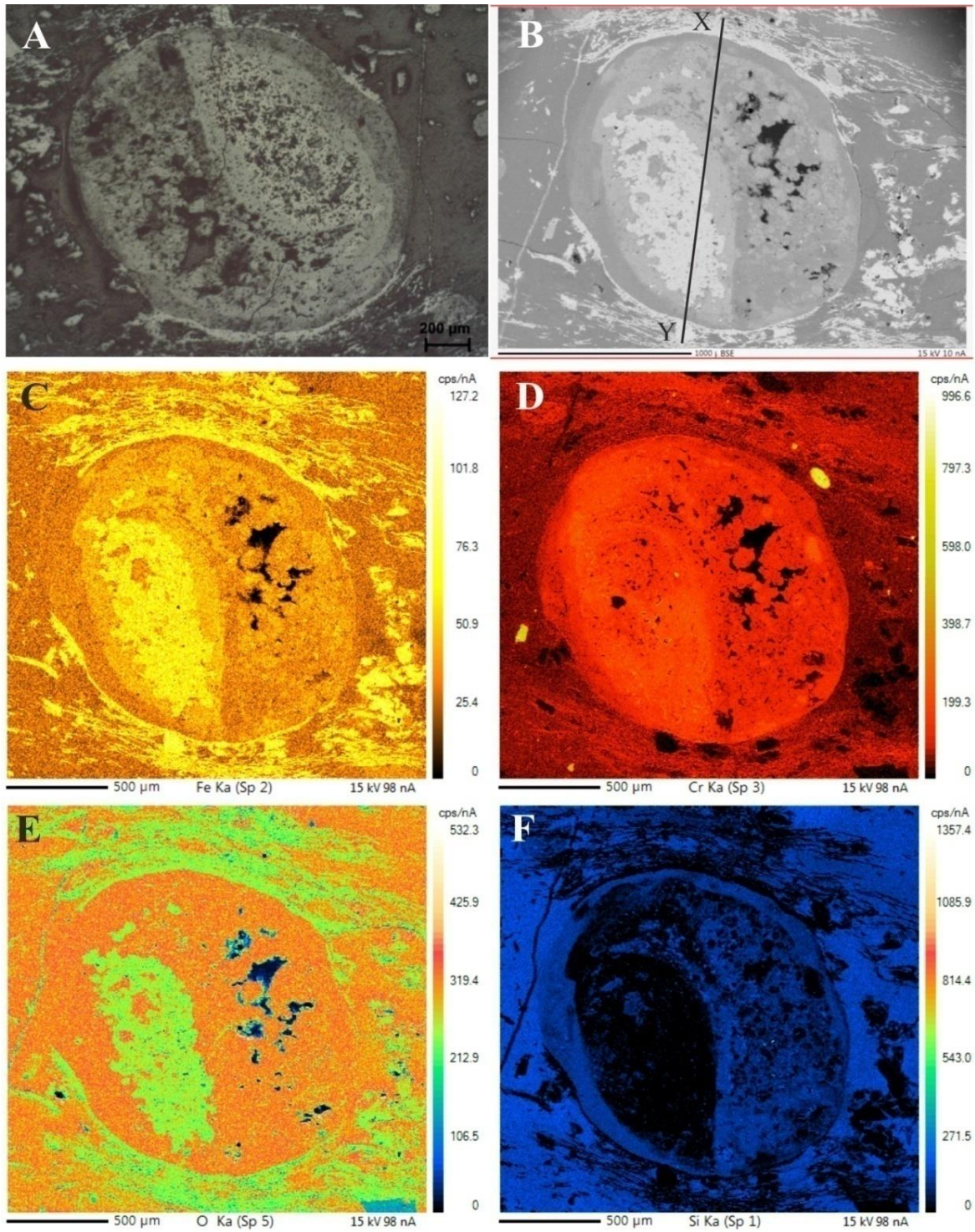


Figure 5.4: (a) Photomicrographs shows chromite crystal altered at margin to Cr-magnetite. (b) BSE images of chromite grain; XY line shown in the figure is used for the EPMA line scan for different oxides as displayed in Figure 8. (C – F) X-ray elemental maps for Fe, Cr, O and Si, respectively.

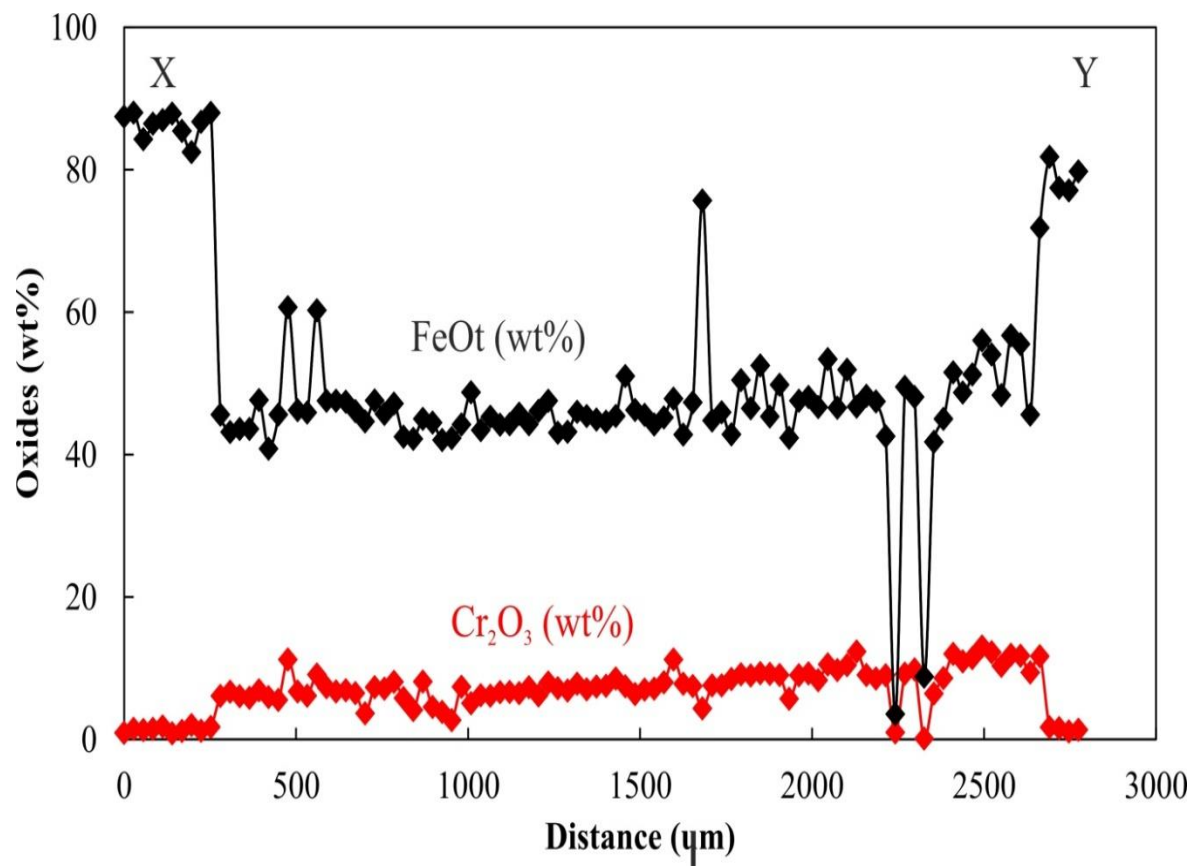


Figure 5.5: EPMA line scans along the line X-Y (as shown in Figure 12B) for various oxides in the studied Cr-magnetite grain.

Table 5.5: EPMA analyses of a selected chrome-magnetite phenocryst along X-Y line from the Phokpur magnetite ore samples of Naga Ophiolite Belt

Wt% Oxide	Cr-Mt	Cr-Mt	Cr-Mt	Cr-Mt	Cr-Mt	Cr-Mt	Cr-Mt	Cr-Mt	Cr-Mt	Cr-Mt
Sample Nos.	5-TP	5- TP	5-TP	5-TP	5-TP	5-TP	5-TP	5-TP	5-TP	5-TP
Point#	111/1	111/2	111/3	111/4	111/5	111/6	111/7	111/8	111/9	111/10
SiO ₂	1.11	1.01	1.02	1.24	0.90	0.82	0.78	1.45	0.92	0.89
TiO ₂	0.38	0.68	0.52	0.52	0.44	0.26	0.30	0.39	0.29	0.33
Al ₂ O ₃	0.53	0.90	0.91	1.26	0.67	0.45	0.45	1.67	0.55	0.68
Cr ₂ O ₃	0.93	1.47	1.32	1.48	1.80	0.84	1.18	2.00	1.20	1.73
V ₂ O ₃	0.00	0.00	0.00	0.00	0.00	0.00	0.00	0.00	0.00	0.00
FeO	87.43	87.99	84.28	86.46	86.95	87.88	85.43	82.45	86.71	87.97
MnO	0.00	0.00	0.00	0.00	0.00	0.00	0.00	0.00	0.00	0.00
MgO	0.00	0.02	0.01	0.03	0.00	0.00	0.00	0.01	0.03	0.00
CaO	0.05	0.10	0.08	0.07	0.08	0.06	0.07	0.06	0.05	0.08
ZnO	0.00	0.00	0.00	0.00	0.00	0.00	0.00	0.00	0.00	0.00
Total	90.43	92.17	88.13	91.06	90.83	90.31	88.22	88.03	89.75	91.70
Point#	111/11	111/12	111/13	111/14	111/15	111/16	111/17	111/18	111/19	111/20
SiO ₂	11.18	12.19	12.56	11.63	10.73	13.17	11.91	7.50	10.19	11.26
TiO ₂	1.66	1.57	1.41	6.10	3.21	1.89	4.31	2.71	1.41	1.07
Al ₂ O ₃	17.84	19.39	19.20	17.36	16.65	20.55	18.19	12.09	17.50	18.83
Cr ₂ O ₃	6.09	6.71	6.06	5.82	6.90	5.94	5.53	11.23	6.72	6.14
V ₂ O ₃	0.00	0.00	0.00	0.00	0.00	0.00	0.00	0.00	0.00	0.00
FeO	45.59	43.16	43.59	43.58	47.65	40.81	45.59	60.68	46.22	45.91
MnO	0.00	0.00	0.00	0.00	0.00	0.00	0.00	0.00	0.00	0.00
MgO	0.48	0.48	0.53	0.50	0.41	0.56	0.60	0.33	0.52	0.61
CaO	0.02	0.02	0.01	0.05	0.02	0.00	0.01	0.03	0.07	0.03
ZnO	0.00	0.00	0.00	0.00	0.00	0.00	0.00	0.00	0.00	0.00
Total	82.87	83.53	83.36	85.03	85.57	82.92	86.14	94.58	82.61	83.86

Table 5.5: Contd----

Wt% Oxide	Cr-Mt	Cr-Mt	Cr-Mt	Cr-Mt	Cr-Mt	Cr-Mt	Cr-Mt	Cr-Mt	Cr-Mt	Cr-Mt
Sample Nos.	5-TP	5-TP	5-TP	5-TP	5-TP	5-TP	5-TP	5-TP	5-TP	5-TP
Point#	111/21	111/22	111/23	111/24	111/25	111/26	111/27	111/28	111/29	111/30
SiO ₂	4.73	10.63	9.86	9.99	10.61	16.58	8.75	11.25	9.24	13.87
TiO ₂	2.28	1.56	1.37	1.45	1.30	0.57	1.82	1.78	2.07	1.05
Al ₂ O ₃	9.70	17.06	17.47	17.99	17.67	20.94	15.53	18.63	16.09	19.99
Cr ₂ O ₃	9.10	7.33	6.74	6.90	6.51	3.64	7.33	7.11	8.07	5.81
V ₂ O ₃	0.00	0.00	0.00	0.00	0.00	0.00	0.00	0.00	0.00	0.00
FeO	60.24	47.56	47.55	47.41	46.09	44.66	47.58	45.71	47.17	42.49
MnO	0.00	0.00	0.00	0.00	0.00	0.00	0.00	0.00	0.00	0.00
MgO	0.25	0.43	0.46	0.44	0.51	0.58	0.42	0.50	0.39	0.56
CaO	0.05	0.03	0.02	0.01	0.02	0.01	0.01	0.01	0.01	0.01
ZnO	0.00	0.00	0.00	0.00	0.00	0.00	0.00	0.00	0.00	0.00
Total	86.36	84.60	83.47	84.17	82.70	86.98	81.45	85.00	83.04	83.79
Point#	111/31	111/32	111/33	111/34	111/35	111/36	111/37	111/38	111/39	111/40
SiO ₂	15.74	11.44	13.69	17.87	18.08	12.70	12.02	13.60	11.59	12.61
TiO ₂	0.72	2.03	0.98	0.58	0.32	1.76	1.81	1.16	1.41	1.41
Al ₂ O ₃	20.57	18.45	20.68	22.47	22.45	18.92	16.84	20.66	18.13	19.99
Cr ₂ O ₃	4.12	8.12	4.56	3.86	2.69	7.40	5.09	6.19	6.13	6.63
V ₂ O ₃	0.00	0.00	0.00	0.00	0.00	0.00	0.00	0.00	0.00	0.00
FeO	42.19	44.99	44.49	42.02	42.31	44.22	48.73	43.43	45.32	44.19
MnO	0.00	0.00	0.00	0.00	0.00	0.00	0.00	0.00	0.00	0.00
MgO	0.76	0.47	0.54	1.02	0.74	0.47	0.50	0.58	0.53	0.58
CaO	0.00	0.00	0.01	0.00	0.00	0.00	0.00	0.00	0.01	0.00
ZnO	0.00	0.00	0.00	0.00	0.00	0.00	0.00	0.00	0.00	0.00
Total	84.09	85.50	84.94	87.82	86.59	85.47	84.99	85.62	83.11	85.41

Table 5.5: Contd----

Wt% Oxide	Cr-Mt	Cr-Mt	Cr-Mt	Cr-Mt	Cr-Mt	Cr-Mt	Cr-Mt	Cr-Mt	Cr-Mt	Cr-Mt
Sample Nos	5-TP	5-TP	5-TP	5-TP	5-TP	5-TP	5-TP	5-TP	5-TP	5-TP
Point#	111/41	111/42	111/43	111/44	111/45	111/46	111/47	111/48	111/49	111/50
SiO ₂	12.67	11.74	11.24	11.24	9.02	12.53	12.43	11.48	11.32	11.45
TiO ₂	1.32	1.34	1.81	1.31	2.18	1.46	1.51	1.80	1.46	1.58
Al ₂ O ₃	18.99	19.70	17.31	18.56	15.14	19.84	18.96	18.91	17.36	19.10
Cr ₂ O ₃	6.65	6.48	7.33	6.18	7.99	7.21	6.86	7.81	7.02	7.43
V ₂ O ₃	0.00	0.00	0.00	0.00	0.00	0.00	0.00	0.00	0.00	0.00
FeO	44.25	45.74	44.24	46.13	47.55	43.05	43.19	45.99	45.41	44.91
MnO	0.00	0.00	0.00	0.00	0.00	0.00	0.00	0.00	0.00	0.00
MgO	0.57	0.58	0.52	0.48	0.41	0.53	0.49	0.43	0.45	0.48
CaO	0.00	0.01	0.01	0.00	0.01	0.00	0.00	0.01	0.01	0.00
ZnO	0.00	0.00	0.00	0.00	0.00	0.00	0.00	0.00	0.00	0.00
Total	84.47	85.59	82.47	83.89	82.28	84.62	83.43	86.43	83.04	84.95
Point#	111/51	111/52	111/53	111/54	111/55	111/56	111/57	111/58	111/59	111/60
SiO ₂	11.41	9.71	6.86	11.05	11.11	13.00	10.02	9.92	12.28	9.33
TiO ₂	1.70	2.13	1.87	1.22	1.37	1.31	2.07	2.64	1.66	1.48
Al ₂ O ₃	17.61	14.71	13.75	18.94	17.83	19.68	15.50	16.66	18.06	16.97
Cr ₂ O ₃	7.52	8.54	7.46	6.36	6.98	7.11	8.02	11.21	7.82	7.50
V ₂ O ₃	0.00	0.00	0.00	0.00	0.00	0.00	0.00	0.00	0.00	0.00
FeO	44.62	45.41	51.02	46.28	45.57	44.22	45.21	47.85	42.79	47.33
MnO	0.00	0.00	0.00	0.00	0.00	0.00	0.00	0.00	0.00	0.00
MgO	0.48	0.39	0.28	0.55	0.44	0.52	0.46	0.40	0.42	0.42
CaO	0.00	0.01	0.01	0.02	0.00	0.01	0.02	0.03	0.01	0.02
ZnO	0.00	0.00	0.00	0.00	0.00	0.00	0.00	0.00	0.00	0.00
Total	83.34	80.90	81.25	84.43	83.30	85.85	81.29	88.72	83.05	83.05

Table 5.5: Contd----

Wt% Oxide	Cr-Mt	Cr-Mt	Cr-Mt	Cr-Mt	Cr-Mt	Cr-Mt	Cr-Mt	Cr-Mt	Cr-Mt	Cr-Mt
Sample No.	5-TP	5-TP	5-TP	5-TP	5-TP	5-TP	5-TP	5-TP	5-TP	5-TP
Point#	111/61	111/62	111/63	111/64	111/65	111/66	111/67	111/68	111/69	111/70
SiO ₂	1.58	10.77	10.24	11.43	7.27	7.10	5.02	10.11	5.86	13.45
TiO ₂	1.63	1.69	1.65	1.70	2.32	2.34	2.27	2.12	2.26	0.92
Al ₂ O ₃	4.49	17.69	16.21	18.63	12.35	13.54	11.55	16.46	12.08	21.49
Cr ₂ O ₃	4.37	7.57	7.60	8.47	9.14	8.97	9.30	9.22	9.03	5.70
V ₂ O ₃	0.00	0.00	0.00	0.00	0.00	0.00	0.00	0.00	0.00	0.00
FeO	75.67	44.78	45.92	42.83	50.44	46.48	52.51	45.34	49.79	42.33
MnO	0.00	0.00	0.00	0.00	0.00	0.00	0.00	0.00	0.00	0.00
MgO	0.05	0.46	0.41	0.47	0.32	0.34	0.28	0.42	0.26	0.86
CaO	0.06	0.01	0.01	0.00	0.01	0.02	0.03	0.00	0.04	0.00
ZnO	0.00	0.00	0.00	0.00	0.00	0.00	0.00	0.00	0.00	0.00
Total	87.85	82.96	82.04	83.54	81.85	78.79	80.96	83.66	79.32	84.75
Point#	111/71	111/72	111/73	111/74	111/75	111/76	111/77	111/78	111/79	111/80
SiO ₂	7.13	7.69	8.71	3.60	8.79	5.64	0.46	7.12	8.35	8.39
TiO ₂	2.05	1.93	1.67	2.60	1.95	2.60	2.87	2.92	1.94	1.97
Al ₂ O ₃	13.74	14.83	16.27	10.43	14.72	10.70	4.39	13.52	14.64	16.31
Cr ₂ O ₃	9.01	9.27	8.31	10.53	9.73	10.44	12.35	9.03	8.53	9.01
V ₂ O ₃	0.00	0.00	0.00	0.00	0.00	0.00	0.00	0.00	0.00	0.00
FeO	47.53	48.06	46.67	53.39	46.55	51.92	46.72	48.25	47.46	42.56
MnO	0.00	0.00	0.00	0.00	0.00	0.00	0.00	0.00	0.00	0.00
MgO	0.32	0.36	0.40	0.20	0.42	0.26	0.00	0.35	0.37	0.25
CaO	0.01	0.04	0.03	0.03	0.04	0.03	0.05	0.01	0.06	0.52
ZnO	0.00	0.00	0.00	0.00	0.00	0.00	0.00	0.00	0.00	0.00
Total	79.80	82.19	82.05	80.77	82.20	81.59	66.85	81.22	81.34	79.01

Table 5.5: Contd----

Wt% Oxide	Cr-Mt	Cr-Mt	Cr-Mt	Cr-Mt	Cr-Mt	Cr-Mt	Cr-Mt	Cr-Mt	Cr-Mt	Cr-Mt
Sample Nos.	5-TP	5-TP	5-TP	5-TP	5-TP	5-TP	5-TP	5-TP	5-TP	5-TP
Point#	111/81	111/82	111/83	111/84	111/85	111/86	111/87	111/88	111/89	111/90
SiO ₂	0.28	6.57	6.90	4.65	13.68	10.66	3.92	6.09	4.43	3.08
TiO ₂	0.00	1.97	1.88	0.00	1.14	1.37	2.35	2.08	2.39	2.60
Al ₂ O ₃	0.90	13.25	13.89	5.79	8.99	17.13	9.97	12.98	10.59	8.43
Cr ₂ O ₃	0.98	9.22	9.83	0.13	6.42	8.60	12.01	10.95	11.40	13.03
V ₂ O ₃	0.00	0.00	0.00	0.00	0.00	0.00	0.00	0.00	0.00	0.00
FeO	3.55	49.50	48.07	8.81	41.78	45.01	51.54	48.71	51.24	56.04
MnO	0.00	0.00	0.00	0.00	0.00	0.00	0.00	0.00	0.00	0.00
MgO	0.00	0.26	0.28	0.12	0.59	0.47	0.16	0.30	0.12	0.11
CaO	34.64	0.08	0.22	32.69	1.11	0.06	0.05	0.07	0.05	0.05
ZnO	0.00	0.00	0.00	0.00	0.00	0.00	0.00	0.00	0.00	0.00
Total	40.35	80.84	81.06	52.20	73.70	83.29	80.00	81.18	80.22	83.33
Point#	111/91	111/92	111/93	111/94	111/95	111/96	111/97	111/98	111/99	111/100
SiO ₂	2.67	6.44	1.80	2.19	9.85	0.33	3.08	3.59	4.71	4.13
TiO ₂	2.58	2.10	2.79	2.73	1.99	2.91	0.50	0.44	0.27	0.44
Al ₂ O ₃	8.22	13.18	6.61	7.51	15.32	3.89	4.01	5.05	6.33	5.19
Cr ₂ O ₃	12.25	10.31	11.87	11.75	9.41	11.69	1.71	1.59	1.13	1.36
V ₂ O ₃	0.00	0.00	0.00	0.00	0.00	0.00	0.00	0.00	0.00	0.00
FeO	54.05	48.33	56.73	55.49	45.62	71.84	81.79	77.43	77.10	79.76
MnO	0.00	0.00	0.00	0.00	0.00	0.00	0.00	0.00	0.00	0.00
MgO	0.10	0.24	0.05	0.10	0.40	0.00	0.10	0.14	0.22	0.19
CaO	0.08	0.03	0.05	0.12	0.02	0.07	0.07	0.04	0.07	0.02
ZnO	0.00	0.00	0.00	0.00	0.00	0.00	0.00	0.00	0.00	0.00
Total	79.95	80.62	79.92	79.90	82.61	90.74	91.26	88.28	89.84	91.10

5.2.3. Mineral chemistry of chlorite

Chlorite is the main silicate mineral identified during EPMA studies and present in substantial amount within the matrix of Phokpur magnetite ore samples. Therefore, in this section, results of the EPMA (Table 5.6) of chlorite grains are discussed to know their mineralogical characteristics.

When the EPMA data are plotted (Fig.5.6) in representation of the compositional fields of Mg-chlorite and Fe-chlorite depending on the dominant cation (after Zane & Weiss, 1998), all the points fall in the compositional field of Fe-rich chlorite (chamosite) having chemical composition iron-aluminium silicates $[\text{Fe}^{+2}\text{Al}(\text{Mg}, \text{Fe}^{+3})(\text{Si}_3\text{Al})\text{O}_{10}(\text{OH})_8]$.

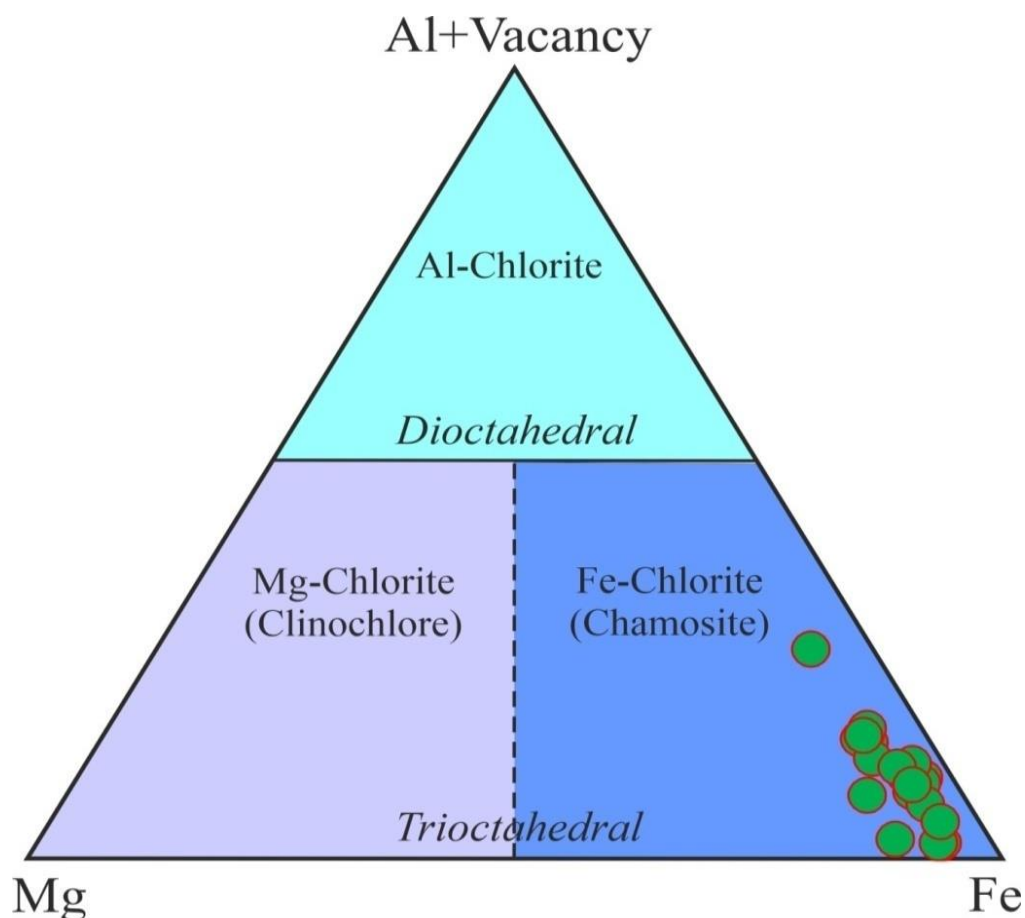


Fig.5.6: Mineral composition of chlorites from Phokpur magnetite ore samples from NOB plotted in representation of the compositional fields of Mg-chlorites and Fe-chlorites depending on the dominant cation (after Zane & Weiss, 1998).

When the chemical composition of chlorites is plotted in FeO-MgO-Al₂O₃ triangular diagram (Fig.5.7) for end-members of chlorite (Fleming and Fawcett, 1976), it shows the substitution between FeO and Al₂O₃ only, which is out of box, and not the characteristic of normal chlorite. It appears new type of chlorite formed under mafic/ultra-mafic system.

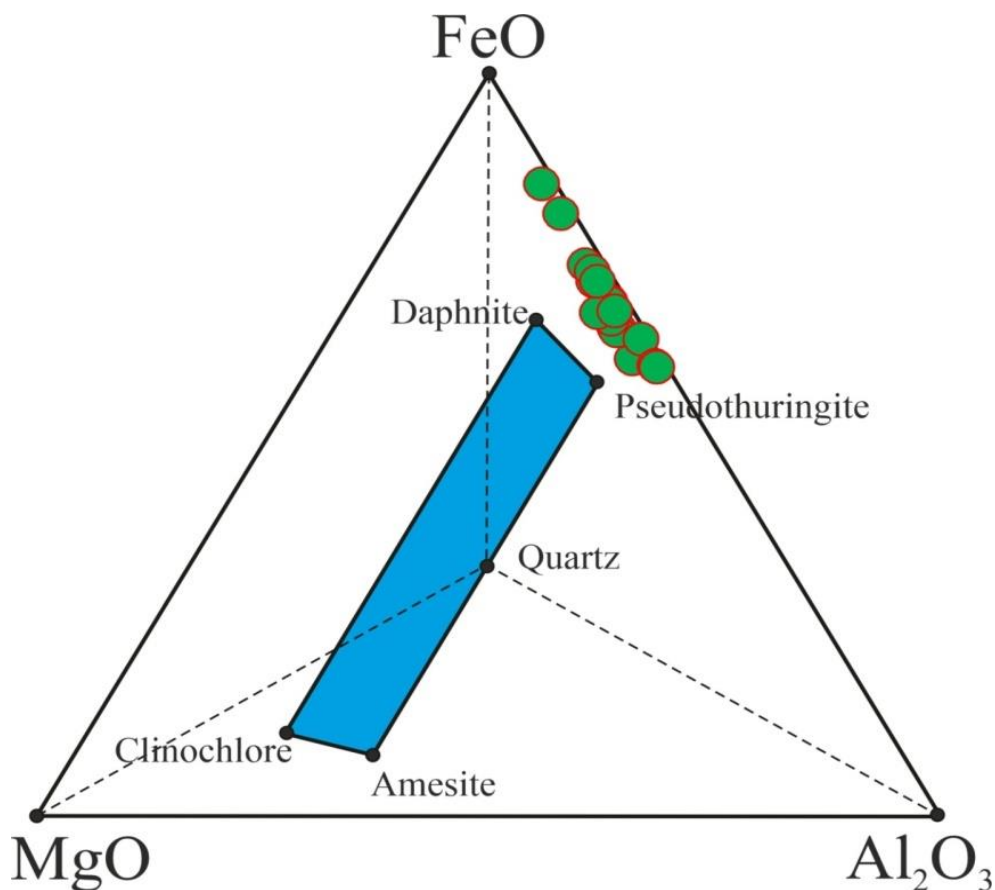


Fig.5.7: Mineral composition of chlorites from Phokpur magnetite ore samples from NOB plotted in FeO-MgO-Al₂O₃ triangular diagram for end-members of chlorite (Fleming and Fawcett, 1976).

The chemical composition of chlorites is plotted in SiO₂ – (MgO + FeO) – Al₂O₃ ternary diagram (Fig.5.8) of chlorite end-members and the substitution considered in chlorite solid solution model (Vidal et al., 2001). It shows the affinity towards Tschermak (TK) substitution, which is prominent between clinocllore-daphnite and amesite than di-trioctahedral substitution.

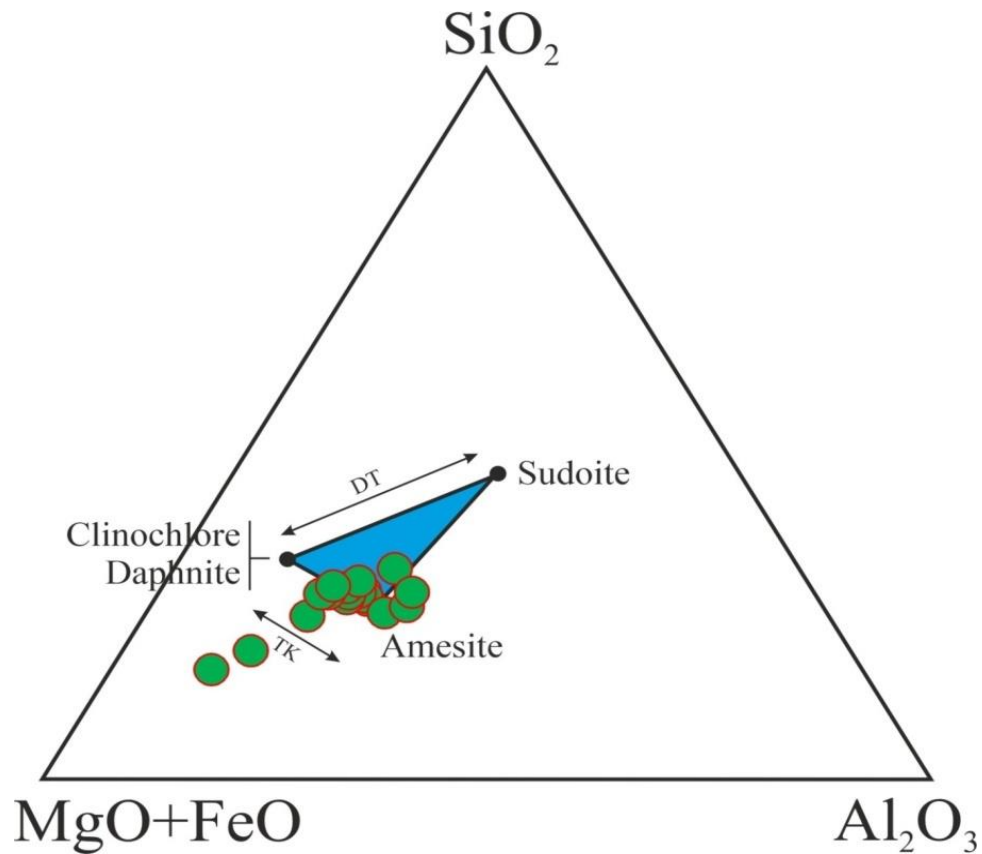


Fig.5.8. Mineral composition of chlorites from Phokpur magnetite ore samples from NOB. $\text{SiO}_2 - (\text{MgO} + \text{FeO}) - \text{Al}_2\text{O}_3$ ternary diagram of chlorite end-members and substitution considered in chlorite solid solution model (Vidal et al., 2001).

Further, when the chemical composition of chlorites is plotted in projection field (R^{2+} -Si diagram, Fig.5.9) for chlorite compositions (after Wiewiora & Weiss 1990; Bourdelle and Cathelineau, 2015), the plotted points does not fall in any standard solid solution diagram. All the plotted points (data) cannot be explained in the existing model. Therefore the chlorite of the study area, derived from the mafic/ultramafic system, may be kept under special category, and needs further detailed study to decipher the possible explanation for its formation. This diagram can also be used for estimating the temperature conditions of formation of the chlorites. Majority of the plotted points concentrate between 300 to 600 °C temperatures. Therefore it can be said that the chlorite of the Phokpur magnetite deposit is formed in the temperature range of 600 to 300 °C. Here, it may also be mentioned that from the $\text{FeO}-\text{Fe}_2\text{O}_3-\text{TiO}_2$ ternary diagram (Fig. 5.1a), the temperature of wustite- magnetite formation is also estimated around 600 °C.

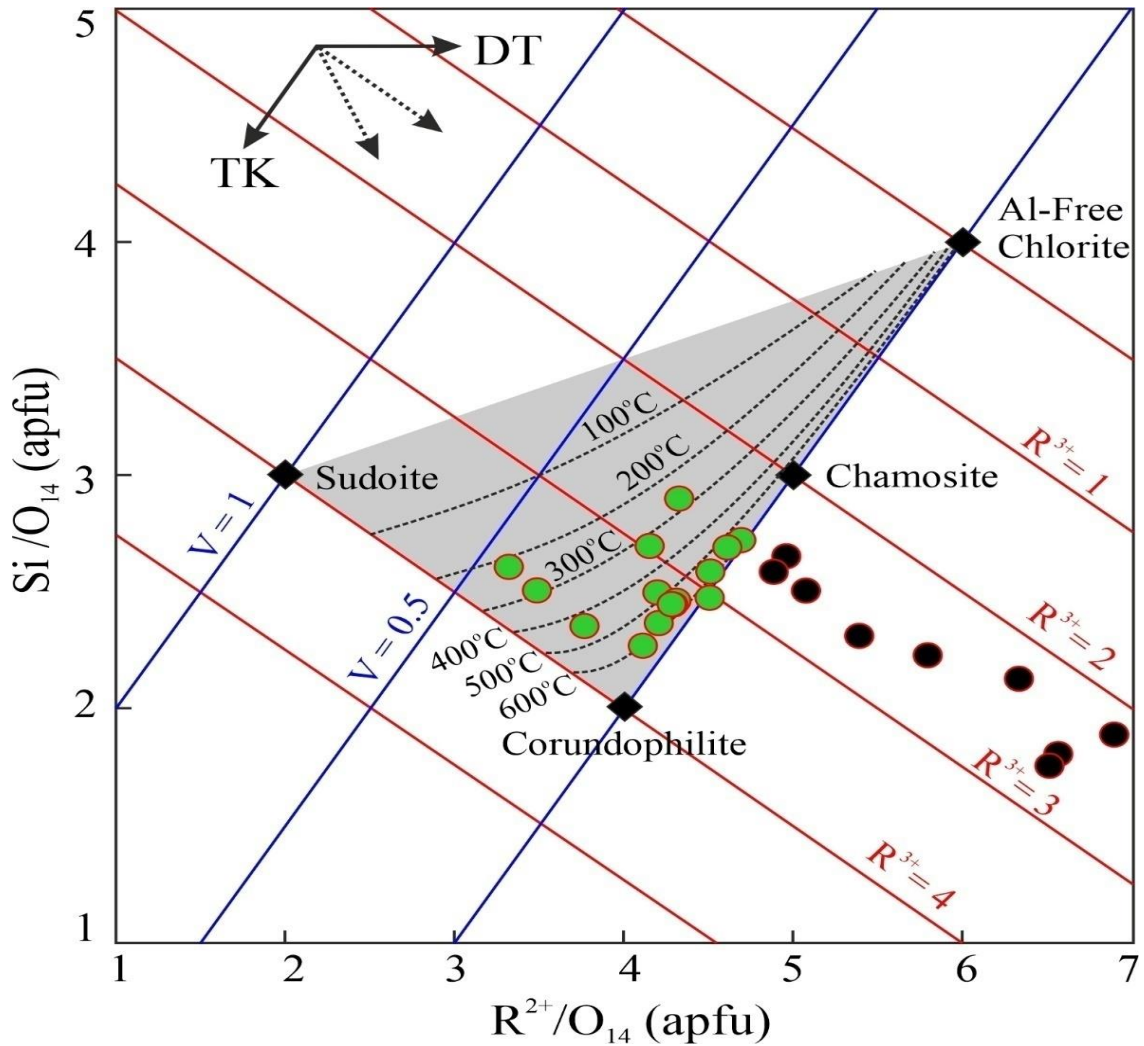


Fig.5.9: Mineral composition of chlorites from Phokpur magnetite ore samples from NOB plotted in projection field (R^{2+} -Si diagram) for chlorite compositions (after Wiewiora & Weiss 1990; Bourdelle and Cathelineau, 2015).

To show the sympathetic or antipathetic relation between the various elements, the Harker's variation diagrams of NiO versus MnO (Fig. 5.10), NiO versus FeO (Fig. 5.11), Cr_2O_3 versus SiO_2 (Fig. 5.12), Cr_2O_3 versus Al_2O_3 (Fig. 5.13), Cr_2O_3 versus FeO (Fig. 5.14) and Cr_2O_3 versus NiO (Fig. 5.15) are plotted. They reflect that in the chlorites of Phokpur magnetite samples, there is a sympathetic relationship between NiO and MnO, and antipathetic relationship between NiO and FeO. Since there are no definite trends between Cr_2O_3 versus SiO_2 , Cr_2O_3 versus Al_2O_3 , Cr_2O_3 versus FeO, and Cr_2O_3 versus NiO; their binary relationships could not be determined.

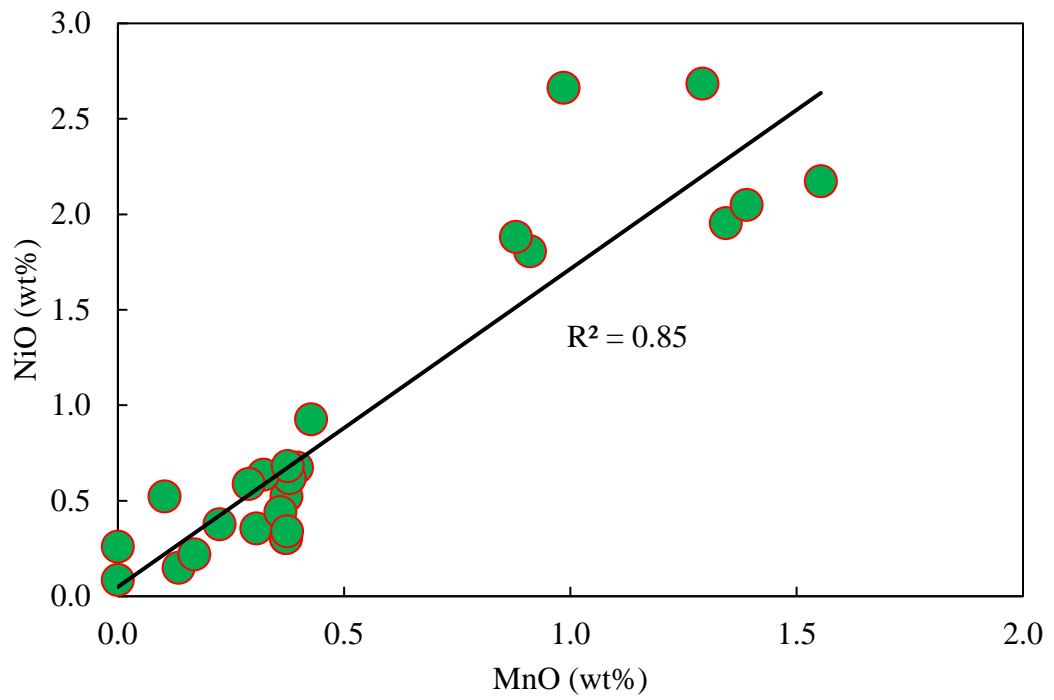
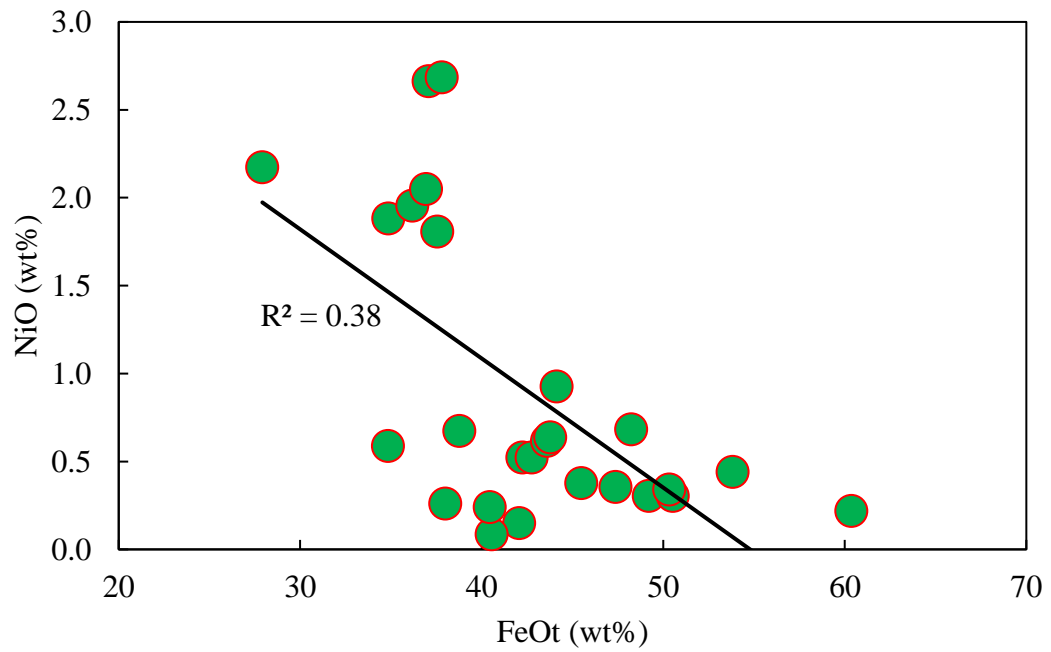


Fig.5.10: Correlation between MnO and NiO content of chlorite from the Phokpur magnetite ore samples from NOB.

Fig.5.11: Correlation between FeO_t and N



content of chlorite from the Phokpur magnetite ore samples from NOB.

iO

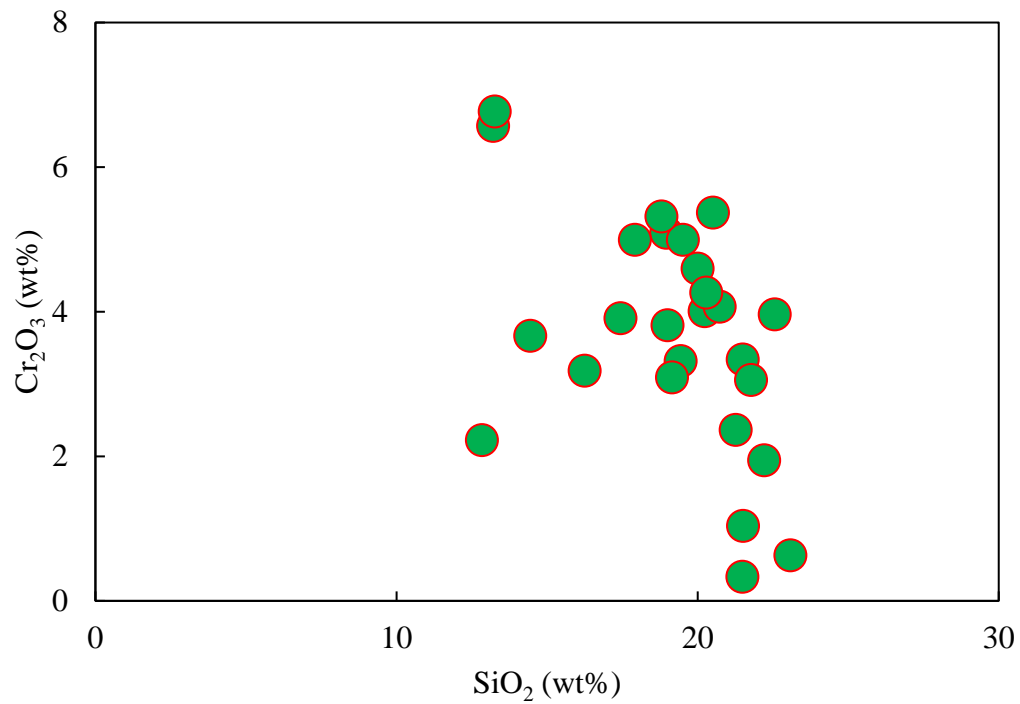


Fig.5.12: Correlation between SiO_2 and Cr_2O_3 content of chlorite from Phokpur magnetite ore samples from NOB.

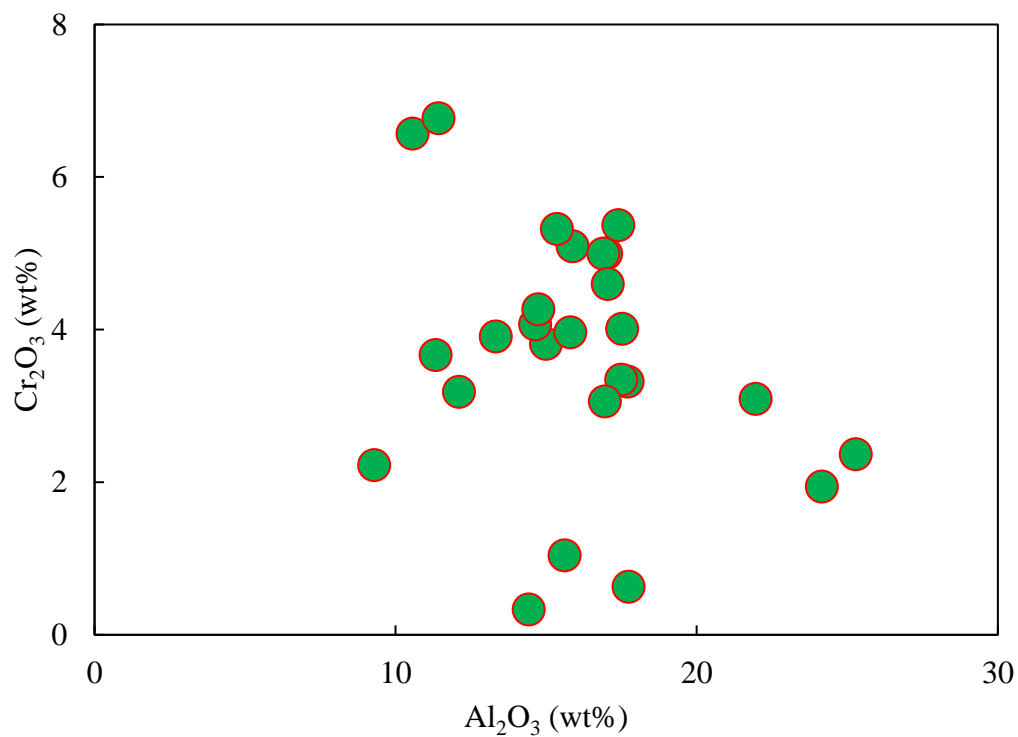


Fig.5.13: Correlation between Al_2O_3 and Cr_2O_3 content of chlorite from Phokpur magnetite ore samples from NOB.

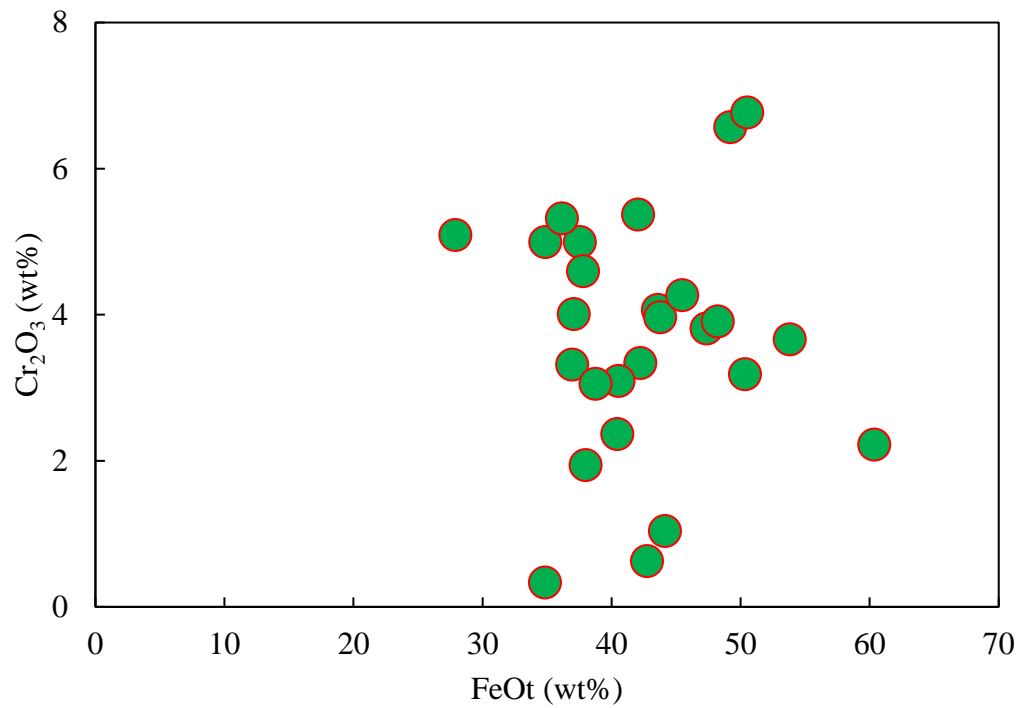


Fig.5.14: Correlation between FeO_t and Cr₂O₃ content of chlorite from Phokpur magnetite ore samples from NOB.

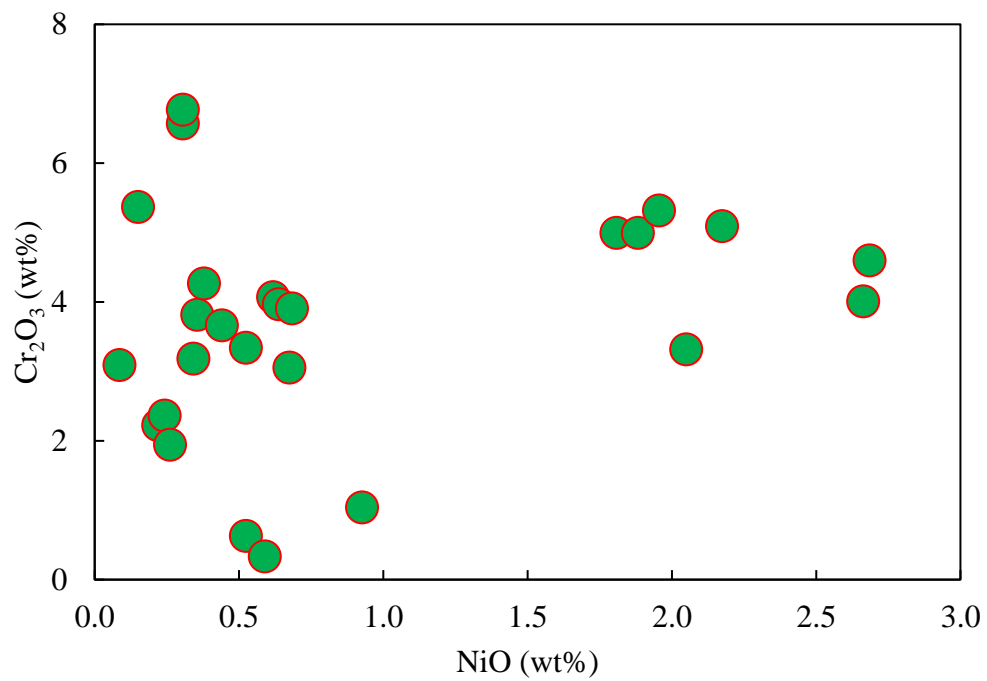


Fig.5.15: Correlation between NiO and Cr₂O₃ content of chlorite from Phokpur magnetite ore samples from NOB.

Table 5.6: Representative EPMA analyses of chlorites in wt% from the Phokpur magnetite ore samples and Fe content reported as total FeO. Structural formulae of chlorite calculated on basis of 28 oxygen atoms.

Sample No. Point No.	1-TP 16 / 1	1-TP 17 / 1	1-TP 18 / 1	1-TP 19 / 1	1-TP 20 / 1	1-TP 23 / 1	1-TP 70 / 1	2-TP 93 / 1	2-TP 94 / 1
SiO ₂	18.96	19.52	20.24	17.92	18.80	19.44	20.01	20.51	21.51
TiO ₂	0.00	0.00	0.00	0.00	0.00	0.00	0.00	0.00	0.00
Al ₂ O ₃	15.88	16.98	17.52	16.89	15.35	17.70	17.04	17.39	17.49
FeO	27.91	37.55	37.08	34.87	36.17	36.94	37.79	42.07	42.24
MnO	1.55	0.91	0.98	0.88	1.34	1.39	1.29	0.13	0.37
MgO	1.49	1.63	1.84	1.52	1.43	1.79	1.73	1.25	1.34
CaO	0.02	0.00	0.00	0.00	0.00	0.02	0.01	0.00	0.00
Na ₂ O	0.03	0.00	0.01	0.02	0.00	0.00	0.17	0.03	0.03
Cr ₂ O ₃	5.09	4.99	4.01	5.00	5.32	3.32	4.60	5.37	3.34
NiO	2.17	1.81	2.66	1.88	1.95	2.05	2.68	0.15	0.52
Total	73.12	83.39	84.34	78.97	80.37	82.65	85.32	86.90	86.84
Calculated									
Fe ₂ O ₃	2.02	0.00	0.00	0.00	0.00	0.00	0.00	0.00	0.00
FeO	26.09	37.55	37.08	34.87	36.17	36.94	37.79	42.07	42.24
Total calc	73.32	83.39	84.34	78.97	80.37	82.65	85.32	86.90	86.84
Oxygen basis	28	28	28	28	28	28	28	28	28
Si	5.231	4.912	5.012	4.751	4.942	4.908	4.911	4.967	5.189
Al _{iv}	2.769	3.088	2.988	3.249	3.058	3.092	3.089	3.033	2.811
Al _{vi}	2.433	1.959	2.132	2.043	1.715	2.193	1.877	1.940	2.166
Ti	0.000	0.000	0.000	0.000	0.000	0.000	0.000	0.000	0.000
Cr	1.110	0.994	0.785	1.048	1.106	0.662	0.892	1.028	0.638
Fe ³⁺	0.420	0.000	0.000	0.000	0.000	0.000	0.000	0.000	0.000
Fe ²⁺	6.019	7.958	7.709	7.801	8.051	7.899	7.923	8.552	8.532
Mn	0.363	0.194	0.207	0.198	0.299	0.297	0.269	0.028	0.076
Mg	0.613	0.612	0.679	0.602	0.559	0.675	0.631	0.453	0.481
Ni	0.482	0.366	0.530	0.401	0.413	0.416	0.530	0.029	0.102
Ca	0.007	0.000	0.000	0.000	0.000	0.005	0.002	0.000	0.000
Na	0.034	0.000	0.005	0.017	0.003	0.000	0.164	0.026	0.028
OH	16.000	16.000	16.000	16.000	16.000	16.000	16.000	16.000	16.000
Total	35.481	36.083	36.047	36.109	36.146	36.147	36.306	36.055	36.022

Table 5.6: Continued....

Sample No.	2-TP	5-TP	5-TP	5-TP	36-TP	36-TP	36-TP	36-TP
Point No.	97 / 1	15 / 1	59 / 1	60 / 1	95 / 1	96 / 1	97 / 1	110 / 1
SiO ₂	23.08	19.15	21.26	22.21	21.78	20.73	22.56	21.49
TiO ₂	0.00	0.98	0.00	0.00	0.00	0.00	0.00	0.00
Al ₂ O ₃	17.73	21.95	25.28	24.15	16.94	14.63	15.80	14.42
FeO	42.75	40.56	40.45	37.99	38.77	43.60	43.78	34.85
MnO	0.10	0.00	0.00	0.00	0.40	0.38	0.32	0.29
MgO	2.59	0.72	0.86	0.78	1.24	1.18	1.27	2.29
CaO	0.00	0.03	0.00	0.00	0.00	0.00	0.00	0.93
Na ₂ O	0.00	0.04	0.04	0.00	0.00	0.00	0.00	0.03
Cr ₂ O ₃	0.63	3.09	2.36	1.94	3.06	4.07	3.97	0.33
NiO	0.52	0.09	0.24	0.26	0.67	0.62	0.64	0.59
Total	87.40	86.60	90.49	87.33	82.86	85.21	88.34	75.22
Calculated								
Fe ₂ O ₃	0.00	0.62	1.65	2.89	1.16	0.00	0.00	0.80
FeO	42.75	40.00	38.96	35.38	37.72	43.60	43.78	34.13
Total calc	87.40	86.66	90.66	87.62	82.97	85.21	88.34	75.30
Oxygen basis	28	28	28	28	28	28	28	28
Si	5.459	4.557	4.725	5.028	5.408	5.182	5.396	5.814
Al _{iv}	2.541	3.443	3.275	2.972	2.592	2.818	2.604	2.186
Al _{vi}	2.401	2.728	3.379	3.530	2.388	1.524	1.850	2.425
Ti	0.000	0.176	0.000	0.000	0.000	0.000	0.000	0.000
Cr	0.118	0.582	0.415	0.348	0.600	0.804	0.750	0.071
Fe ³⁺	0.000	0.111	0.276	0.493	0.218	0.000	0.000	0.163
Fe ²⁺	8.463	7.961	7.240	6.700	7.834	9.317	8.759	7.720
Mn	0.021	0.000	0.000	0.000	0.083	0.080	0.065	0.066
Mg	0.913	0.254	0.285	0.265	0.461	0.440	0.452	0.922
Ni	0.100	0.016	0.043	0.047	0.135	0.124	0.123	0.128
Ca	0.000	0.007	0.000	0.000	0.000	0.000	0.000	0.271
Na	0.000	0.040	0.031	0.000	0.000	0.003	0.000	0.029
OH	16.000	16.000	16.000	16.000	16.000	16.000	16.000	16.000
Total	36.014	35.877	35.670	35.391	35.727	36.295	36.009	35.806

GENESIS OF PHOKPUR MAGNETITE DEPOSIT

6.1 Magnetite: Historical Information

The name magnetite is thought to be derived from the ancient locality *Magnesia* near Macedonia (Greece). According to Pliny (AD 23-79), the name was derived after the name of the shepherd Magnes who first noticed magnetite on Mount Ida while herding his sheep, when pieces of magnetite (lodestone) stuck to the metal nails in his shoes.

Magnetite has been used for thousands of years as amulets and talismans. It was said to give protection from enchantments and evil spirits, and to provide invulnerability to soldiers. It was also said to attract power, favor and love, and to guard against unfaithfulness.

6.2 Magnetite Ore Mineral: General Information

Magnetite, one of the two common naturally occurring iron oxides (chemical formula, Fe_3O_4) and a member of the spinel group. Magnetite is the most magnetic of all the naturally occurring minerals on Earth. Naturally magnetized pieces of magnetite, called lodestone, will attract small pieces of iron, and this was how ancient people first noticed the property of magnetism.

The chemical formula for magnetite is Fe_3O_4 ($\text{Fe}^{2+}\text{O} \cdot \text{Fe}^{3+}_2\text{O}_3$) - which is combination of the formulas for wustite (FeO) and one part of hematite (Fe_2O_3), and contains about 72.4% iron in pure form. Magnetite occurs in almost all igneous and metamorphic rocks as accessory mineral. It is black or brownish-black with a metallic luster. It has a Mohs hardness of 5.5 – 6 and a black streak. Sub-conchoidal fracture is developed in brittle materials characterized by semi-curving surfaces. The specific gravity of magnetite is 5.15.

The relationships between magnetite and other iron-rich oxide minerals such as ilmenite, hematite, and ulvospinel have been much studied on the basis of the reactions between these minerals and oxygen influence. Magnetite is a very important mineral which preserves a record of the Earth's magnetic field. It is a critical tool in paleomagnetism, a science important in understanding plate tectonics and as historic data for magneto-hydrodynamics and other scientific fields.

Magnetite has been very important in understanding the conditions under which rocks form. Magnetite reacts with oxygen to produce hematite, and the mineral pair forms a buffer that can control oxygen fugacity. Usually igneous rocks contain two solid solutions of the iron bearing minerals, one of magnetite and ulvospinel and the other of ilmenite and hematite. Compositions of these mineral pairs are used to calculate the oxygen fugacity of the magma: a range of redox conditions are found in magmas. Magnetite is also crystallized from dunites and peridotites by the process of serpentinization.

Magnetite is one of the spinel group of minerals of cubic system. It occurs commonly as euhedral octahedral crystals. It is also found as fine to coarse granular massive, and as laminated masses. It shows simple spinel twinning on {111}. It has no cleavage, but commonly shows octahedral parting on {111}.

6.3 Transformation of ferrous hydroxide into magnetite

Under anaerobic conditions, the ferrous hydroxide [Fe (OH)₂] can be oxidized into magnetite by the protons of water. Molecular hydrogen is released in this process, which can be shown by following reaction:



Ferrous hydroxide → magnetite + hydrogen + water

Since, the well crystallized magnetite (Fe₃O₄) is thermodynamically more stable than the ferrous hydroxide [Fe (OH)₂].

6.4 Earlier Views on the Genesis of Phokpur Magnetite Deposit

The following hypotheses have been suggested for the origin of Phokpur magnetite deposit by the various workers.

1. Ghose (1980) suggested that the nickel and chromium bearing Phokpur magnetite, a rare occurrence in the ophiolite, have been formed by increased activity of water in ultramafic cumulate zone on layered sequence favouring formation of amphibole in association with ore. The magnetite ore of Naga Hills whether truly influence by hydrothermal activity or represent intrusive equivalents of the massive flow is not clear at present.
2. Chattopadhyay and Bhattacharya (1986) opined that the magnetite, being a part of the cumulate sequence, is formed by crystal fractionation and gravitational settling magma of different composition. The chloritic matrix probably represent metamorphosed equivalent of magma of the second type which occur as interstratified material with magnetite.
3. Ghosh and Goswami (1986) suggested that the Phokpur magnetite ore body was formed by the replacement of earlier formed chromite by magnetite during serpentinisation of host dunite.

6.5 Discussion on the Genesis of Phokpur Magnetite Deposit

Crystallochemically, chromite occurs in a very stable phase and preserves the geochemical characteristics of its parental materials (Irvine, 1967; Dick and Bullen, 1984; Kamenetsky et al. 2001; Mondal et al., 2006; Arai et al., 2006; Dare et al., 2009; Pal, 2011) particularly in highly altered ophiolitic/ silicate rocks. Chemistry of chromite provides significant information about mantle-crustal processes, viz. melting of source material, melt-rock interaction, oxygen fugacity and crystallization of rocks in the ophiolites (Irvine, 1967; Dick and Bullen, 1984; Kamenetsky et al., 2001; Arai et al., 2011; Pal, 2011). Chromites of magmatic origin reflect the nature of the parental melts, whereas the chromites from mantle reflect information about the melt migration and its extraction in the ophiolite sequence (Rollinson, 2008). There are two types of ophiolites: (a) ophiolites formed by the rocks of

the mid oceanic ridge (MOR), and (b) ophiolites formed by the rocks in the supra-subduction zone (SSZ) setting. The formation of Phanerozoic ophiolite sequence is generally explained in terms of the SSZ environment (Pearce et al., 1984; Dare et al., 2009; Pagé et al., 2009; Pal, 2011). In SSZ settings, subduction zone fluids influence mantle melting and melt–rock interaction in the mantle (Boudier and Nicolas, 1995; Kelemen et al., 1997; Zhou et al., 2005). Melt–rock interaction plays a significant role in the crystallization and concentration of chromite within lower crust (Bedard, 1999; Bedard et al., 2000). In such case of the lower crust chromite, the composition of the Cr-spinels is controlled by the composition of magma and magmatic assimilation (Bedard and Hebert, 1998).

Naga Ophiolite Belt, an important part of the IMR, is located along the eastern part of the Indian plate. The ophiolites were emplaced by thrusting during terminal collision (Late Oligocene) between the Indian plate and the Myanmar micro-plate (Sengupta et al., 1990; Acharyya, 2006). In the Naga ophiolite belt, the rocks are highly dismembered slices in an accretionary prism overlying Eocene-Oligocene sediments. The Andaman Islands, located to the south of the Nagaland-Manipur ophiolite belt, reflect characteristics of an active subduction tectonics; the Nagaland-Manipur ophiolite belt represents a collisional tectonics arc (relic). Recent study (Pal, 2011) of the Andaman ophiolite has revealed evidence of polygenetic MORB-SSZ tectonic setting. Although very little petrogenetic information on Naga Ophiolite Belt is available, but they are possibly of SSZ origin (Pal et al., 2014). Recently, Ghosh et al. (2014) reported grain scale-deformation of the chromite of the Naga-Manipur ophiolite belt. On the basis of the study of structures of the ophiolites of the IMR, Bhattacharjee (1991) suggested that subduction commenced during Cretaceous time. He also opined that collision took place in two stages. The first collision occurred between the subducting Indian plate and an island arc, and the second collision occurred between the subducting Indian plate and the Myanmar micro-plate. This is also evident in the studies of Acharyya (2006).

The ultramafics and mafic rocks were usually formed by gravity settling in upper part of the mantle (Wyllie, 1967) which was emplaced as low temperature solid/semi-solid

crystal mush during tectonic movement along weaker zones. The occurrence of high angle faults along the contacts of major ultramafic bodies conforms to the idea of tectonic emplacement of ultramafics (Chattopadhyay and Roy, 1975), which have been reported from adjacent areas of the same belt (Manipur). The low temperature, during emplacement is evident by very little baking effect, absence of chilled margin and very low grade of metamorphism (Mukhopadhyay and Rapa, 1974; Chattopadhyay and Roy, 1975). All these similar features observed in the present area also conform to the view.

From the mode of occurrence of Phokpur magnetite ore body and its relation with the ultramafic host rocks it can be said that such magma may be developed on a subduction zone near the continental margin (Roy et.al., 1984) which was later tectonically emplaced onto the continental margin and formed the part of Indo-Myanmar orogenic belt.

In the Phokpur magnetite ore samples, chromite occurs as euhedral to anhedral discrete as well as rounded to sub-rounded corroded/ zoned grains which are often replaced by magnetite along their grain boundaries and fracture planes. Therefore in the present study EPMA of spinel minerals present on the magnetite ore samples has been studied to know the overall geological conditions responsible for the formation of the Phokpur magnetite ore deposit.

The FeO-Fe₂O₃-TiO₂ ternary diagram (Fig. 5.1a) depicts the low oxygen fugacity, moderate temperature of around 600 °C and low-silica environment prevailed during the wustite-magnetite formation and wustite changed with temperature in the FeO-Fe₃O₄ system (Darken and Gurry, 1945; Myers and Eugster, 1983). The textural relationships of the minerals suggest that the Phokpur magnetite may have formed slightly later than chromite, can be both interstitial (Wang et al., 2008), which explains the unusual association of chromite with Phokpur magnetite in the NOB.

Phokpur magnetite is characterised by the significant quantity of aluminium, which are classified in Cr-Al-Fe³⁺ ternary discrimination diagram (Fig. 5.1b, after Stevens, 1944). This indicates that the Phokpur magnetite was formed from Al-chromite according to the following stages: Al-chromite (initial stage) → Fe-chromite (intermediate stage) → Cr-magnetite (final stage).

Composition of the Phokpur magnetite ore samples exhibit extended range of chromium number (Cr# 0.47 to 0.92). Cr₂O₃ vs. Al₂O₃ variation diagram plotted for Phokpur chrome-magnetite (Fig. 5.2a) shows that most of the samples fall in the stratiform chromitite field. According to Dick and Bullen (1984), chromian spinel with low Cr# (<0.60) is derived from oceanic crust whereas high Cr# (>0.60) belongs to volcanic arcs, stratiform complexes and oceanic plateau basalts. The Phokpur magnetite ore samples plotted in Al₂O₃ vs. TiO₂ diagrams (Fig. 5.2b) indicates their association with volcanic-arc with some contributions from MORB lineage. This is important to emphasize that the spinel compositions from volcanic-arc and MORB trends is coincident with pronounced changes in the mantle petrological-geochemical signatures and conditions of mantle melting (Kamanetsky et al., 2001). Further evidence about the tectonic setting is inferred from Cr₂O₃ vs. Al₂O₃ diagram (Fig. 5.2a), that shows an arc-cumulate affinity, which is further substantiated from Al₂O₃ vs. TiO₂ diagrams (Fig. 5.2b). Some of the podiform chromite deposits show deformation as well as relict cumulus texture that may indicate disrupted stratiform layers (Thayer, 1969; Jackson and Thayer, 1972).

Compositional variation in Fe²⁺/Fe³⁺ versus Al₂O₃ plot (Fig. 5.3a) shows that the composition of Phokpur magnetite ore samples falls exclusively in supra-subduction zone (SSZ) peridotites. Petrogenetic regeneration of magma in the SSZ conditions suggests that they were formed during the early stages of subduction. This suggests that the early formed magma in response to the intra-oceanic subduction was appeared in the partial melting of the hydrated oceanic lithosphere in the mantle wedge (Pearce et al., 1984; Stern and Bloomer, 1992). This led to the development of iron-rich hydrothermal fluid responsible for the massive metasomatic replacement of Cr³⁺ by Fe³⁺ along grain boundaries and cracks of the pre-existing chromite and ultimately the formation of Phokpur magnetite deposit in the NOB.

Ore microscopic studies show evidence of cataclastic texture and martitization along fractures and grain boundaries. Lattice controlled replacement of magnetite by hematite and discrete grains of chromite associated with the magnetite are noticed. Magnetite appears to have been formed later than the chromite.

The textural studies of Phokpur magnetite ore samples shows pull-apart texture in the chromite grains (Chapter 4). This may be the result of stretching and fracturing due to directed pressure (cataclastic metamorphism). The interspaces are filled with the altered silicates mostly serpentine. The stretching and elongation of chromite and magnetite grains may be due to shearing/ volume expansion during the process of serpentinization. Magnetite formed due to serpentinisation, mainly along the fractures within olivine, is well documented by the various workers.

Widespread occurrence of native metals in serpentinite, it has been noted by many authors that the process of serpentinization is followed by the conditions of very low oxygen fugacity ($f O_2$). This is also evident by the presence of hydrogen gas (H_2) in spring draining areas of active serpentinisation (Hahn-Weinheimer and Rost, 1961; Thayer, 1966; Barnes et.al., 1972; Frost, 1985). Process of serpentinization of olivine and accompanied reducing environment can be shown by the following reaction:



Hydrogen released in this process acts as the reducing agent and helps formation of magnetite in which one-third of the iron is present in the ferrous (Fe^{2+}) state and two-third iron is present in ferric (Fe^{3+}) state.

From the detailed textural and mineralogical studies of Phokpur magnetite ore samples as well as the work done by various authors on the ultramafics of the study area, it can be said that the chrome-bearing Phokpur magnetite and associate ophiolite sequence is an outcome of a polygenetic tectonic setting comprising of mid oceanic ridge (MOR) and supra-subduction zone (SSZ) environments. This is very well reflected in the various EPMA discrimination diagrams of the Phokpur magnetite ore samples. The Phokpur magnetite ore body might have formed in two ways: (i) by the process of serpentinisation of the underlying dunites and pyroxenites as explained above, and (ii) by metasomatic replacement of earlier formed syngenetic chromites/ chromitites which is an integral part of the Naga ophiolite belt. These chromatic rocks may have undergone a very prominent

metasomatic reaction caused by a high temperature hydrothermal fluid released during the magmatic differentiation within the ultramafic/ mafic domain before or during emplacement of the ophiolitic rocks. The magmatic differentiation may have produced the iron-rich fluids during the transition stage of its evolution. These iron-rich fluids reacted with the earlier formed chromites/chromitites and probably responsible for the metasomatic substitution of chromium (Cr^{3+}) by iron (Fe^{3+}) and also the addition of iron in various proportions in the Phokpur magnetite ore deposit. The unusual concentration of chromium in the chlorite-silicate matrix of the Phokpur magnetite ore samples may be due to the enrichment of this replaced chromium within the matrix.

The above replacement process may be understood in the following lines. The chemical formula of chromite is FeCr_2O_4 ($(\text{FeO}.\text{Cr}_2\text{O}_3)$) and its theoretical composition of 32.0% FeO and 68.0% Cr_2O_3 . The chemical formula of magnetite is Fe_3O_4 ($\text{FeO}.\text{Fe}_2\text{O}_3$). During replacement/ substitution reaction, the chromium atoms/ molecules may have been replaced by the iron atoms/ molecules, ultimately, resulting in the compositional and mineralogical changes and the formation of magnetite.

It is important to mention here that in the Manipur part of the ophiolite belt, there are chromites but no any incidence of magnetite has been reported. So Phokpur magnetite ore deposit is very peculiar in its nature as well as in distribution.

Overall, the present study suggests that the host rock chromite-dunite has been serpentinised, fractured and subsequently modified by influx of epigenetic magnetite released during serpentinisation. The original magmatic layering of the cumulate emphasized by deformation probably acted as the locales of magnetite concentration by the replacement of chromite.

SUMMARY AND CONCLUSIONS

7.1 Introduction

Ophiolite suites are usually considered as fragments of the oceanic lithosphere emplaced during obduction of the continental margins. They have been proved potential sites for exploration of various metallic deposits like copper sulphides, chromium bearing magnetite, podiform chromite etc. and constitute favourable locales for occurrences of precious metals like PGE and gold. Consequently, the ophiolite belts are being explored for their mineral wealth.

The Naga Ophiolite Belt (extended up to Manipur) forms a part of the Indo-Burman Ranges comprising the Arakan Yoma, Chin and Naga Hills. The ophiolite belt within India extends for about 200 km from Chokla (Nagaland) in the north to Moreh (Manipur) in the south with width ranging from 5 to 16 km. The part of the ophiolite belt within Nagaland extends for about 90 km and is termed as Naga Ophiolite Belt. It is placed between the Nimi Formation in the east and the Disang flysch in the west.

Nickel (Ni) - cobalt (Co) - chromium (Cr) - bearing magnetite deposit associated with Naga Ophiolite Belt is a rare type of occurrence. The main deposit, popularly known as the Phokpur magnetite deposit, occurs at eastern-most part of the Nagaland. It is located at the Matungse Kein Hill, about 4 km east of Phokpur village in Kiphire district of Nagaland. A number of small magnetite incidences have also been reported at Phor, Ziphu, Mollen, Washelo, Reguri, Molhe Peaks, Ghoos Camp in Meluri Subdivision of Phek district of Nagaland.

The Phokpur magnetite deposit occurring in the northern part of the Naga Ophiolite Belt is exposed as a massive sheet like band over serpentinised peridotite with almost a sharp contact and is overlain by Mio-Pliocene molassic sediments (Jopi Formation) with an unconformity. The ore body has been traced for a strike length of approximately 1 km

in NNE-SSW direction with moderate to steep westerly dips. The thickness varies between 3 m to 15 m with an outcrop width of about 300 m along the dip direction. The ore body represents a low plunging (SSW) synformal warp truncated on its west and east by high angle faults giving the body a form of a 'horst' like block. The basal contact with the serpentinite body is marked with discrete grains of chromite.

In most cases it has been observed that the magnetite occurrences are exposed along the inner rims of a broad synformal structure (Mollen-Jopi-Ziphu ridge) and are overlain by Mio-Pliocene sediments concealing the magnetite bodies beneath them.

Thus nickel and cobalt containing magnetite deposit in Nagaland is of vital and strategic importance for our nation. Our defence needs a lot of nickel and cobalt and their alloy products for the manufacture of superior military equipments. Due to scarcity of raw materials for nickel and cobalt in the country, every possible indigenous source of these metals should be exploited. In this context, the nickel bearing magnetite of Phokpur, Nagaland, in spite of its low nickel and cobalt content, can be considered a potential source of these metals of our country.

Therefore, the proposed research work entitled "Study of magnetite mineralization associated with Naga Ophiolite belt at Phokpur in Kiphire district of Nagaland" has been undertaken to document a detailed and unified picture of the geological, petrographic, geochemical and petrogenetic aspects of evolution of the Phokpur magnetite deposit.

7.2 Geological Setting

The Naga Ophiolite Belt (NOB), along Indo-Myanmar border, forms a part of the Naga - Arakan Yoma flysch of upper Cretaceous-Middle Eocene age. This N-S to NNE - SSW trending narrow arcuate Ophiolite Belt of Nagaland and Manipur extends approximately for 200 km from northeast of Chokla in Nagaland to south of Moreh in Manipur. In Nagaland it extends over 90 km in length and width varying widths ranging from 2-15 km. The Ophiolite have tectonic contacts on either side with evidence of their transport into and onto the Disang flysch in the west and, in turn, have been over-ridden in places, by Nimi Formation/ Naga Metamorphics (possibly Mesozoic age) from the east.

The contact between ophiolites and Disang formation is marked by shearing, brecciation and silicification with occasional development of tight to isoclinal folds.

The rocks of the study area comprise mainly mafic, ultramafics, mafic volcanics, and volcanoclastic sediments. The rock-types under this group include peridotite, pyroxenite, serpentinites and dunite. Usually, the ultramafics are altered to serpentinites. The NOB contains economically important chromite and magnetite deposits with minor Nickel. The magnetite bodies are associated with the cumulate ultramafic rock. The magnetite bodies at Phokpur and Thongsunyu villages are the biggest magnetite deposits in the ophiolite and Phor Magnetite also occupy an extensive area compare to the other parts of ophiolite of NOB.

The ore is usually hard, massive, compact, and jointed. Sometimes, it is highly fractured (fragmented) showing cataclastic effects. The best studied magnetite ore body in NHO is located 4 km east of Phokpur village occur in the form of sheet-like magnetite body. The strike length of the Phokpur magnetite body is about 1 km along NNE-SSW to N-S direction with a 30° to 40° westerly dip. The magnetite occurs as a broad synformal warp with slickensides and groove lineation suggesting scale sliding. The thickness of the body varies from 5 to 15 m with an average outcrop width of about 300 m. It is underlain by cumulate ultramafics, viz, serpentinite, harzburgite and pyroxenite. The contact is generally sharp and at places gradational being marked by gradual decrease in magnetite content from the underlying ultramafics. At places it is observed that serpentinised dunite with magnetite disseminations grade into bands of magnetite ore. The magnetite body is non-conformably overlain by the sediments (shale, sandstone and conglomerate of varying thickness) of Phokphur Formation at places.

7.3 Petrography and Geochemistry of Phokpur Magnetite

Phokpur magnetite ore is usually hard and compact, massive and jointed. Thin partings of silicates and hydrated iron oxides are usually present within the ore. The hydrated iron oxides might have formed due to weathering of magnetite grains. Reflected light microscopic studies of the polished thin sections of the ore samples reveal that

magnetite and chromite are the main mineral phases. In addition, maghemite, martite and goethite are observed as secondary minerals. Secondary magnetite formed due to serpentinisation of olivine is also observed.

7.3.1 Ore microscopic Studies

The chromite (FeCr_2O_4), grains are generally seen to be anhedral as well as rounded to elliptical in form. Most of the grains are seen to contain outer rims of magnetite formed due to replacement along chromite grain boundaries; replacement by magnetite also occurs along the fractures. The chromite grains present a typical cataclastic texture and in some cases there is pronounced distortion due to brittle fracturing, producing a pull apart texture, the original shapes are appreciably lost. Fine and closely spaced fractures of some grains are seen to be healed by magnetite as well as hematite i.e., martite. The magnetite and chromite intergrowth occur in part as irregularly interlaced and in others in distinct cubic patterns generally in similar proportions presenting network like features.


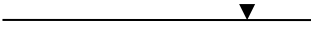




Detailed textural and mineralogical studies of Phokpur magnetite samples reveal that magnetite and chromite occurs as composite as well as discrete ore mineral phases constituents of the ore body. Ore minerals are fractured in nature with indications of deformational activities after the formation of chromite and magnetite grains. Usually the fractures are occupied by goethite and maghemite. They are also filled with secondary silicate matrix composed probably of chlorite and serpentines, which also served as the major constituents of the ore and host rocks. The isolated chromite grains are often rimmed by magnetite. There is also presence of replacement texture where chromite grains are being replaced by magnetite along the fractures and cleavage planes as well as surrounding boundaries. Magnetite grains also display conspicuous rims of maghemite/goethite, which indicates secondary alteration and deposition of oxidized iron from the diffusion process possibly combined with martitization.

Ferrochromite/maghemite and martite/goethite are observed as the common alteration products along fractures in chromite and magnetite respectively. Chromite is corroded and replaced by magnetite and the fracture planes in chromite are infilled by magnetite. In general, the opaque grains are corroded and at places show highly sutured

margins. Zoning texture is common in chromite grains of Phokpur magnetite ores. This may be due to metasomatic alteration of the chromite grains. Two types of alteration products are possible: (1) the iron-rich high reflecting phase, and (ii) the Mg and Al-rich low reflecting phase. In the Phokpur magnetite ore samples, the chromite grains alter to a high reflecting phase of magnetite with an intermediate phase of ferro-chromite having medium reflectance. The high reflecting magnetite phase is almost devoid of chromium. The intermediate phase with medium reflectivity between magnetite and chromite shows a decrease in chromium and magnesium content but slightly increase in iron and aluminium.

Based on the degree of crystallinity, mineral inclusions and textural relationships, the paragenetic sequence of the Phokpur magnetite deposit is presented in Table 7.1.

Table 7.1: Paragenetic sequence based on textural relationship

Time		
Mineral	Primary	Secondary
Chromite		
Magnetite		
Chlorite-Serpentine		
Hematite		
Goethite		

7.3.2 Modal Mineralogy

Phokpur magnetite ore body is highly altered and occurs in very irregular form. Magnetite constitutes about 40 to 55% proportion (average 45%) whereas chromite constitutes about 8 to 15% proportion (average 10%) of the studied ore samples. Hematite and goethite, etc. constitutes an average proportion of 7%. Remaining part of the ore is occupied by the highly weathered aphanitic silicate matrix (average 38%) containing disseminated grains of chromite and magnetite as well as fine aggregates of silicate matrix.

7.3.3 Geochemistry of Phokpur Magnetite

The chemical analyses of the 10 samples from the Phokpur magnetite ore samples was carried out in National Metallurgical Laboratory, Jamshedpur, Jharkhand by using ICP-OES instrumentation technique. The iron content ranges from 40.51 to 55.95% with an average concentration of 50.54%. The concentration of nickel in the magnetite ore ranges from 0.14 to 0.91 % with an average concentration of 0.49 %, and the concentration of chromium ranges from 1.33 to 3.79 % with an average concentration of 2.38%. Cobalt (average 0.04%), titanium (average 0.56%), and vanadium (average 0.02%) have been reported in very small amount in the magnetite ore samples, though titanium and vanadium are usually rich in magnetites of magmatic origin.

Magnetite is an illustrious petrogenetic indicator and occurs in various ore deposits, which contains several discriminator elements that display systematic variations. Trace elements in magnetite provide a tool to understand the processes that aid discrimination based on their different environments of formation, which helps to understand petrogenetic and provenance studies in the exploration of ore deposits. Generally, magnetite related to mafic-ultramafic complex, hydrothermal deposits, granodiorite-porphyry and ophiolites are known for their low Cr, Ni, and Co content. In resemblance, magnetite ores from the Phokpur deposit belongs to Naga Ophiolite belt are also characterized by slightly low Ni and Co content. Therefore, magnetite trace element compositions have capability to be powerful tool in exploration of economic mineral deposit.

7.4 Mineral Chemistry of Magnetite Ore

Electron probe micro analysis (EPMA) of selected ore samples from Phokpur magnetite ore body was carried out at the Department of Geology (Centre of Advanced Study), Institute of Science, Banaras Hindu University, Varanasi. Fe^{3+} in ore minerals were calculated on the basis of stoichiometry, i.e., 32 oxygens. Standard deviations, mainly those for major elements involved in the transformation from chromite to magnetite, were significantly large. The compositional variations from chromite to magnetite is observed because change in chemistry of all the grains studied from core to rim.

Composition of spinel can be used as an important petrogenetic indicator which may help in discriminating tectonic setting. Study of the spinel group minerals from different host rocks/ores is also indicators of the physical and chemical conditions of subsolidus re-equilibration. Therefore, the mineral chemistry of Phokpur magnetite has been also been studies to find out the various physico-chemical and tectonic environments responsible for its formation. Phokpur magnetite compositions, plotted in the FeO-Fe₂O₃-TiO₂ diagram, fall along the wustite-magnetite solid solution line. The wustite-magnetite formation is rarity in nature stems most probably required low oxygen fugacity, moderate temperature (around 600°C) and low-silica environment, however, composition of wustite changes with temperature in the FeO-Fe₃O₄ system. The textural relationships of the mineral suggest that the magnetite may have formed slightly later than chrome-magnetite, can be both interstitial, which explains the unusual association of chromite with Phokpur magnetite in the NOB. Compositional variations for wide range of mafic-ultramafic rocks derived from variable tectonic settings have been obtained from global spinel database (Barnes and Roeder, 2001). Phokpur Cr-magnetite contains significant quantity of aluminium, which are classified in Cr-Al-Fe³⁺ ternary discrimination diagram. This also reflects that the Cr-magnetite was formed from Al-chromite according to the following stages: Al-chromite (initial stage) → Fe-chromite (intermediate stage) → Cr-magnetite (final stage).

Composition of chrome-magnetite from Phokpur deposits exhibit extended range of Cr-number (0.47 - 0.92). In order to decipher the nature of the chrome-magnetite from Phokpur deposits, various discrimination diagrams are plotted. Cr₂O₃ vs. Al₂O₃ variation diagram plotted for Phokpur chrome-magnetite shows that most of the samples fall in the stratiform chromitite field and some of them fall away from this field. According to Dick and Bullen (1984), chromian spinel with low Cr# (<0.60) is derived from oceanic crust whereas high Cr# (>0.60) belongs to volcanic arcs, stratiform complexes and oceanic plateau basalts. The compositional variation of Phokpur chrome-magnetite plotted in Al₂O₃ vs. TiO₂ diagrams indicates that most of the points are associated to volcanic-arc with some contributions from MORB lineage. This may be emphasized here that the composition of spinel mineral from volcanic-arc and MORB trends is coincident with pronounced changes in the mantle petrological-geochemical characteristics and conditions

of mantle melting. Further clarification about the tectonic setting is inferred from Cr_2O_3 vs. Al_2O_3 diagram (Fig. 8a) and found that they exhibit an arc-cumulate affinity, which is further substantiated from Al_2O_3 vs. TiO_2 diagrams. Some of the podiform chromite deposits show deformation as well as relict cumulus texture that may indicate disrupted stratiform layers.

Compositional variation in $\text{Fe}^{2+}/\text{Fe}^{3+}$ versus Al_2O_3 diagram shows that the magnetite composition from Phokpur deposit falls exclusively in supra-subduction zone (SSZ) peridotites. Petrogenetic regeneration of magma in the SSZ conditions suggests that they were formed during the early stages of subduction. Authentication from the SSZ sources suggests that the early formed magma was derived in response to the intra-oceanic subduction emerged in the partial melting of the hydrated oceanic lithosphere in the mantle wedge. This led to the development of Fe-rich hydrothermal fluid responsible for the massive metasomatic replacement of Cr^{3+} by Fe^{3+} along grain boundaries and cracks of the pre-existing chromite and ultimately the formation of Phokpur magnetite deposit in NOB.

7.5 Genesis of Phokpur Magnetite Deposit

From the detailed textural and mineralogical studies of Phokpur magnetite ore samples as well as the work done by various authors on the ultramafics of the study area, it can be said that the chrome-bearing Phokpur magnetite and associate ophiolite sequence is an outcome of a polygenetic tectonic setting comprising of mid oceanic ridge (MOR) and supra -subduction zone (SSZ) environments. This is very well reflected in the various EPMA discrimination diagrams of the Phokpur magnetite ore samples. The Phokpur magnetite ore body might have formed in two ways: (i) by the process of serpentinisation of the underlying dunites and pyroxenites as explained above, and (ii) by metasomatic replacement of earlier formed syngenetic chromites/ chromitites which is an integral part of the Naga ophiolite belt. These chromitic rocks may have undergone a very prominent metasomatic reaction caused by a high temperature hydrothermal fluid released during the magmatic differentiation within the ultramafic/ mafic domain before or during emplacement of the ophiolitic rocks. The magmatic differentiation may have produced the

iron-rich fluids during the transition stage of its evolution. These iron-rich fluids reacted with the earlier formed chromites/chromitites and probably responsible for the metasomatic substitution of chromium (Cr^{3+}) by iron (Fe^{3+}) and also the addition of iron in various proportions in the Phokpur magnetite ore deposit. The unusual concentration of chromium in the chlorite-silicate matrix of the Phokpur magnetite ore samples may be due to the enrichment of this replaced chromium within the matrix.

The above replacement process may be understood in the following lines. The chemical formula of chromite is FeCr_2O_4 ($\text{FeO} \cdot \text{Cr}_2\text{O}_3$) and its theoretical composition of 32.0% FeO and 68.0% Cr_2O_3 . The chemical formula of magnetite is Fe_3O_4 ($\text{FeO} \cdot \text{Fe}_2\text{O}_3$). During replacement/ substitution reaction, the chromium atoms/ molecules may have been replaced by the iron atoms/ molecules, ultimately, resulting in the compositional and mineralogical changes and the formation of magnetite.

It is important to mention here that in the Manipur part of the ophiolite belt, there are chromites but no any incidence of magnetite has been reported. So Phokpur magnetite ore deposit is very peculiar in its nature as well as in distribution.

Overall, the present study suggests that the host rock chromite-dunite has been serpentinised, fractured and subsequently modified by influx of epigenetic magnetite released during serpentinisation. The original magmatic layering of the cumulate emphasized by deformation probably acted as the locales of magnetite concentration by the replacement of chromite.

The Phokphur magnetite ore samples are characterised by higher nickel contents. Higher concentration of Ni is mostly observed in the chlorite-silicate matrix. The magnetite and chromite grains of the ore samples are usually extremely low in nickel concentration. On the basis of the unique, substantial and consistently higher concentration of chromium in most of the analyzed (EPMA as well as bulk chemistry of the ore) ore samples of the study area, *it may be concluded to use the term **Chrome-magnetite deposit** for the Phokpur magnetite ore body* associated with Naga ophiolite belt.

REFERENCES

Acharyya, S.K. (1986): Tectono-stratigraphic History of Naga Hills Ophiolites. Geological Survey of India, Memoirs, V. 119, pp. 94-103.

Acharyya, S.K. (2007): Collisional emplacement history of the Naga-Andaman ophiolites and the position of the eastern Indian suture. Journal of Asian Earth Sciences, V. 29, pp. 229–242.

Acharyya, S.K., Ray, K.K. and Roy, D.K. (1989): Tectono-stratigraphy and emplacement history of the ophiolite assemblage from the Naga Hills and Andaman Island Arc, India. Journal of Geological Society of India, V. 33 (1), 4–18.

Acharyya, S.K., Ray, K.K. and Sengupta, S. (1990): Tectonics of ophiolite belt from Naga Hills and Andaman Islands, India. Proc. Indian Acad. Sci. (Earth Planet. Sci.), V. 99 (2), pp. 187–199.

Acharyya, S.K., Srivastava, R.K., Bhattacharyya, S., Venkataramana, P., Ghose, S., Vidyadharan, K.T. and Jena, S.K. (1984): Geology and tectonic frame of Naga Hills Ophiolite, Northern Indo-Burmese Range, India. 27th International Geological Congress, Moscow, Sec. 7, Tectonics, 89-90.

Acharyya, S.K., Roy, D.K. and Mitra, N.D. (1986): Stratigraphy and Palaeontology of the Naga Hills Ophiolite Belt. Memoirs, Geological Survey of India, V.119, 64–74.

Agrawal, O.P. and Ghose N.C. (1986): Geology and stratigraphy of the Naga Hills ophiolite between Melury and Awankhoo, Phek district Nagaland, India. In: Ghose N.C. and Varadarajan, S. (Eds.), Ophiolite and Indian Plate Margin. Sumna Publishers, Patna, pp.163-195.

Agrawal, O.P. and Ghose, N.C. (1989): Mineral resources in the ophiolite belt of Nagaland, N.E. India. In: Ghose, N.C. (Ed.), Phanerozoic ophiolites of India. Sumna Publishers, Patna, pp. 245–280.

Agrawal, O. P. and Kacker, R.N. (1980): Nagaland Ophiolites, India- A subduction zone Ophiolites complex in Tethyan orogenic belt. Proceeding International Ophiolite Symposium, Cyprus 1979, pp. 454-461.

Agrawal, O.P. and Rao, K.S., (1971): Discovery of Pokphur magnetite deposit. Unpublished report, DGM, Nagaland.

Agrawal, O.P. and Rao, K.S. (1972): Geological traverses in the ultramafic complex of Thonoknyu and Pungro areas, Tuensang district. Discovery of Pokphur Magnetite Deposit, DGM, Nagaland, Unpublished Report.

Agrawal, O.P. and Rao, K.S. (1978): Status of Geological work and inventory of mineral discoveries, in Nagaland. Misc. Pub. No.1, DGM, Nagaland, 38p.

Ahmed, A.H., Arai, S. and Attia, A.K. (2001): Petrological characteristics of podiform chromitites and associated peridotites of the Pan African Proterozoic ophiolite complexes of Egypt. Mineralium Deposita, V. 36, pp.72-84.

Ahmad, T., Tanaka, T., Sachan, H.K., Asahara, Y., Islam, R. and Khanna, P.P. (2008): Geochemical and isotopic constraints on the age and origin of the Nidar Ophiolitic Complex, Ladakh, India: implications for the Neo-Tethyan subduction along the Indus suture zone. Tectonophysics, V. 451, pp. 206-224.

Anon (1986): Geology of Nagaland Ophiolite. Geological Survey of India Memoirs, V. 119, 113p.

Anonymous (1972): Penrose field conference on ophiolites. Geotimes, V. 17, pp. 24–25.

Arai, S., Kadoshima, K., Morishita, T. (2006): Widespread arc-related melting in the mantle section of the northern Oman ophiolite as inferred from detrital chromian spinels. Journal of Geological Society of London, V. 163, pp.869–879.

Arai, S., Okamura, H., Kadoshima, K., Tanaka, C., Suzuki, K. and Ishimaru, S. (2011): Chemical characteristics of chromian spinel in plutonic rocks: implications for deep magma processes and discrimination of tectonic setting. Island Arc, V. 20, pp. 125 - 137.

Awasthi, N., Ray, J.S. and Pande, K. (2015): Origin of the Mile Tilek Tuff, South Andaman: evidence from ^{40}Ar – ^{39}Ar chronology and geochemistry. Current Science, Vol. 108, No. 2, pp. 205-210.

Bandyopadhyay, S., Subramanyam M.R. and Sharma P.N. (1973): The geology and mineral resources of the Andaman and Nicobar Islands. Records, Geological Survey of India, V. 105, pp. 25–68

Barnes, I., Rapp, J.B., O'Neill, J.R., Sheppard, R.A. and Gude, A.J. (1972): Metamorphic assemblages and the direction of flow of metamorphic fluid in four instances of serpentinisation. Contribution to Mineralogy and Petrology, V. 35, pp. 263-276.

Baxter, A.T., Aitchison, J. C., Zyabrev, S.V. and Ali, J.R. (2011): Upper Jurassic radiolarians from the Naga Ophiolite, Nagaland, northeast India. *Gondwana Res.* V. 20 (2–3), pp. 638–644.

Barnes, I., Rapp, J.B., O’Neil, J.R., Sheppard, R.A. and Gude, A.J. (1972): Metamorphic assemblages and the direction of flow of metamorphic fluids in four instances of serpentinisation. *Contribution to Mineralogy and Petrology*, V.35, pp.263-276.

Barnes, S. and Roeder, P. (2001): The Range of spinel Composition in Terrestrial Mafic and Ultramafic Rocks, *Journal of Petrology* .V. 42(12), pp. 2279-2302

Bedard, J.H. (1999): Petrogenesis of boninites from the Betts Cove Ophiolite, Newfoundland, Canada: identification of subducted source components. *Journal of Petrology*, V.40, pp.1853–1889.

Bedard, J.H. and Hebert, R. (1998): Formation of chromitites by assimilation of crustal pyroxenites and gabbros into peridotitic intrusions: North Arm Mountain massif, Bay of Islands ophiolite, Newfoundland. Canada. *Journal of Geophysical Res.*, V.103, pp. 51-65.

Bedard, J.H., Hebert, R., Berclaz, A. and Varfalvy, V. (2000): Syntexis and the genesis of lower oceanic crust. *Geological Society of America, Special Pap* 349, pp.105–119.

Berthelsen, A. (1953): On the geology of the Rupshu District, N.W. Himalaya. *Medd. Dan. Geol. Foren.* 12, 350 – 415.

Bhattacharjee, C.G. (1991): The Ophiolites of Northeast India- a subduction zone ophiolite complex of the Indo-Burman Orogenic belt. *Tectonophysics*, V. 191, 213-222

Bhattacharyya, K.K. (2010): Petrography, chemistry and economic potential of the magnetite ores of Pokphur area, Nagaland. *Memoirs Geol Soc India* V. 75:341–348.

Bhowmik, N., Majumdar, M. and Ahmed, S.A. (1973): Investigation on nickeliferous magnetite near Pokphur, Tuensang district, Nagaland. *Geological Survey of India, Unpublished Progress Report.*

Bonavia, F.F., Diella, V. and Ferrario, A., (1993) : Precambrian podiform chromitite from Kenticha Hill, southern Ethiopia. *Economic Geology*, V. 88, pp. 198-202.

Boudier, F. and Nicolas, A. (1995): Nature of the Moho transition zone in the Oman Ophiolite. *Journal of Petrology*, V. 36, pp.777–796.

Bourdelle, F. and Cathelineau, M. (2015): Low-temperature chlorite geothermometry: a graphical representation based on a T-R₂+Si diagram. *European Journal of Mineralogy*, V. 27(5). pp. 617-626.

111

Brunnschweiler, R. O. (1966): On the geology Indo-Burman-Ranges. *Journal of Geological Society of Australia*, V. 13 (1), pp.137-194

Buddington, A.F. and Lindsley, D.H. (1964): Iron-titanium oxide minerals and synthetic equivalents. *Journal of Petrology* V. 5, 310-357.

Cawood, P.A., Kröner, A., Collins, W.J., Kusky, T.M., Mooney, W.D. and Windley, B.F. (2009): Accretionary orogens through Earth history. *Geological Society of London, Special Publication*, V. 318, pp. 1– 36.

Chatterjee, N. and Ghose, N.C. (2010): Metamorphic evolution of the Naga Hills eclogite and blueschist, Northeast India: implications for early subduction of the Indian Plate under the Burma Microplate. *Jour. Met. Geol* V. 28:209–225.

Chattopadhyay, B. And Roy, R.K. (1975): Systematic geological mapping and mineral investigation in Manipur East, Manipur. Unpub. Prog. Rept. Geological Survey of India .

Chattopadhyay, B. and Bhattacharya, S. (1986): The nickeliferous magnetite associated with the Naga Hills Ophiolite at Phokpur, Tuensang district, Nagaland, India. *Record, Geological Survey of India*, V. 114 (4), pp.15-24.

Chattopadhyay, B., Venkataramana, P., Roy, D.K., Bhattacharyya, S. and Ghose. S. (1983): Geology of Naga Hills Ophiolite. *Record, Geological Survey of India*, V. 112 (2), pp. 59-115.

Chauhan, H., Tripathi, A., Pandit, D. and Chalapathi Rao, N.V. (2020): A new Analytical Protocol for high precision U-Th-Pb Chemical Dating of Xenotime from the TTG Gneisses of the Bundelkhand Craton, Central India, using CAMECA SXFive Electron Probe Micro Analyzer. *Journal of Earth System Science*, 129, 210.

Chungkham P. and Jafar S.A. (1998): Late Cretaceous (Santonian-Maestrichtian) integrated Coccolith-Globotruncanid biostratigraphy of pelagic limestone from the accretionary prism of Manipur, northeast India. *Micropalaeontology* V. 44:68–83.

Cloos, M. (1993): Lithospheric buoyancy and collisional orogenesis: Subduction of oceanic plateaus, continental margins, island arcs, spreading ridges, and seamounts *Geological Society of America Bulletin* V. 105(6), 715-737.

Coleman, R.G. (1977): Ophiolites, Ancient Oceanic Lithosphere? In: Wyllie, P. J. (Ed.), Springer-Verlag, New York, 229 p.

Coleman, R.G. (1977): Emplacement and metamorphism of ophiolite. *Ophioliti*, V. 2, pp. 41-74.

112

Coleman, R.G. (1984): The diversity of ophiolite. *Geol. Minjb.* V. 63, pp.141-150.

Dare, S.A.S., Barnes, S.J., Beaudoin, G., Meric, J., Boutroy, E. and Potvin-Doucet, C. (2014): Trace elements in magnetite as petrogenetic indicators. *Miner. Deposita*, V. 49, pp.785-796.

Dare, S.A.S., Pearce, J.A., McDonald, I. and Styles, M.T. (2009): Tectonic discrimination of peridotites using fO₂-Cr# and Ga-Ti-Fe^{III} systematics in chrome-spinel. *Chem. Geol.*, V. 261, pp.199–216.

Darken, L.S. and Gurry, R.W. (1945): The System Iron-Oxygen. I. The Wüstite Field and Related Equilibria. *Journal of American Chemical Society*, V. 67(8), pp.1398–1412.

Davis, B.L., Rapp, Jr. G. and Walawender, M.J. (1968): Fabric and structural characteristics of the martitization process. *American Jour. of Science*, V. 266, pp.482-496.

de Sigoyer, J. (1998): Mécanismes d'exhumation des roches de haute pression basse température, en contexte de convergence continentale (Tso Moriri, NO Himalaya), Thèse Univ. Claude Bernard, Lyon, pp. 236.

Della Giusta, A., Carbonin, S. and Russo, U. (2011): Chromite to magnetite transformation: compositional variations and cation distributions (south Aosta Valley, Western Alps, Italy). *Periodico di Mineralogia*, V.80, 1, 1-17. DOI: 10.2451/2011PM0001.

Devaraju, T.C., Jayaraj, K.R., Sudhakara, T.L., Alapieti, T.T., Spiering, B. and Kaukonen, R.J. (2014): Mineralogy, geochemistry and petrogenesis of the V-Ti-bearing and chromiferous magnetite deposits hosted by Neoarchaean Channagiri mafic-ultramafic complex, Western Dharwar Craton, India: implications for emplacement in differentiated pulses. *Central European Journal of Geosciences*, V. 6, 518-548. DOI: 10.2478/s13533-012-0193-9.

Dewey, J.F. and Bird, J.M. (1971): Origin and emplacement of the ophiolite suite: Appalachian ophiolites in Newfoundland. *J. Geophys. Res.* V. 76, pp. 3179–3206.

DGM-Nagaland (2015): Assessment of Multi-metal Magnetite Deposits in Naga Hills Ophiolites. Technical Publication DGM/FSP/2012-14/No. 06, 33p.

Dick, H.J.B. and Bullen, T. (1984): Chromian spinel as a petro genetic indicator in abyssal and alpine-type peridotites and spatially associated lavas. *Contrib. Mineral. Petrol.* V. 86, pp. 54-76.

Dilek, Y. and Flower, M.F. (2003): Arc-trench rollback and forearc accretion: 2. A model template for ophiolites in Albania, Cyprus, and Oman. *Geol. Soc. Lon. Spec. Pub.* V. 218, pp. 43-68.

113

Dilek, Y. and Furnes, H. (2011): Ophiolite genesis and global tectonics: Geochemical and tectonic fingerprinting of ancient oceanic lithosphere. *Geol. Soc. Am. Bull.* V. 123, pp. 387–411.

Dilek, Y., Thy, P., Hacker, B. and Grundvig, S. (1999): Structure and petrology of Tauride ophiolites and mafic dike intrusions (Turkey): Implications for the Neotethyan ocean. *Geol. Soc. Am. Bull.* V. 111, pp.1192–1216.

Duran, C.J., Barnes, S.J., Mansur, E.T., Dare, S.A.S., Bedard, L.P. and Sluzhennikin, S.F. (2020): Magnetite Chemistry by LA-ICP-MS Records sulphide Fractional Crystallisation in Massive Nickel Copper-Platinum group Element ores from Norilsk-Talnakh Mining District (Siberia, Russia): Implication for Trace Elements Partitioning into Magnetite. *Economic Geology*, V, 115 (6), pp.1245-1216.

Eliopoulos, D.G. and Eliopoulos, M.E. (2019): Trace element distribution in magnetite separates of varying origin: genetic and exploration significance. *Minerals*, V. 9, 759. doi: 10.3390/min9120759.

Evans B.W., Trommsdorff, V. and Richter, W. (1979): Petrology of an eclogite metarodingite suite at Cima di Gagnone, Ticino, Switzerland. *American Mineralogists*, V. 64, pp. 15-31.

Fleming, P.D. and Fawcett, J.J. (1976): Upper stability of chlorite + quartz in the system MgO-FeO-Al₂O₃-SiO₂-H₂O at 2 kbar water pressure. *American Mineralogist*, V. 61, pp. 1175-1193.

Frost, B.R. (1985): On the stability of Sulfides, Oxides and Native metals in Serpentine. *Journal of Petrology*, V.26, pp. 31-63.

Fuchs, G. and Linner, M. (1996): On the Geology of the Suture Zone and Tso Moriri Dome in Eastern Ladakh (Himalaya). *Jb. Geol. B.*139, pp.191-207.

Geological Survey of India (2015): Collaboration on Phanerozoic ophiolites of India. Official Project Report, Dy. DG and Head, CHQ, Kolkata, 7th May 2015, 6p.

Ghosh, B., Mahoney, J. and Ray, J. (2007): Mayodia Ophiolites of Arunachal Pradesh, Northeastern Himalaya. *Journal of the Geological Society of India*, V.70 (4), pp. 595-604.

Ghose, N.C. (1980): Occurrence of magnetite and chromite in the ophiolite belt of Naga Hills, N.E. India. UNESCO International Symposium on Metallogeny of Mafic and Ultramafic Complexes, Athens, V. 3, pp. 293-314.

114

Ghose, N. C. (2014): Occurrence of native gold and gold-silver alloy in the olivine gabbro of layered cumulate sequence of Naga Hills ophiolite, India. *Current Science*, V.106 (8), pp. 1125-1130.

Ghose, N.C. and Agrawal, O.P. (1989): Geological framework of the central part of Naga Hills. In: Ghose, N.C. (Ed.), *Phanerozoic Ophiolites of India and Associated Mineral Resources*. Sumna Publications, Patna, pp. 165-188.

Ghose, N.C., Chatterjee, N. and Fareeduddin (2014): A Petrographic Atlas of Ophiolite – An Example from the Eastern India- Asia Collision. Springer India, 234 p.

Ghose, N. C. and Shrivastava, M. P. (1986): Podiform chromite of Naga Hills ophiolite, N.E. India. In: Petrascheck W. et al. (eds) *Chromites: Theophrastus Publication*, Athens, pp. 263–284

Ghosh, S. and Goswami, H.K. (1986): Mineral occurrences and metallogenic aspect. *In: Geology of Nagaland ophiolite. Memoir, Geological Survey of India*, V. 119, pp.80-93.

Hahn-Weinheimer, P. and Rost, F. (1961). Akzessorische Mineralien und Elemente in Serrpentin von Leupoldsgrün (Münchenberger Gneissmasse). *Geochim. Cosmochim. Acta*. 21, pp.165-181.

Haughton, D., Roder, P.L. and Skinner, B.J. (1974): Solubility of Sulphur in mafic magmas. *Economic Geology*, V.69, pp.451-467

Hébert, R., Huot, F., Wang, C. S. and Liu, Z. F. (2003): Yarlung Zangbo ophiolites (Southern Tibet) revisited: geodynamic implications from the mineral record, Ophiolite in Earth History. *Geol. Soc. Lond. Spec. Publ.*, Vol. 218, pp. 165-190

Irvine, T.N. (1967): Chromium spinel as a petrogenetic indicator, Part II, Petrologic applications. *Canadian Journal of Earth Sciences*. V. 4, pp.71-103.

Jackson, E.D. and Thayer, T.P. (1972): Some criteria for distinguishing between stratiform, concentric and alpine peridotite-gabbro complexes. *Proceedings of the 24th International Geological Congress*, V. 2, pp.289–296.

Jena, S.K. and Acharyya, S.K. (1983): Report on reference geological section of Naga Hills Ophiolite. Prog. Rept. Geological Survey of India, F.S., 1981-82 (Unpublished).

Jonnalagadda, M.K., Benoit, M., Harshe, S., Tilhac, R., Duraiswami, R.A., Grégoire, M. and Karmalkar, N. R. (2022): Geodynamic evolution of the Tethyan lithosphere as recorded in the Spontang Ophiolite, South Ladakh ophiolites (NW Himalaya, India). *Geoscience Frontiers*, 13, <https://doi.org/10.1016/j.gsf.2021.101297>.

115

Kamenetsky, V.S., Crawford, A.J. and Meffre, S. (2001): Factors controlling chemistry of magmatic spinel: An empirical study of associated olivine, Cr-spinel and melt inclusions from primitive rocks. *Journal of Petrology*, V. 42(4), pp. 655–671.

Kelemen, P.B., Hirth, G., Shimizu, N., Spiegelman, M. and Dick, H.J.B. (1997): A review of melt migration processes in the adiabatically upwelling mantle beneath oceanic ridges. *Phil Trans R Soc Lond A* 355, pp.67–102.

Lagabriele, Y., Guivel, C., Maury, R.C., Bourgois, J., Fourcade, S., Martin, H. (2000): Magmatic–tectonic effects of high thermal regime at the site of active ridge subduction: the Chile Triple Junction model. *Tectonophysics*, V. 326 (3–4), pp.255–268.

Lopez-Garcia, J.A., Oyarzun, R., Lillo, J., Manteca, J.I. and Cubas, P. (2016): Geochemical characterization of magnetite and geological setting of the iron-oxide \pm iron silicate \pm iron carbonate rich Pb-Zn sulfides from the La Union and Mazarron stratabound deposits (SE Spain). *Resource Geology*, V. 67, pp. 139-157.

Lukram, J.S. and Kachhara, R.P. (2010): Molluscan biostratigraphy of the Disang Group of rocks in parts of Manipur, India. *Mem Geol Soc India* V. 75, pp. 149–163.

Maheo, G., Bertrand, H., Guillot, S., Villa, I.M., Keller, F., Capiez, P. (2004): The South Ladakh ophiolites (NW Himalaya, India): an intra-oceanic tholeiitic arc origin with implication for the closure of the Neo-Tethys. *Chem. Geol.*, V. 203, pp. 273–303.

Majumdar, M. and Pandey, B.N. (1974): Geological mapping in parts of the mineralized belt, East of Pokphur, Tuensang dist., Nagaland. Joint unpublished report of GSI (Manipur-Nagaland Circle) and DGM, Nagaland.

Mukhopadhyay, G. and Rapa, D.A. (1974): Geological mapping and preliminary mineral investigation in parts of ultramafic belt in Manipur, Central District, Manipur. Unpub. Prog. Rept. Geological Survey of India

Majumdar, M. and Prabhakar, A. (1975): Geological mapping in parts of mineralized belt, east of Pokphur, Tuensang district, Nagaland. Geological Survey of India, Unpublished Progress Report.

Majumdar, M., Prabhakar, A. and Srivastava, S.N.P. (1976): A note on the nickel and cobalt bearing magnetite and chromite around Pokphur, Tuensang district, Nagaland, India. Symposium on Geology and mineral resources of NE India, Geological Survey of India, Shillong, pp. 45-56.

Mavrogonatos, C., Voudouris, P., Berndt, J., Klemme, S., Zaccarini, F., Spry, P.G., Melfos, V., Tarantola, A., Keith, M., Klemd, R. and Haase, K. (2019): Trace elements

116

in magnetite from the Pagoni Rachi porphyry prospect, NE Greece: implications for ore genesis and exploration. *Minerals*, 9, 725. doi: 10.3390/min 9120725.

Mitchell, AHG (1981): Phanerozoic plate boundaries in mainland SE Asia, the Himalayas and Tibet. *J Geol Soc Lond.*, V. 138, pp. 109–122.

Mitchell, A.H.G. (1993): Cretaceous–Cenozoic tectonic events in the western Myanmar (Burma) Assam region. *Journal of Geological Society of London*, V. 150, pp. 1089–1102.

Mohapatra, B.K., Rath, P.C. and Sahoo, R.K. (1995): Chromiferous chamosite from Pokphur magnetite body, Nagaland, India. *Current Science*, V. 68(10), pp.1036-1039.

Mondal, S.K., Ripley, E.M., Li, C. and Frei, R. (2006): The genesis of Archaean chromitites from the Nuasahi and Sukinda massifs in the Singhbhum craton, India. *Precambrian Research*, V. 148(1), pp. 45–66.

Mukherjee, R., Mondal, S.K., Rosing, M.T. and Frei, R. (2010): Compositional variations in the Mesoproterozoic chromites of the Nuggihalli schist belt, western Dharwar craton (India): Potential parental melts and implications for tectonic setting. *Contributions to Mineralogy and Petrology*, V. 160(6), pp. 865–885.

Myers, J. and Eugster, H. P. (1983): The system Fe-Si-O: Oxygen buffer calibrations to 1,500K. *Contributions to Mineralogy and Petrology*, V. 82 (1), pp. 75-90.

Nadoll, P., Angerer, T., Mauk, J.L., French, D. and Walshe, J. (2014): The chemistry of hydrothermal magnetite: a review. *Ore Geology Review*, V. 61, pp. 1-32.

Nayak B, Vaish A.K., Singh S.D. and Bhattacharyya K.K. (2010): Petrography, chemistry and economic potential of the magnetite ores of Pokphur area, Nagaland. *Memoir Geological Society of India*, V. 75, pp.341–348.

Nayak, R. and Rao, B. V. (2017): Petrogenesis and geochemical characteristics of plagiogranites from Naga Ophiolite Belt, northeast India: Fractional crystallization of MORB-type magma. *Chemie der Erde*, 77, pp.183–194.

Nicolas, A. (1989): Structures of Ophiolites and Dynamics of Oceanic Lithosphere. Kluwer Academic Publishers, Dordrecht, 320p.

Ningthoujam, P.S., Dubey, C.S., Guillot, S., Fagion, A.S. and Shukla, D.P. (2012): Origin and serpentinization of ultramafic rocks of Manipur Ophiolite Complex in the Indo-Myanmar subduction zone, North-east India. *J Asian Earth Sci* V. 50, pp.128–140.

Pagé, P., Bedard, J.H. and Tremblay, A. (2009): Geochemical variations in depleted fore-arc mantle: the Ordovician Thetford Mines Ophiolite. *Lithos*, V. 113, pp. 21–47.

117

Pal, T. (2011): Petrology and geochemistry of the Andaman ophiolite: melt-rock interaction in a suprasubduction zone setting. *Journal of the Geological Society, London*, V. 168, pp.1031- 1045. <https://doi.org/10.1144/0016-76492009-152>.

Pal, T., Bhattacharya, A. and Nagendran, G., Yanthan, N.M., Singh, R. and Raghumani, N. (2014): Petrogenesis of chromites from the Manipur ophiolite belt, NE, India: evidence for a suprasubduction zone setting prior to India-Myanmar collision. *Miner. Petrol.*, Vol. 108, pp.713-726, DOI 10.1007/s00710-014-0320-z.

Pal, T., Chakraborty, P.P., Gupta, T.D. and Singh, C.D. (2003): Geodynamic evolution of the outer-arc-forearc belt in the Andaman Islands, the central part of the Burma–Java subduction complex. *Geol. Mag.*, V. 140, pp. 289–307.

Palme, H. and O'Neill, H. S. C. (2014): Cosmochemical estimates of mantle composition. In: Holland, H. D. and Turekian, K. K. (ed.), *Treatise on Geochemistry* (2nd Edn) Oxford:Elsevier, V.2, pp.1–38. <http://dx.doi.org/10.1016/B978-0-08-095975-7.00201-1>

Pandey, A., Chalapathi Rao, N. V., Chakrabarti, R., Pandit, D., Pankaj, P., Kumar, K. and Sahoo, S. (2017a): Petrogenesis of a Mesoproterozoic shoshonitic lamprophyre dyke from the Wajrakarur kimberlite field, eastern Dharwar craton, southern India: geochemical and isotopic evidence for a modified sub-continental lithospheric mantle source. *Lithos*, pp. 218-233.

Pandey, A., Chalapathi Rao, N.V., Pandit, D., Pankaj, P., Pandey, R., Sahoo, S. and Kumar, A. (2017b): Subduction – Tectonics in the evolution of the eastern Dharwar craton, southern India: Insights from the post-collision calc-alkaline lamprophyres at the western margin of the Cuddapah basin. *Precambrian Research*, V. 298, pp. 235-251.

Pandey, M., Pandit, D., Arora, D., Chalapathi Rao, N. V. and Pant, N. C. (2019): Analytical Protocol for U-Th-Pb chemical dating of monazite using CAMECA EPMA

SX5 installed at the Deep Mantle Petrology Laboratory, Department of Geology, Banaras Hindu University, Varanasi, India. *Journal of Geological Society of India*, V. 93, pp.46-50.

Pandey, R., Chalapathi Rao, N.V., Pandit, D., Sahoo, S. and Dhote, P. (2017c): Imprints of modal metasomatism in the post-Deccan sub-continental lithospheric mantle: petrological evidence from the ultramafic xenoliths in an Eocene lamprophyre, NW India. *Geological Society of London Special Publication*, V. 463, pp.117-136.

Pearce, J.A., Alabaster, T., Shelton, A.W. and Searle, M.P., 1981. The Oman ophiolite as a Cretaceous arc-basin complex: evidence and implications. *Philos. Trans. R. Soc. London*. V. 300, pp. 299-317.

118

Pearce, J.A., Lippard, S.J. and Roberts, S. (1984): Characteristics and tectonic significance of suprasubduction zone ophiolites. *Geological Society, London, Special Publications*, V. 16(1), pp. 77–94.

Pedersen, R.B., Searle, M. P., Carter, A. and Bandopadhyay, P.C. (2010): U–Pb zircon age of the Andaman ophiolite: implications for the beginning of subduction beneath the Andaman–Sumatra arc. *Jour. Geol. Soc. (London)*, V. **167**, pp. 1105–1112.

Pisiak, L.K., Canil, D., Lacourse, T., Plouffe, A. and Ferbey, T. (2017): Magnetite as an indicator mineral in the exploration of porphyry deposits: a case study in till near the Mount Polley Cu-Au deposit, British Columbia, Canada. *Economic Geology*, V. 112, pp. 919-940.

Rao, M.V.S., Balaram,V., Rao, B.V., Charan, S.N., Srikanth, B. and Ezung, O.C. (2005): Prospects of Platinum Group Element (PGE) Occurrence in the Ultramafic Rock associations of the Naga Ophiolite Belt, North-East India: Need for Detailed Investigations. *In: Douli, S. K. and Mahanta, C. (Eds.) Science and Technology for Regional Development: Case for North-East India*, pp. 84-88.

Ravikumar and Prabhakar, A. (1977): Geological mapping and exploratory drilling for Ni, Co, and Cr bearing magnetite deposit in Tuensang dist., Nagaland. *Geological Survey of India, Unpublished Progress Report*.

Ravi Kumar and Prabhakar, A. (1981): Final report on exploratory drilling in the North Block of the Ni-bearing magnetite deposit east of Pokphur, Tuensang District, Nagaland, GSI., S.E. Asia, Bangkok.

Rengma, K. and Singh, S. K. (2021): Ni-Co-Cr-bearing Phokpur Magnetite Deposit Associated with Naga Ophiolite Belt, North-East India and its Economic Viability. *Jour. Sci, Res., Banaras Hindu University, Varanasi*, V. 65 (1), pp. 26-31.

Rollinson, H.R. (2008): The geochemistry of mantle chromitites from the northern part of the Oman ophiolite: inferred parental melt compositions. *Contribution in Mineralogy and Petrology*, V. 156, pp. 273–288.

Roy, R. K. (1989): Meso-Cenozoic accretionary prism on the margin of Indo-Burman range ophiolite and its implications. In: Ghose NC (ed.) *Phanerozoic ophiolites of India*. Sumna Publishers, Patna, pp. 145–164.

Roy, R.K., Agrawal, O.P. and Kacker, R.N. (1984): Nature and evolution of the stratiform igneous magnetite deposits of Naga Hills. *Symp. Stratiform ore deposit of India*. Jadavpur University, Calcutta.

119

Sarma, D.S., Jafri, S. H., Fletcher, I. R. and Mc Naughton, N.J. (2010): Constraints on the tectonic setting of the Andaman ophiolites, Bay of Bengal, India, from SHRIMP U–Pb zircon geochronology of plagiogranite. *J. Geol.*, V. 118, pp. 691–697.

Searle, M.P., Noble, S.R., Cottle, J.M. et al. (2007): Tectonic evolution of the Mogok metamorphic belt, Burma (Myanmar) constrained by U–Th–Pb dating of metamorphic and magmatic rocks. *Tectonics*, V. 26, TC3014.

Sen, S. and Chattopadhyay, B. (1979): The ophiolite belt of NE India and associated mineralization. *Third Regional Conference on Geology and Mineral Resources of Southwest Asia*, Bangkok, Thailand, Nov. 1978, pp.14-18.

Sengupta, S., Ray, K.K., Acharyya, S.K. and de Smeth, J.B. (1990): Nature of ophiolite occurrences along the eastern margin of the Indian plate and their tectonic significance. *Geology* V. 18(5), pp. 439–442.

Sengupta, S., Sukla, V.K., Mitra, N.D. and de Ghose, S. (1987): Structure of Naga Hills Ophiolite Belt. *Indian Minerals*, V. 41, pp. 46-51.

Singh, A. K. (2013): Petrology and geochemistry of Abyssal Peridotites from the Manipur Ophiolite Complex, Indo-Myanmar Orogenic Belt, Northeast India: Implication for melt generation in mid- oceanic ridge environment. *J Asian Earth Sci.*, V. 66, pp. 258–276.

Singh A. K., Singh N.B., Debala Devi L. and Singh R.K.B. (2012a): Geochemistry of Mid-Ocean Ridge mafic intrusives from the Manipur ophiolite complex, Indo-Myanmar orogenic belt, N.E.India. *J Geol Soc India* V. 80, pp. 231–240.

Singh, A. K., Devala Debi L, Ibotombi Singh N. and Subramanyam K.S.V. (2012b): Platinum group of elements and gold distributions in the peridotites and associated

podiform chromitites of the Manipur ophiolite complex, Indo-Myanmar orogenic belt, NorthEast India. *Chemie der Erde*, <http://dx.doi.org/10.1016/j.chemer.2012.07.004>

Singh, L.R. (2022): Petrology and Geochemistry of the Ultramafic Rocks from Parts of the Manipur Ophiolite Belt with Reference to Chromite Mineralisation. Unpublished Ph.D. Thesis, Nagaland University, 163p.

Singh, R.N. and Ghose, N.C. (1981): Geology and stratigraphy of the ophiolite belt of Naga Hills, East of Kiphire. N.E. India. *Recent Researches in Geology*, V. 8, pp. 359–381.

Singh, R.N., Singh, S.K. and DasGupta, S.P. (1989): Ophiolite and associated metallogeny in Naga Hills, India. *In*. *Phanerozoic Ophiolites of India*, (Ed.) N. C, Ghose, Sumna Publ., pp. 235-243.

120

Sharma, D.P. (1983): Interim report on investigation of the Nickel-Cobalt-Chromium associated magnetite deposit (South Block) at Pokphur, Tuensang District, Nagaland. Unpublished Report, DGM, Nagaland.

Stern, R.J. and Bloomer, S.H. (1992): Subduction zone infancy: Examples from the Eocene Izu-Bonin-Mariana and Jurassic California arcs. *Geological Society of America Bulletin*, V. 104(12), pp.1621–1636.

Stevens, R.E. (1944): Composition of some chromites of the western hemisphere. *American Mineralogist*, V. 29, pp. 1–64.

Tamura, A. and Arai, S. (2001): Harzburgite–dunite–orthopyroxenite suite as a record of supra-subduction zone setting for the Oman ophiolite mantle. *Lithos*, V. 90, pp. 43–56. doi:10.1016/j.lithos.2005.12.012

Tan, W., Liu, P., He, H., Wang, C.Y. and Liang, X. (2016) Mineralogy and origin of exsolution in Ti-rich magnetite from different magmatic Fe-Ti oxide-bearing intrusions. *Can. Mineral.*, V. 54, pp. 539–553.

Thayer, T.P. (1966) Serpentinization considered as constant-volume metasomatic process. *Am. Miner.* V. 51, pp. 685-710.

Thayer, T.P. (1969) Gravity differentiation and magmatic re-emplacement of Podiform chromite deposits. *In*: Wilson, H.D.B. (ed), *Magmatic ore deposits*, Econ. Geol. Monograph V. 4, pp. 132-146.

Venkataramana, P. and Bhattacharyya, S. (1989): Mode of occurrence and origin of chromite, magnetite and Ni-bearing laterite in Naga Hills Ophiolite, N. E. India. *In*. Ghose, N. C. (ed) Phanerozoic ophiolites of India. Sumna Publishers, Patna, pp. 213–234.

Venkataramana, P., Ghose, S., Dutta A. and Goswami, H.K. (1984): Mode of occurrence and chemistry of chromite in the Naga Hills Ophiolite. Record, Geological Survey of India, V. 113 (4), pp.1-6.

Venkataramana, P., Ghose, S. and Bhattacharyya, S. (1986): Petrology and chemistry of leucocratic rocks from Naga Hills Ophiolite. Record, Geological Survey of India, V. 114 (4), pp.1-6.

Venkataramana, P., Datta, A.K. and Acharyya, S.K. (1986): Petrology and petrochemistry. *In* Geology of Nagaland Ophiolite (ed), D. B. Ghosh Commemorative Volume, Memoir Geological Survey of India V. 119, pp. 33–63.

121

Vidal, O., Parra, T. and Trotet, F. (2001): A thermodynamic model for Fe-Mg aluminous chlorite using data from phase equilibrium experiments and natural pelitic assemblages in 100 - 600 °C, 1-25 kbar P-T range. American Journal of Science, V. 301, pp.557-592.

Vidyadharan, K.T., Shrivastava, R.K., Bhattacharyya, S., Joshi, A. and Jena, S.K. (1986): Distribution and description of major rock types. Geol. Nagaland Ophiolite, Mem. Geol. Surv. India V. 119, pp. 18–27.

Vidyadharan, K.T., Joshi, A., Ghosh, S., Gaur, M. P., Shukla, R. (1989): Manipur ophiolites: its geology, tectonic setting and metallogeny. *In*: Ghose, N.C. (ed.) Phanerozoic ophiolites of India. Sumna Publishers, Patna, pp. 197–212.

Wang, Y., Morin, G., Ona-Nguema, G., Manguy, N., Juillet, F., Aubry, E., Guyt, F., Calas, G. and Broun, G. (2008): Arsenic Sorption at the magnetite-water interface during aqueous preprecipitation of magnetite: EXAFS evidence for a new arsenite surface complex. *Geochimica et Cosmochimica Acta*, V. 72 (11), pp. 2573-2586. DOI:10.1016/j.gca.2008.03.011

Wiewiora, A. and Weiss, Z. (1990): Crystallochemical Classifications of phyllosilicates based on the unified system of projection of chemical composition: II. The Chlorite Group. *Clay Minerals*, V. 25 (1), pp. 83-92.

Wyllie, P.J. (1967): Ultramafic and related rocks. John Willey and Sons, New York.

Zane, A. and Weiss, Z. (1998): A procedure for classifying Rock-Forming Chlorite based on Microprobe Data. *Rendiconti Lincei*, 9, pp.51-56. DOI. Org/10.1007/BF02904455

Zhou, MF., Robinson, P.T., Malpas, J., Edwards, S.J. and Qi, L. (2005): REE and PGE geochemical constraints on the formation of dunites in the Luobusa Ophiolite, Southern Tibet. *Journal of Petrology*, V. 46, pp. 615–639.



Fig.1: Field photograph showing the panoramic view of the physiographic feature around the study area.



Fig.2: Field photograph showing the view of the study area, the Phokpur section of the Matungse Kein Hill, where the largest magnetite deposit occurs.

PLATE II



Figure 1: Field Photograph showing huge block of Phokpur magnetite deposit with amount of dip around 30° towards west



Figure 2: Field Photograph of Phokpur magnetite deposit along road cutting showing its jointed and compact nature.

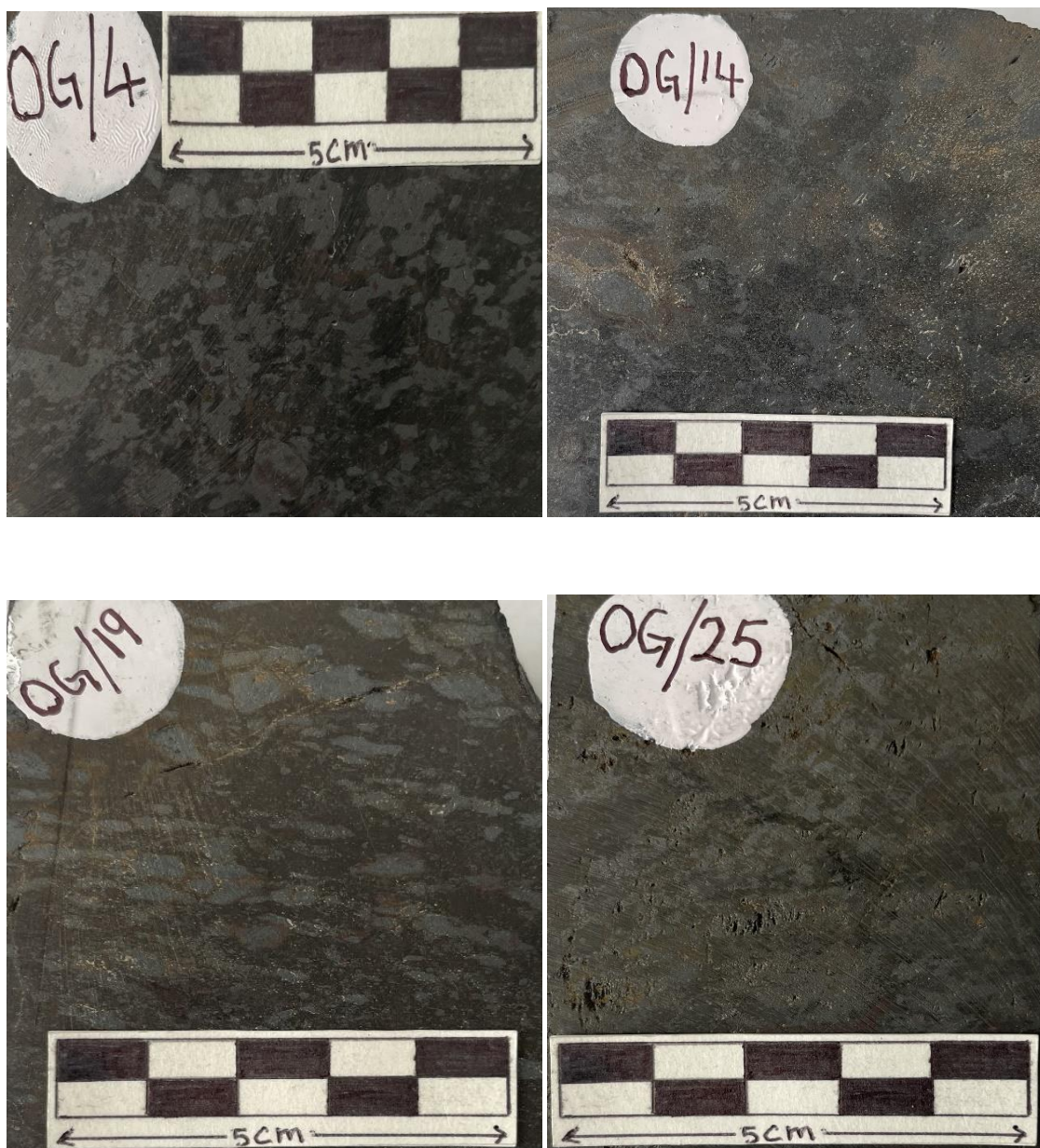


Figure 1: Field Photograph of Phokpur magnetite deposit slightly away from road cutting showing a massive block of magnetite.



Figure 2: Field Photograph of Phokpur magnetite deposit along road cutting showing its highly fractured/ fragmented nature.

PLATE IV



Figs.: Hand specimen photographs of cut and polished Phokpur magnetite samples from NOB showing: 1. Anhedral magnetite grains (gray) within dark gray to black silicate matrix; 2. Randomly oriented anhedral to subhedral magnetite grains (gray) within grayish-black silicate matrix; 3. Elongated magnetite grains (gray) oriented in a linear pattern. Smaller grains of magnetite are also observed within grayish-black silicate matrix; 4. Poorly oriented grains of magnetite (gray) within grayish-black silicate matrix.

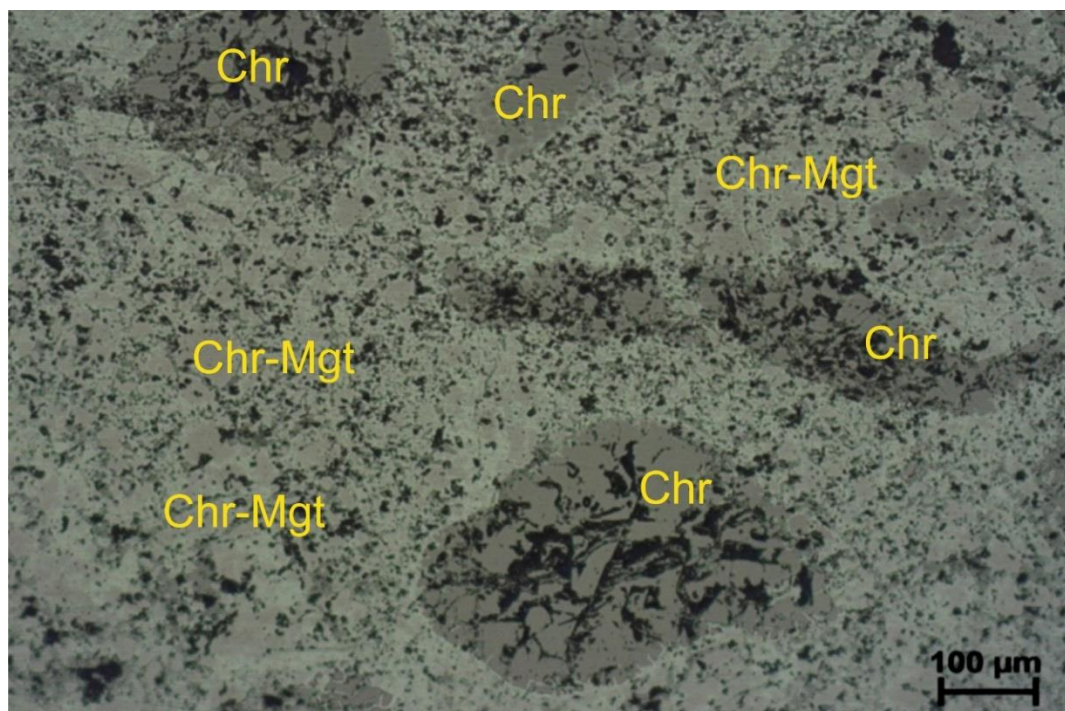


Fig.1: Reflected light photomicrographs of Phokpur magnetite sample from NOB showing chrome-magnetite and chromite grains within the matrix of magnetite (dull white). Dark grains of gangue silicates are also present as inclusions.

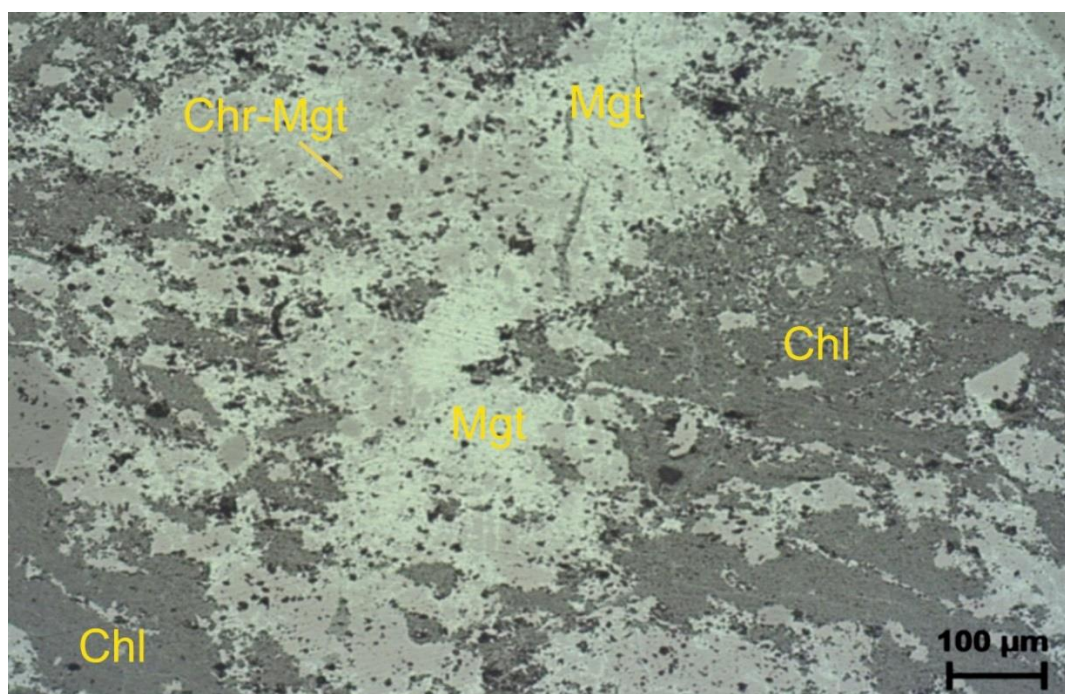


Fig. 2: Reflected light photomicrographs of Phokpur magnetite sample from NOB showing anhedral magnetite and chrome-magnetite grains with martite-chlorite-silicate matrix.

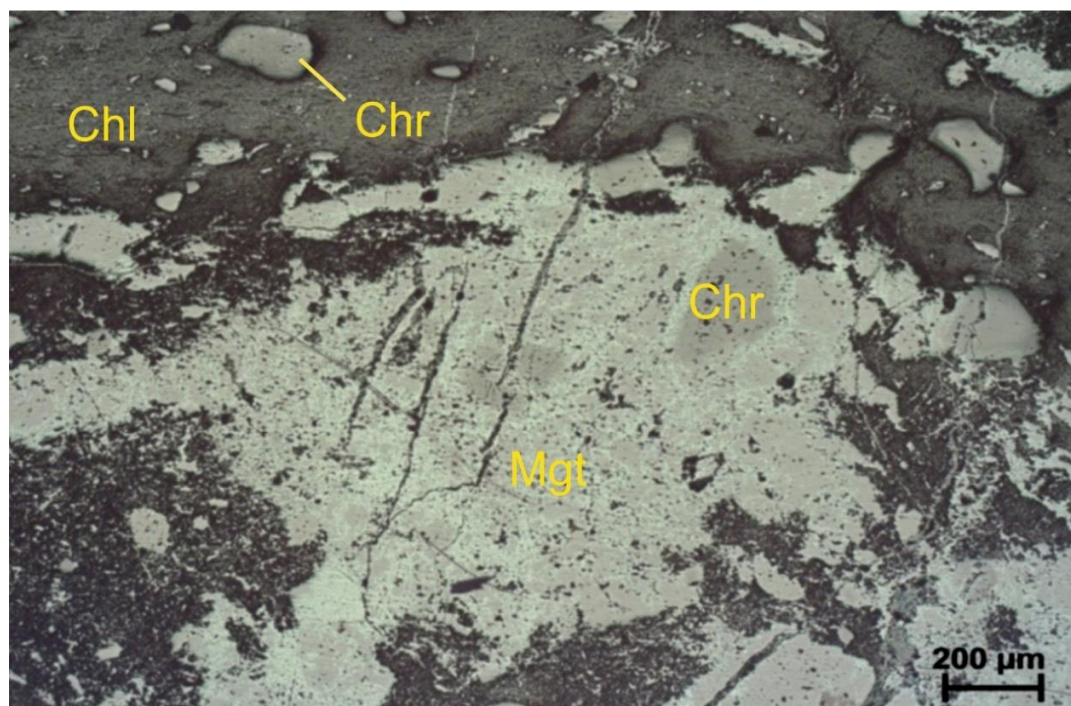


Fig.1: Reflected light photomicrographs of Phokpur magnetite sample from NOB showing a big anhedral grain of magnetite with relics of chromite. Fine grains of martitised-magnetite and chromite are also observed in chlorite-silicate matrix.

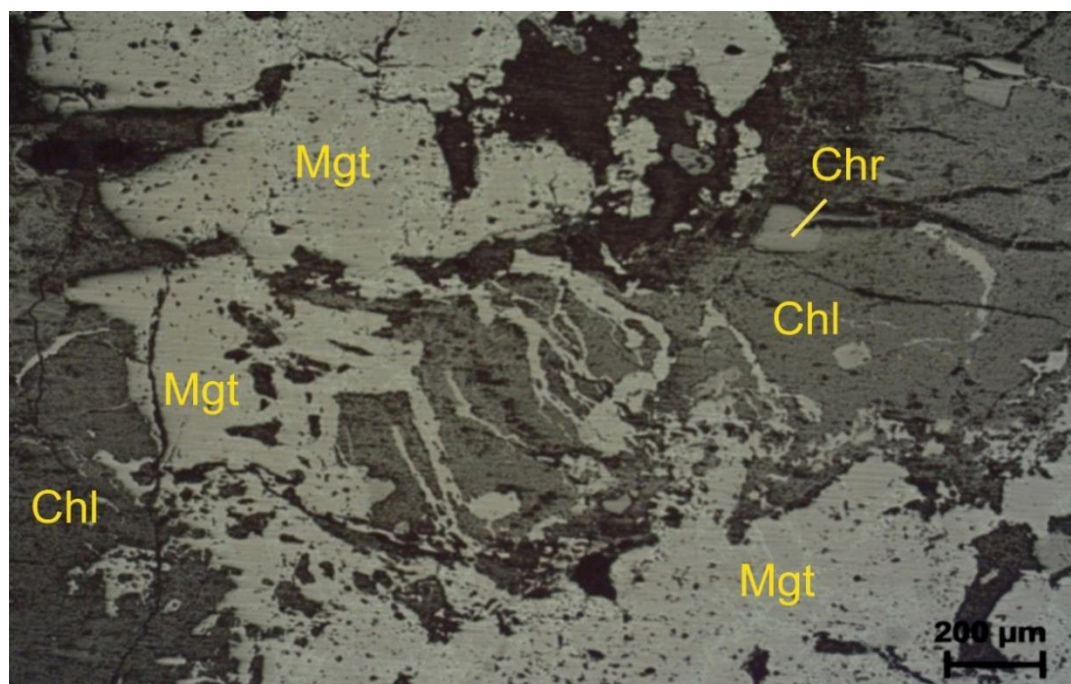


Fig.2: Reflected light photomicrographs of Phokpur magnetite sample from NOB showing anhedral and dendritic magnetite grains, smaller chromite grains along with chlorite-silicate matrix.

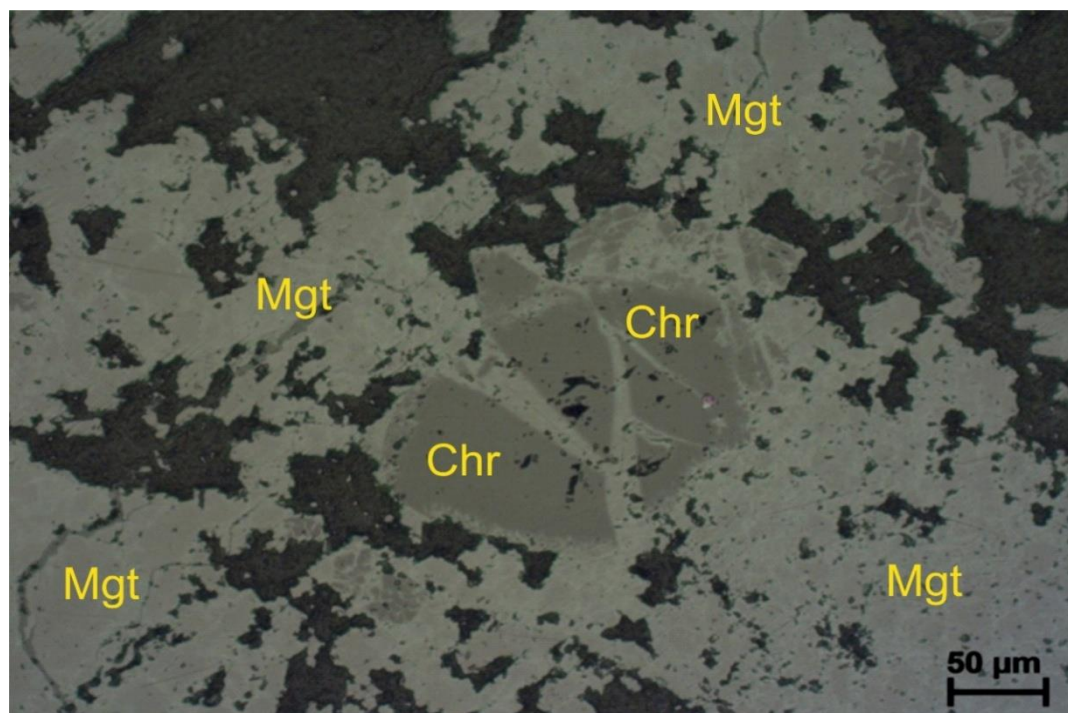


Fig.1: Reflected light photomicrographs of Phokpur magnetite sample from NOB showing altered chromite grains in the matrix of magnetite and silicates (dark). Martite veins are also observed along the cracks within chromite grains.

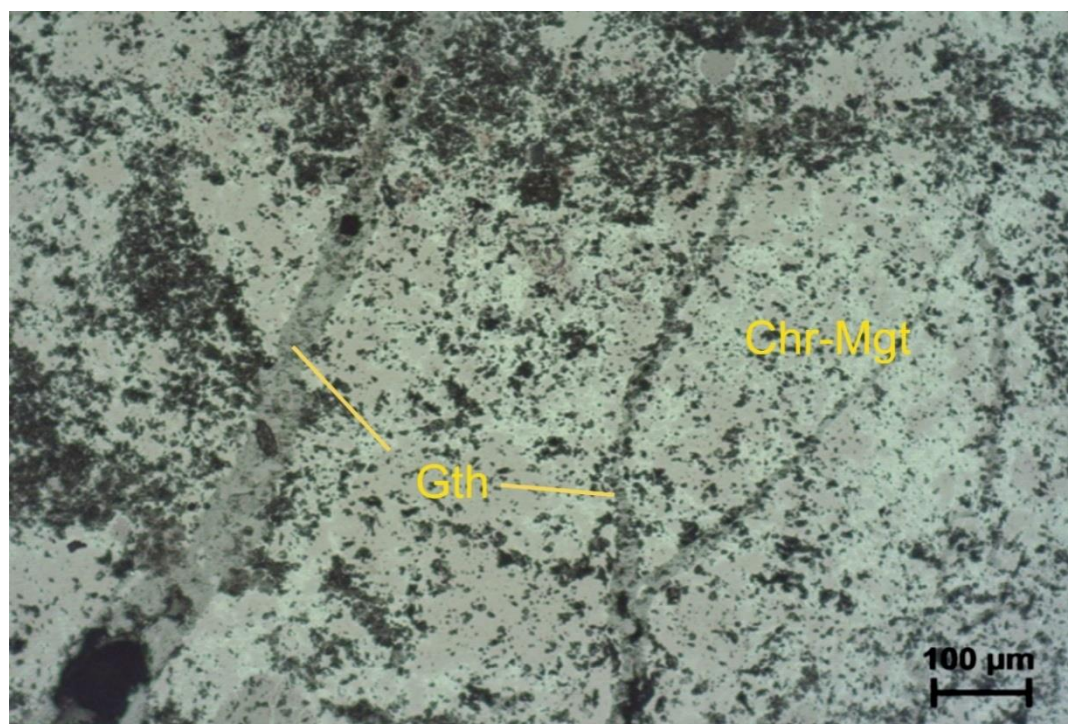


Fig.2: Reflected light photomicrographs of Phokpur magnetite sample from NOB showing anhedral magnetite/chrome-magnetite along with goethite veins.

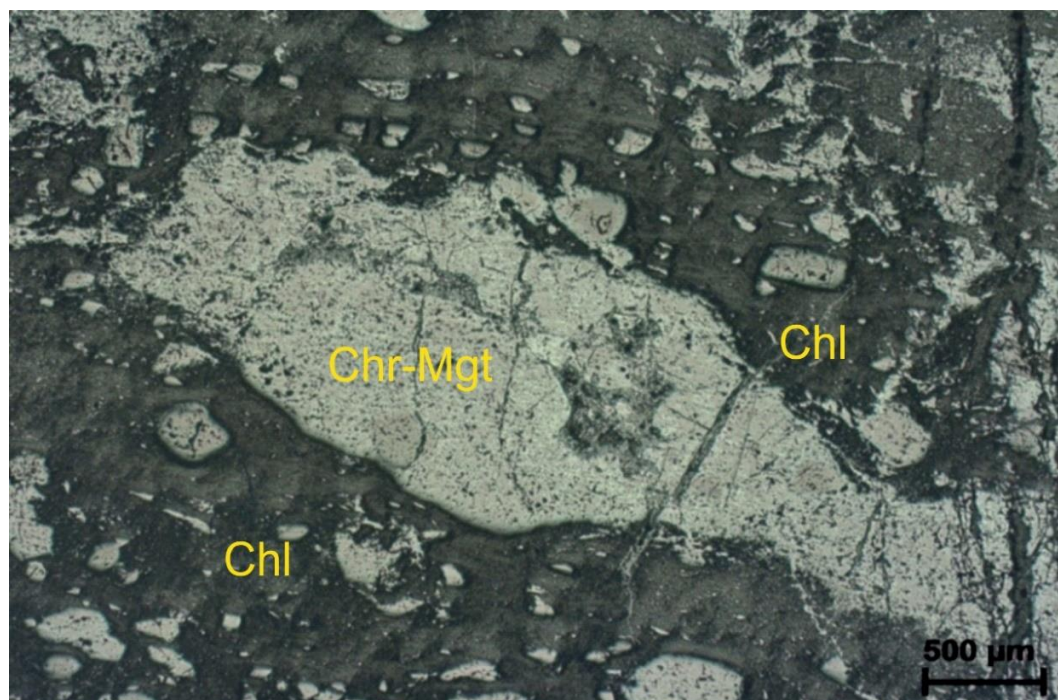


Fig. 1: Reflected light photomicrographs of Phokpur magnetite sample from NOB showing a large elongated chrome-magnetite grain along with smaller fragmented and oriented grains of chromite indicating the affect of tectonic activity.

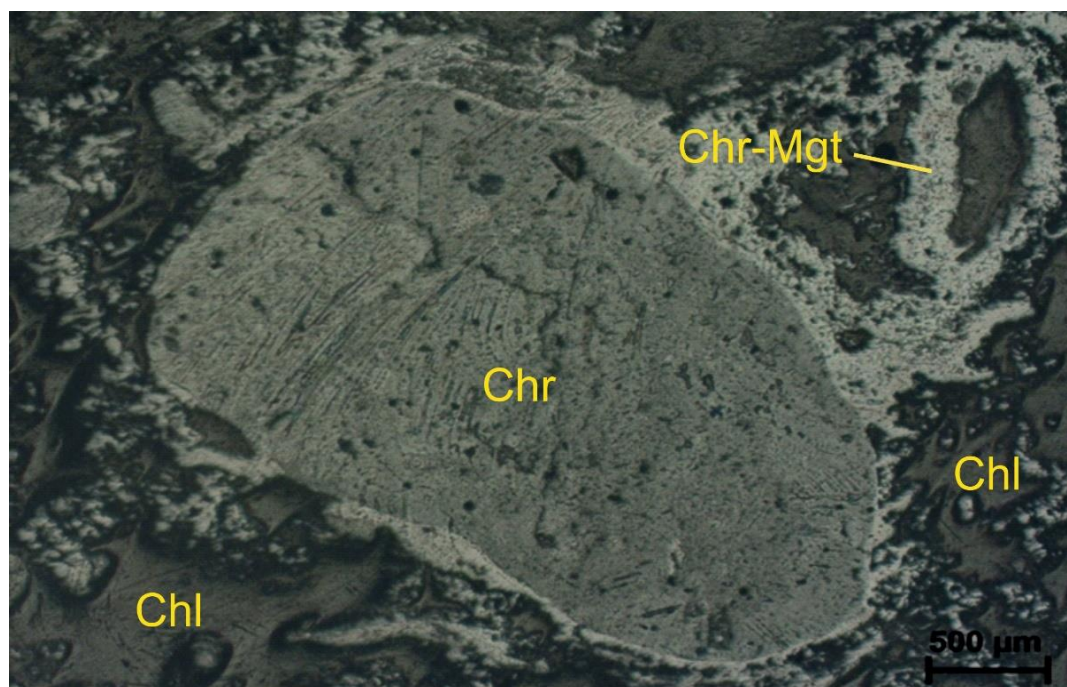


Fig.2: Reflected light photomicrographs of Phokpur magnetite sample from NOB showing alteration of a large grain of chromite to chrome-magnetite at margin. A ring of chrome-magnetite and fine disseminated grains of magnetite are also present within chlorite-silicates matrix.

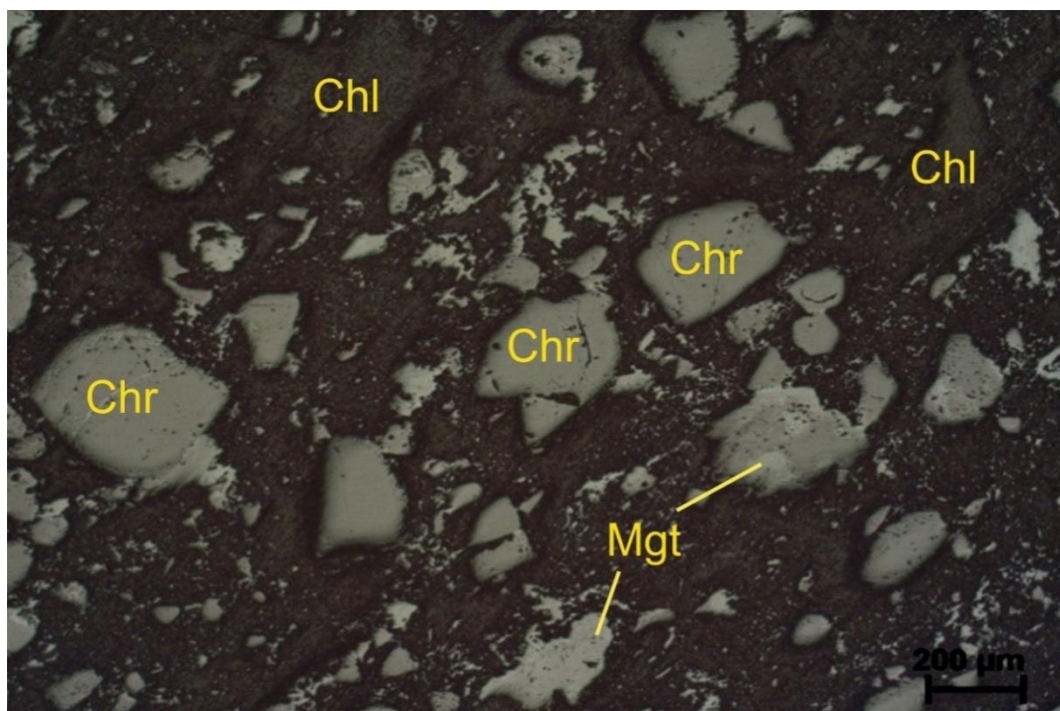


Fig.1: Reflected light photomicrographs of Phokpur magnetite sample from NOB showing orientation of chromite grains along with smaller disseminated grains of magnetite in chlorite-silicate matrix indicating the effect of tectonism.

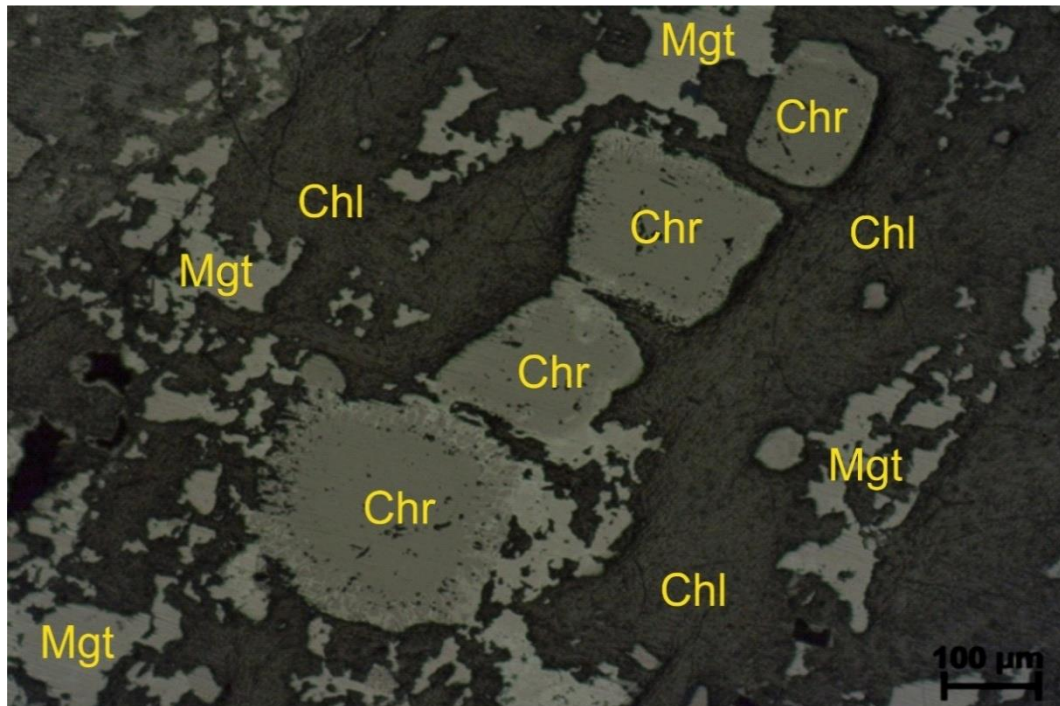


Fig.2: Reflected light photomicrographs of Phokpur magnetite sample from NOB showing discrete and altered chromite grains oriented in one direction along with smaller anhedral broken magnetite grains indicating the effect of tectonism.

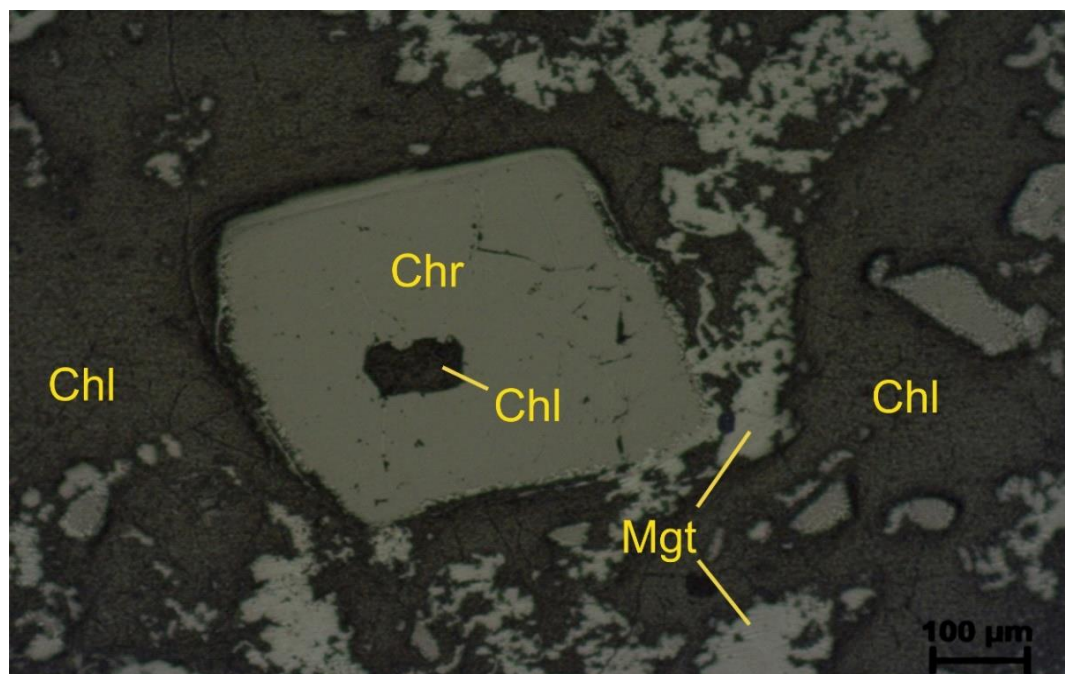


Fig. 1: Reflected light photomicrographs of Phokpur magnetite sample from NOB showing octahedral chromite (with a small inclusion of chlorite) along with smaller anhedral magnetite grains within chlorite-silicate matrix.

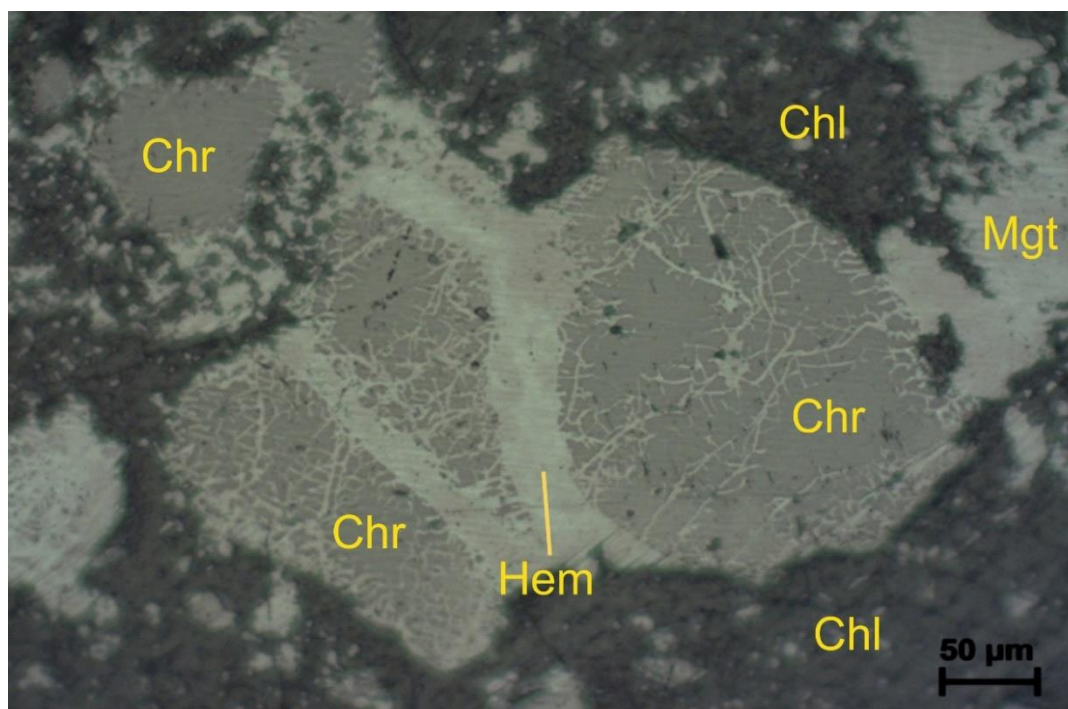


Fig. 2: Reflected light photomicrographs of Phokpur magnetite sample from NOB showing compositional transformation of dark grey chromite to dull white magnetite along the margins and fractures forming net and branching textures. Hematite vein is also present at the contact of chromite grains due to martitization.

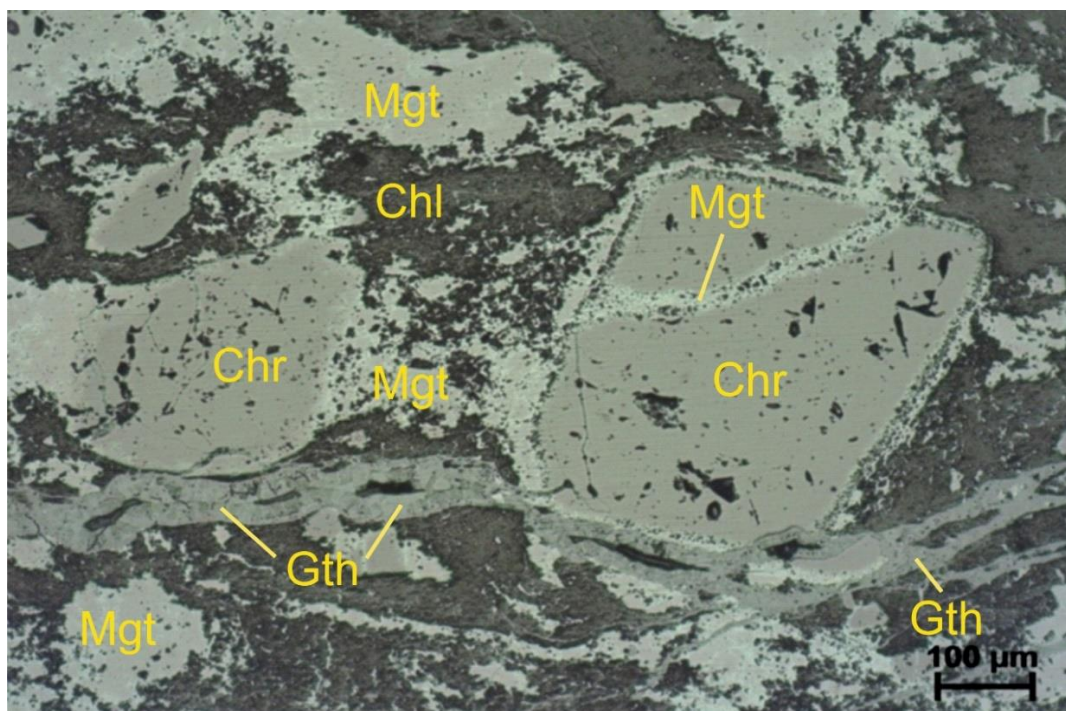


Fig.1: Reflected light photomicrographs of Phokpur magnetite sample from NOB with euhedral chromite showing alteration to magnetite from margin and crack. Goethite veins running almost parallel below the chromite grains are also present.

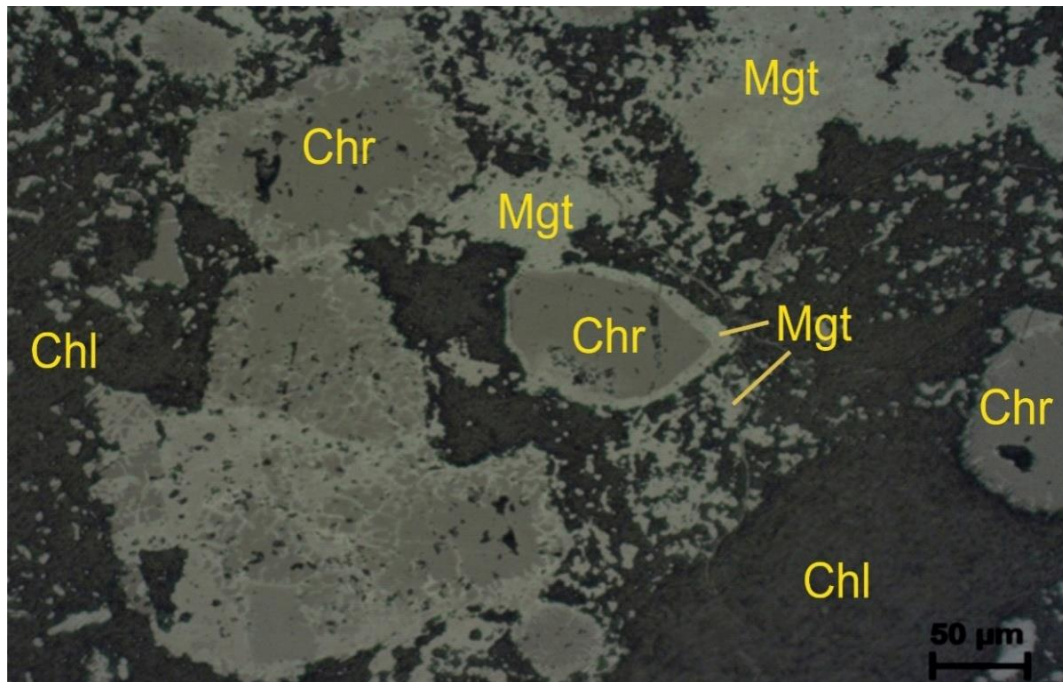


Fig.2: Reflected light photomicrographs of Phokpur magnetite sample from NOB showing a chromite grain with magnetite rim. Chromite grains are also showing their transformation to magnetite along margins and fractures. Fine disseminated grains of magnetite and hematite are also present within chlorite matrix.

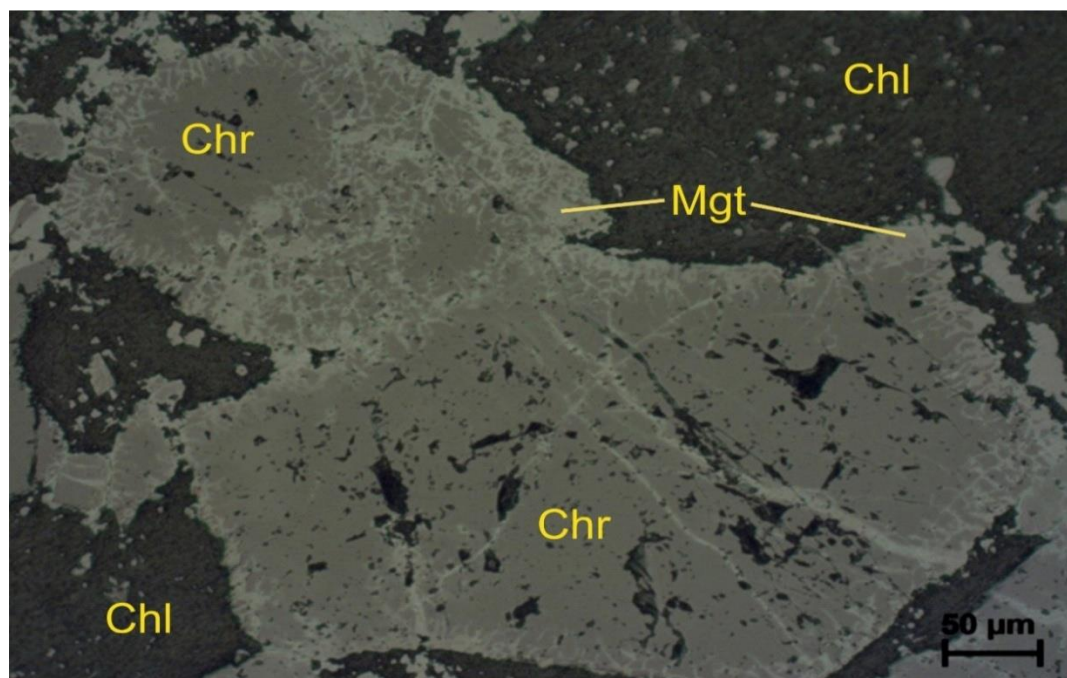


Fig.1: Reflected light photomicrographs of Phokpur magnetite samples from NOB showing formation of magnetite along grain boundaries and fractures of chromite grains in the matrix of chlorite. Hematite veins are also observed within chromite.

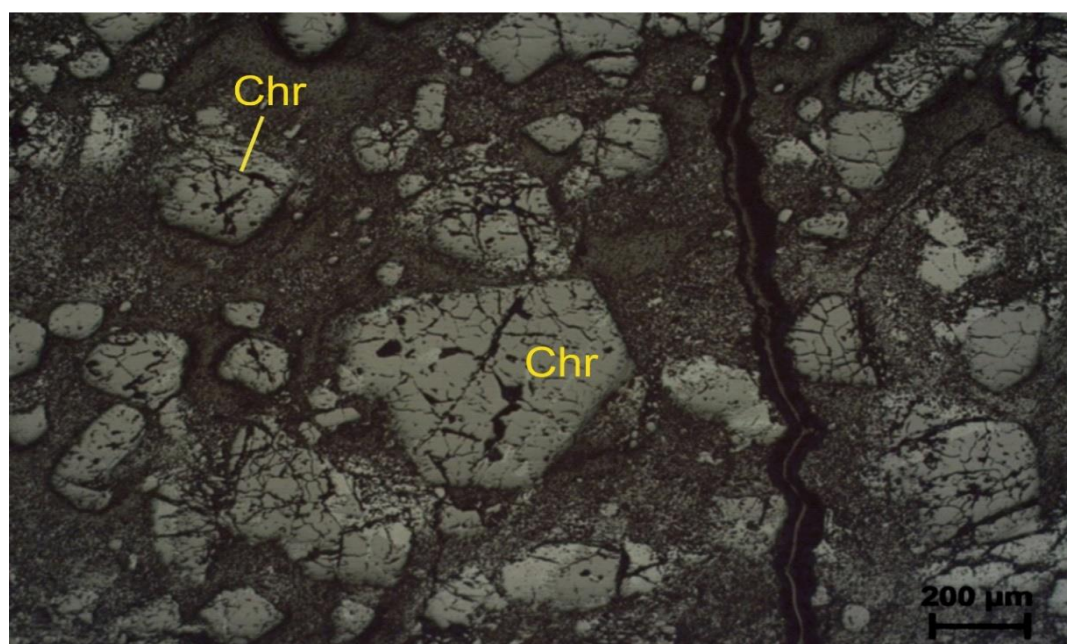


Fig.2: Reflected light photomicrographs of Phokpur magnetite samples from NOB showing deformational cracks/ fractures within euhedral to subhedral brecciated chromite grains in the matrix of chlorite. These cracks/ fractures are filled with silicate gangues. A dark silicate vein containing a thin goethite vein is also present. This may be the ground preparation for transformation of chromite to magnetite.

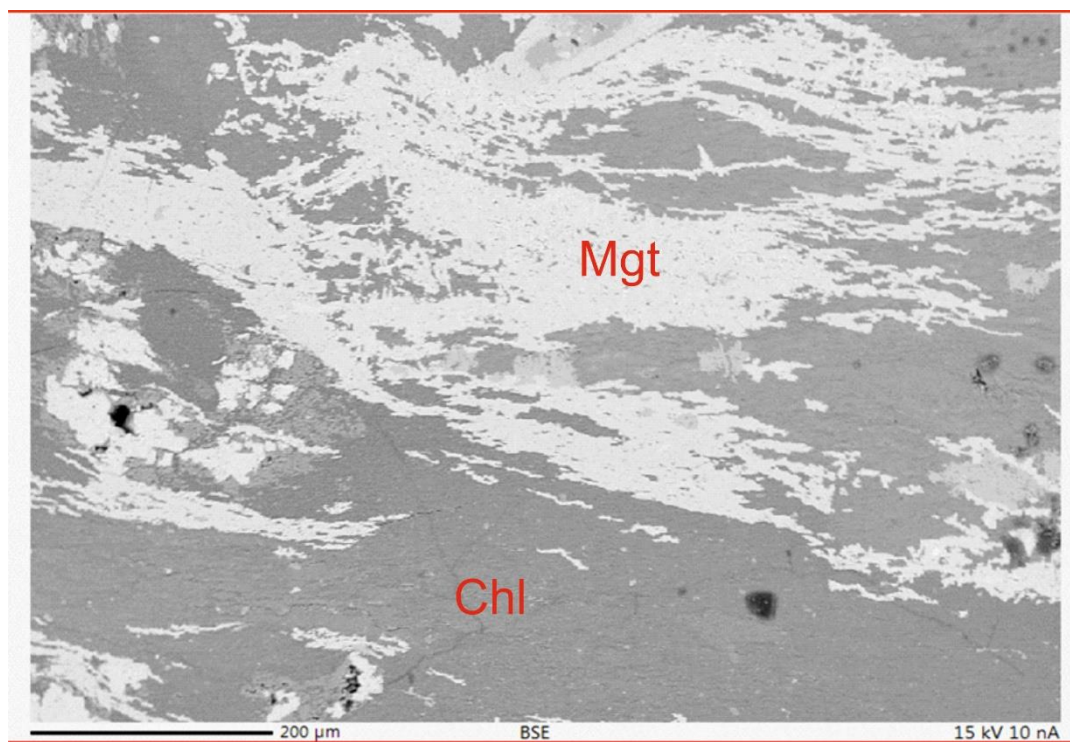


Fig. 1: BSE image of Phokpur magnetite sample from NOB showing anhedral and deformed magnetite grains within the chlorite-serpentine matrix.

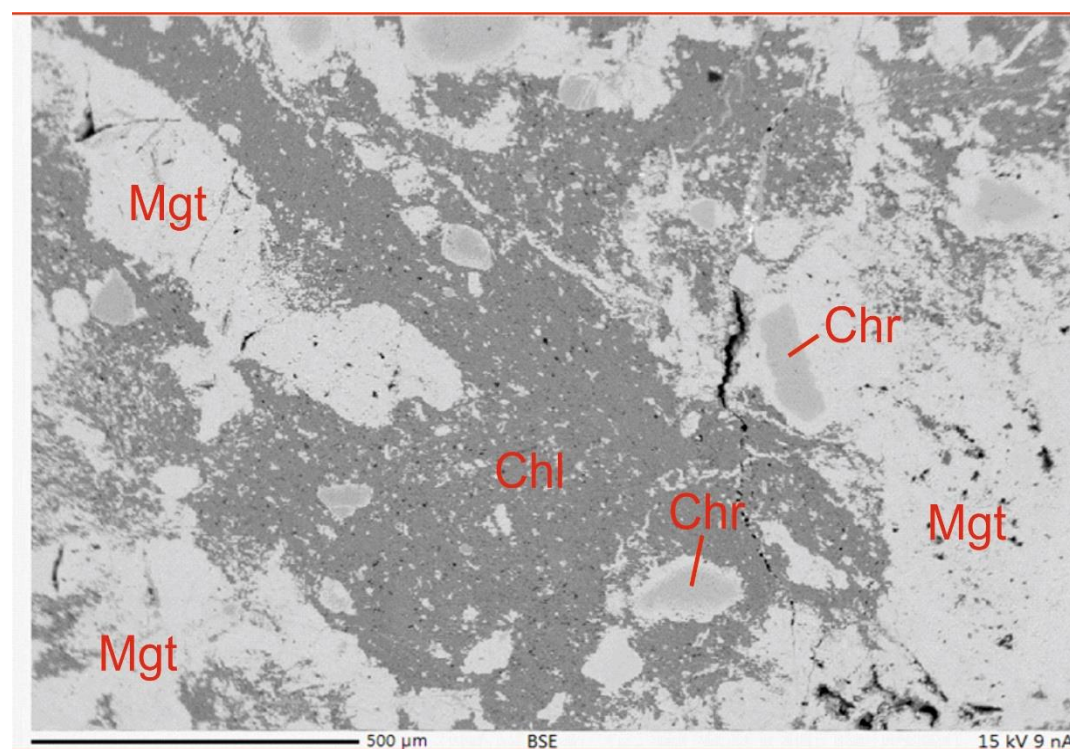


Fig. 2: BSE image of Phokpur magnetite sample from NOB showing anhedral to subhedral magnetite and chromite along with fine magnetite/ hematite grains within chlorite-serpentine matrix.

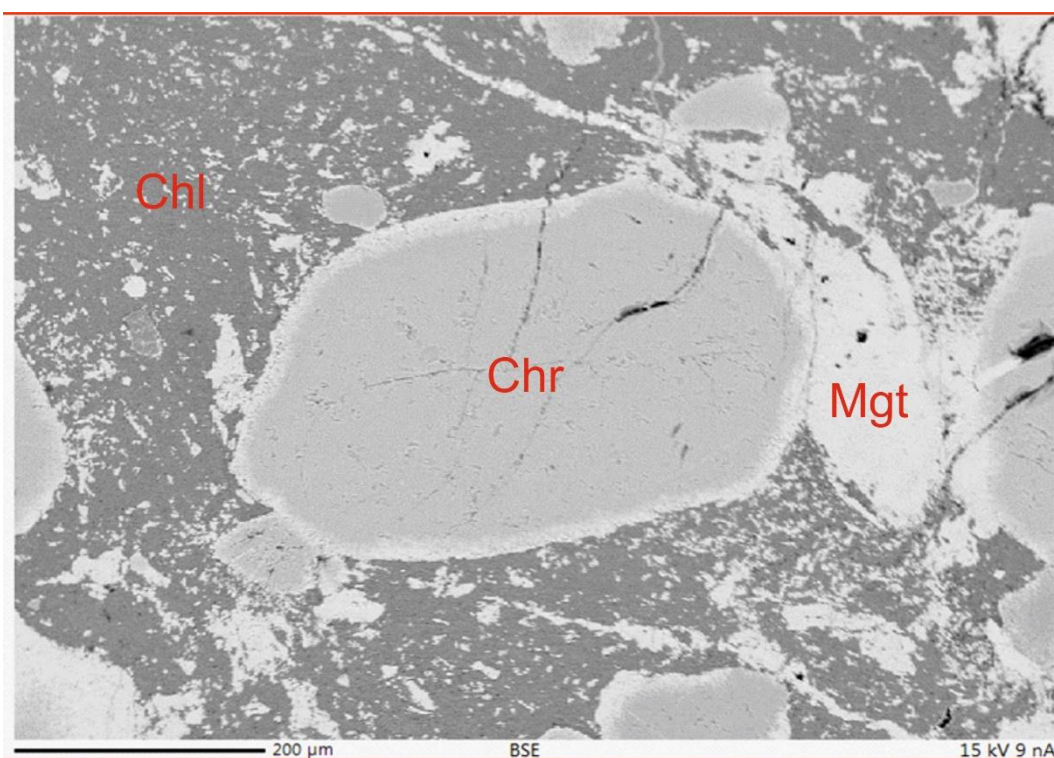


Fig. 1: BSE image of Phokpur magnetite sample from NOB showing alteration of a large chromite grain to chrome-magnetite at margin (rim) having smooth contact with chlorite-serpentine matrix.

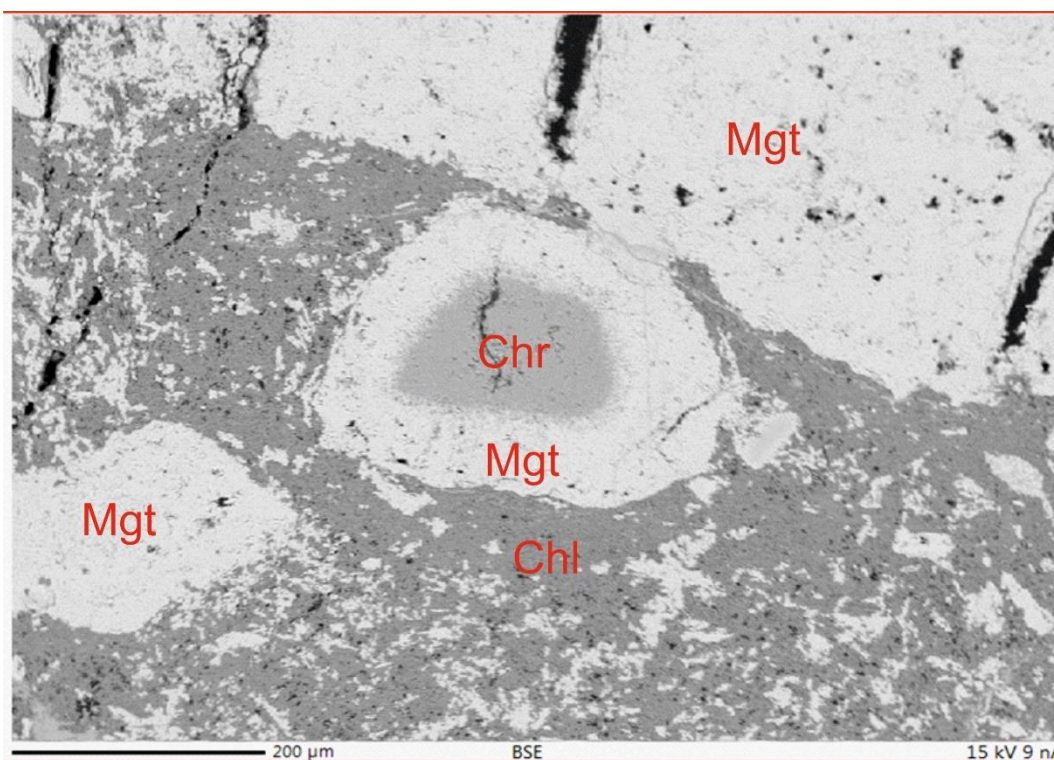


Fig. 2: BSE image of Phokpur magnetite sample from NOB showing a zoned chromite grain surrounded by the thick rim of magnetite. Fine magnetite grains are also present within the matrix of chlorite-serpentine.

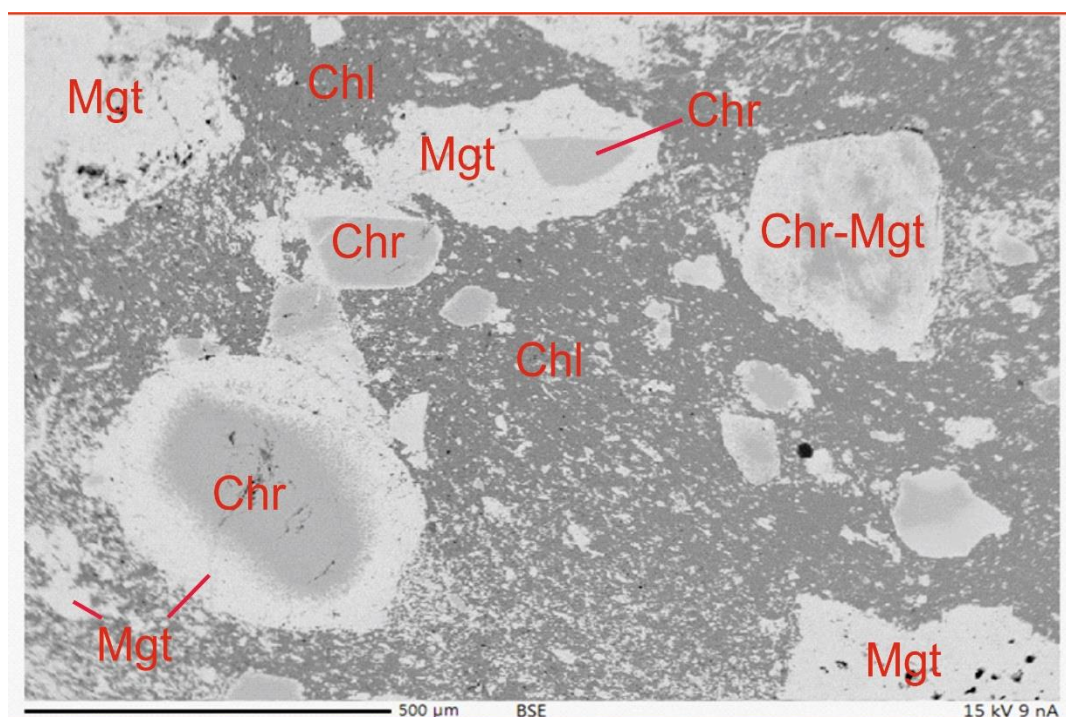


Fig.1: BSE image of Phokpur magnetite sample from NOB showing various proportions of alteration of chromite grains into magnetite along their grain boundaries. Fine magnetite grains are present within chlorite-serpentine matrix.

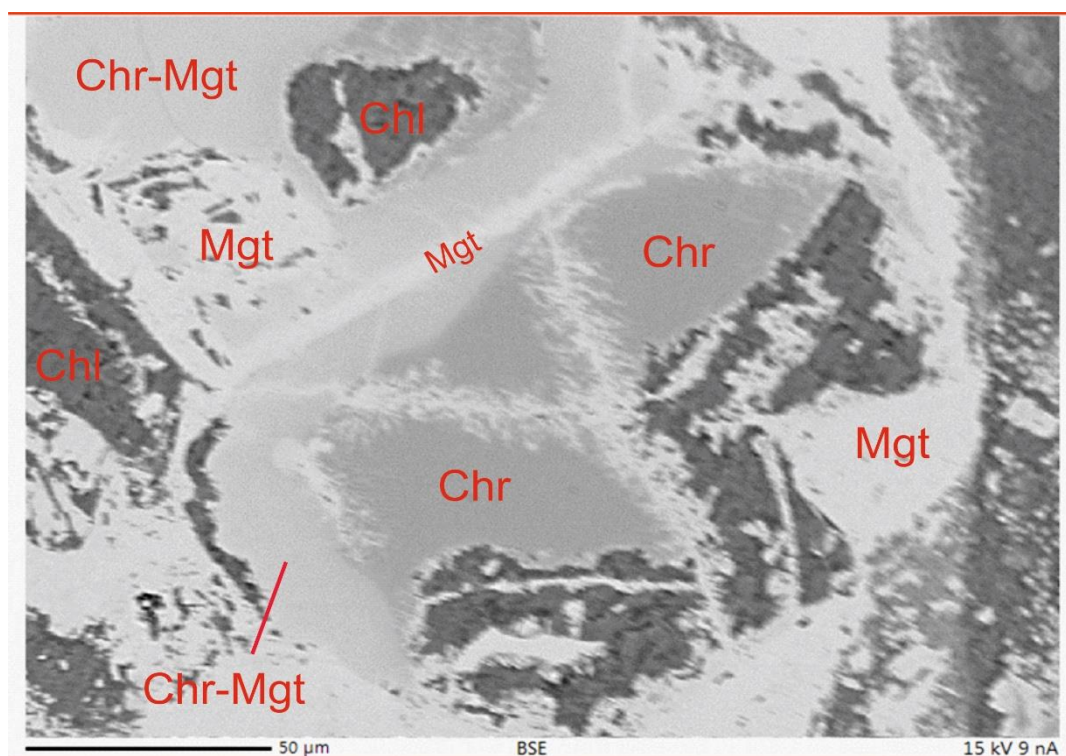


Fig.2: BSE image of Phokpur magnetite sample from NOB showing transformation of chromite grains to chrome-magnetite/ magnetite along their grain boundaries and fractures. A straight vein of magnetite is formed at the contact of two chromite grains. Chlorite is also present as inclusions within chromite grains.

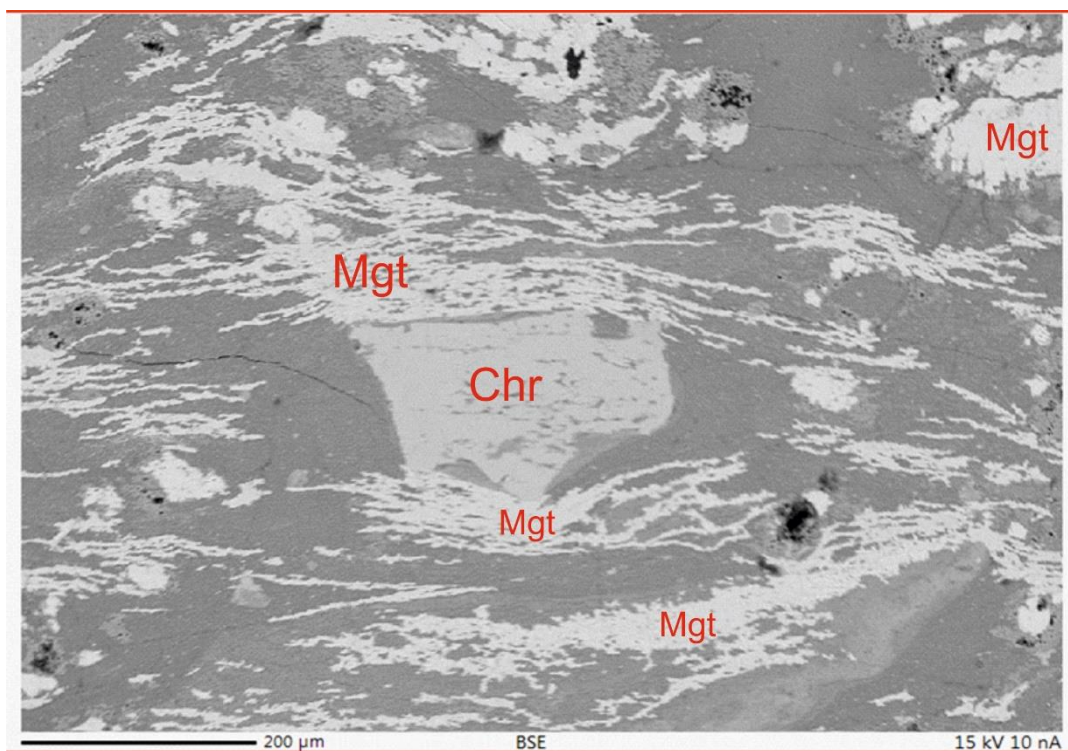


Fig. 1: BSE image of Phokpur magnetite sample from NOB showing elongated and oriented magnetite grains along with a large grain of chromite at the centre within chlorite-serpentine matrix.

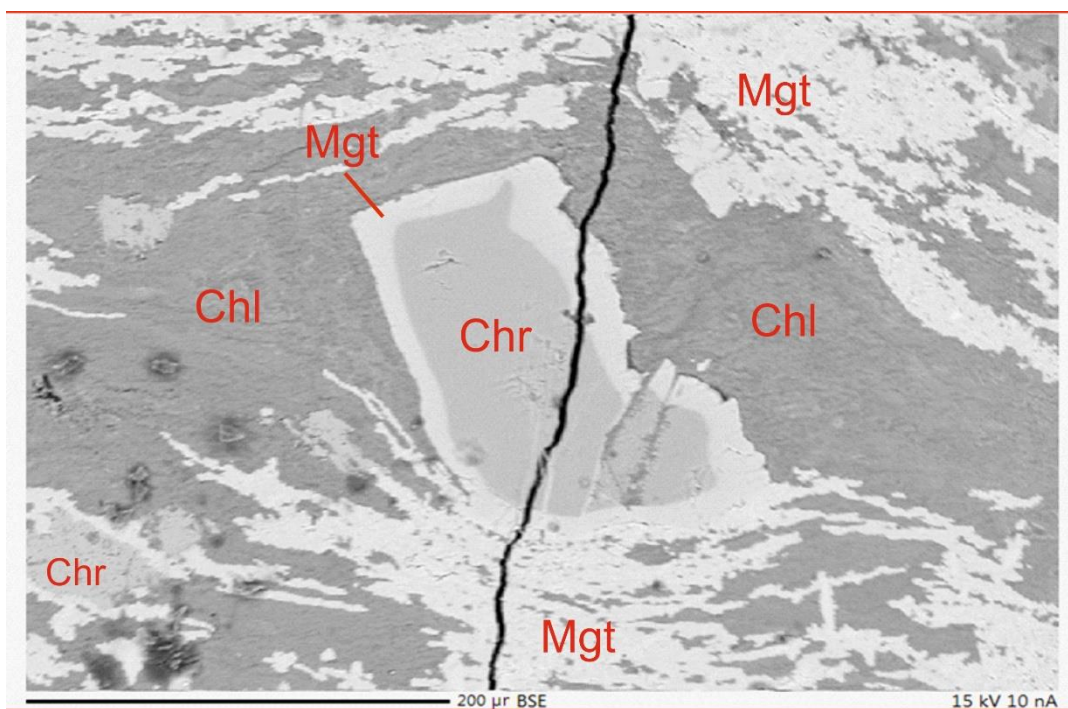


Fig. 2: BSE image of Phokpur magnetite sample from NOB showing a zoned chromite with magnetite rim between elongated and deformed magnetite grains. A fracture filled dark thin vein of gangue silicate is also present cutting across all the minerals - magnetite, silicate matrix and chromite.

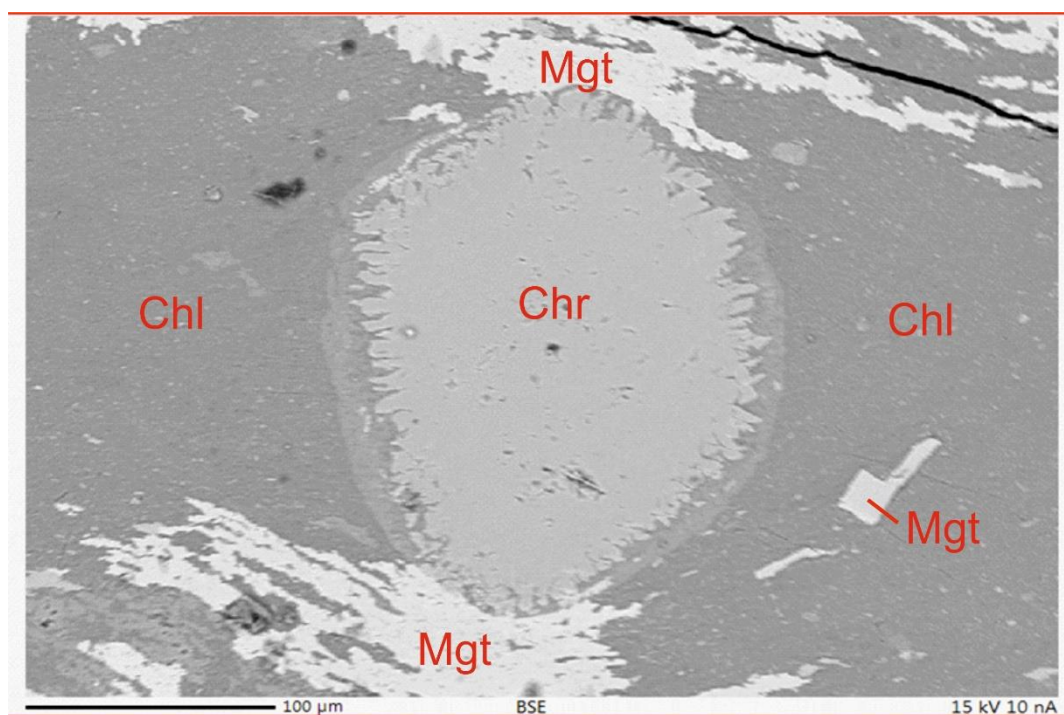


Fig. 1: BSE image of Phokpur magnetite sample from NOB showing corroded margin of chromite with rim of goethite hosted within chlorite-serpentine matrix.

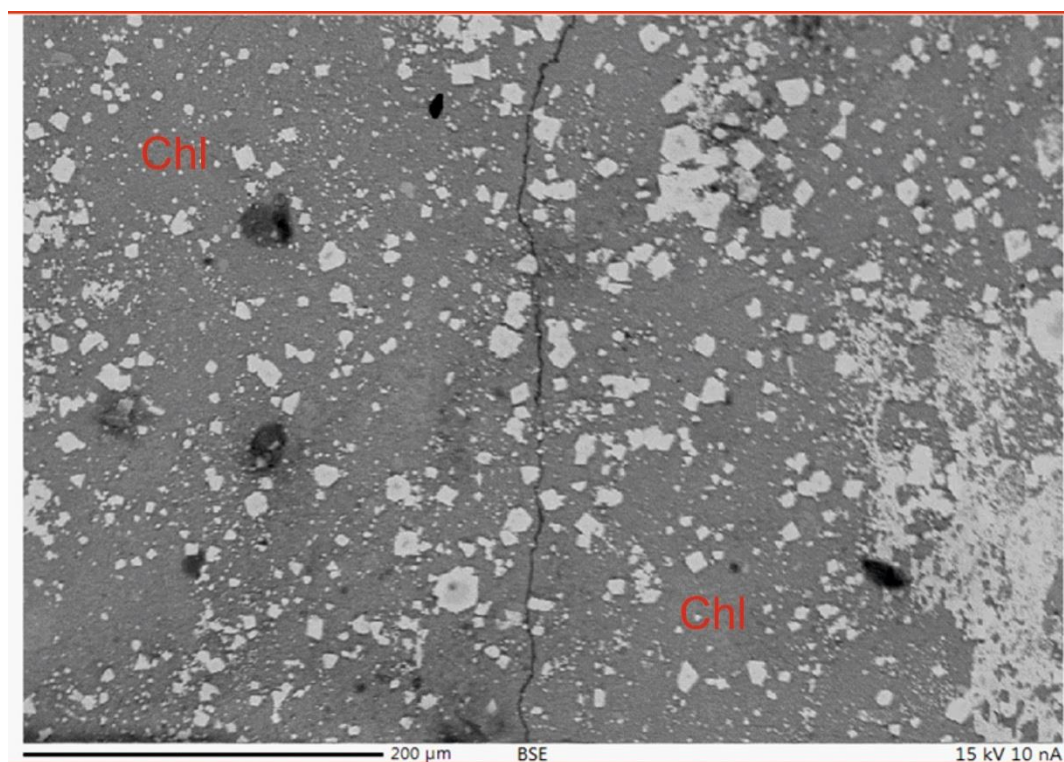


Fig.2: BSE image of Phokpur magnetite sample from NOB showing fine to medium disseminated grains of chromite, magnetite and hematite within the matrix of chlorite along with a minor fracture filled silicate vein.